Supporting Information

Mapping yearly fine resolution global surface ozone through the Bayesian Maximum Entropy data fusion of observations and model output for 1990–2017

Marissa N. DeLang[1], Jacob S. Becker[1], Kai-Lan Chang[2,3], Marc L. Serre[1], Owen R. Cooper[2,3], Martin G. Schultz[4], Sabine Schröder[4], Xiao Lu[5], Lin Zhang[5], Makoto Deushi[6], Beatrice Josse[7], Christoph A. Keller[8,9], Jean-François Lamarque[10], Meiyun Lin[11,12], Junhua Liu[8,9], Virginie Marécal[7], Sarah A. Strode[8,9], Kengo Sudo[13,14], Simone Tilmes[10], Li Zhang[11,12,15], Stephanie E. Cleland[1], Elyssa L. Collins[1], Michael Brauer[16,17], J. Jason West[*,1]

[1]Department of Environmental Sciences and Engineering, University of North Carolina at Chapel Hill, Chapel Hill, NC, USA
[2]Cooperative Institute for Research in Environmental Sciences, University of Colorado, Boulder, CO, USA
[3]NOAA Chemical Sciences Laboratory, Boulder, CO, USA
[4]Jülich Supercomputing Centre (JSC), Forschungszentrum Jülich, Jülich, Germany
[5]Laboratory for Climate and Ocean-Atmosphere Studies, Department of Atmospheric and Oceanic Sciences, School of Physics, Peking University, Beijing, China
[6]Meteorological Research Institute (MRI), Tsukuba, Japan
[7]Centre National de Recherches Météorologiques, Université de Toulouse, Météo-France, CNRS, Toulouse, France
[8]NASA Goddard Space Flight Center, Greenbelt, MD, USA
[9]Universities Space Research Association, Columbia, MD, USA
[10]National Center for Atmospheric Research, Boulder, CO, USA
[11]NOAA Geophysical Fluid Dynamics Laboratory, Princeton, NJ, USA
[12]Program in Atmospheric and Oceanic Sciences, Princeton University, Princeton, NJ, USA
[13]Graduate School of Environmental Studies, Nagoya University, Nagoya, Japan
[14]Japan Agency for Marine-Earth Science and Technology (JAMSTEC), Yokosuka, Japan
[15]Department of Meteorology and Atmospheric Science, Pennsylvania State University, University Park, PA. USA
[16]Institute for Health Metrics and Evaluation, University of Washington, Seattle, Washington, USA
[17]School of Population and Public Health, University of British Columbia, Vancouver, British Columbia, Canada

Pages: 74
Figures: 48
Tables: 4

This supporting information provides (1) model weights by region and year to create multi-model composites, (2) spatial and temporal covariance parameters, (3) fine resolution addition method and example, (4) yearly maps for all relevant scenarios, (5) cross validation statistics, (6) M^3Fusion method comparison, (7) population weighted ozone by region statistics, (8) population weighted ozone by country, and (9) ozone trends with uncertainty intervals.

(1) Multi-model Composite Weights by Region and Year

Figure S1: Region Classification.

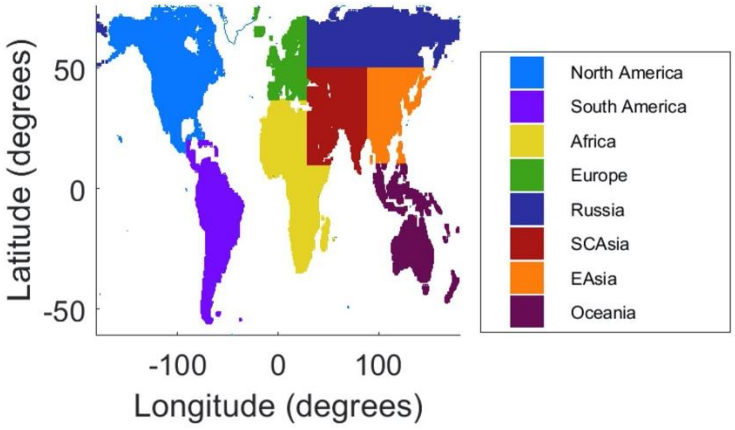

Table S1: Regionally optimized model weights. A blank cell represents zero weight and a dashed line represents a model not available.

Africa

	CESM1 CAM4-Chem	CESM1 WACCM	CHASER	GFDL AM3	GFDL AM4	MERRA2-GMI	MOCAGE	MRI-ESM1r1	MRI-ESM2.0
2017	-	-	-	-	-	1	-	-	
2016	-	-	-	-	0.91		0.09	-	
2015	-	-	-	-	0.91		0.09	-	
2014	-	-	-		1			-	
2013	-	-	-		0.83		0.17	-	
2012	-	-	-		0.85		0.15	-	
2011	-	-	-		0.64	0.25	0.11	-	
2010			0.38	0.08	-	0.18	0.36		-
2009			0.13	0.20	-	0.32	0.35		-
2008		0.06	0.20	0.71	-		0.03		-
2007			0.27	0.50	-	0.22	0.01		-
2006		0.13	0.24	0.02	-	0.61			-
2005			0.23	0.11	-	0.58	0.08		-
2004			0.49	0.11	-		0.40		-
2003			0.43		-		0.57		-
2002			0.12	0.66	-		0.22		-
2001			0.05	0.44	-		0.51		-
2000			0.13	0.29	-		0.58		-
1999			0.29	0.40	-	0.02	0.29		-
1998			0.29	0.40	-	0.02	0.29		-
1997			0.29	0.40	-	0.02	0.29		-
1996			0.29	0.40	-	0.02	0.29		-
1995			0.29	0.40	-	0.02	0.29		-
1994			0.29	0.40	-	0.02	0.29		-
1993			0.29	0.40	-	0.02	0.29		-

1992			0.29	0.40	-	0.02	0.29		-
1991			0.29	0.40	-	0.02	0.29		-
1990			0.29	0.40	-	0.02	0.29		-

East Asia

	CESM1 CAM4-Chem	CESM1 WACCM	CHASER	GFDL AM3	GFDL AM4	MERRA2-GMI	MOCAGE	MRI-ESM1r1	MRI-ESM2.0
2017	-	-	-	-	-	0.94	-	-	0.06
2016	-	-	-	-	0.59	0.22	0.19	-	
2015	-	-	-	-	0.60	0.15	0.25	-	
2014	-	-	-		0.66	0.13	0.21	-	
2013	-	-	-	0.27	0.26	0.44	0.03	-	
2012	-	-	-		0.29	0.67	0.04	-	
2011	-	-	-		0.20	0.68	0.12	-	
2010	1				-				-
2009	1				-				-
2008	0.90			0.10	-				-
2007		0.72		0.28	-				-
2006		0.90			-		0.10		-
2005	0.86			0.09	-		0.05		-
2004		0.44			-	0.39	0.17		-
2003	0.89			0.11	-				-
2002	0.23			0.44	-	0.25	0.08		-
2001	0.63				-	0.26	0.11		-
2000	0.60			0.40	-				-
1999	0.93			0.03	-		0.05		-
1998	0.93			0.03	-		0.05		-
1997	0.93			0.03	-		0.05		-
1996	0.93			0.03	-		0.05		-
1995	0.93			0.03	-		0.05		-
1994	0.93			0.03	-		0.05		-
1993	0.93			0.03	-		0.05		-
1992	0.93			0.03	-		0.05		-
1991	0.93			0.03	-		0.05		-
1990	0.93			0.03	-		0.05		-

Europe

	CESM1 CAM4-Chem	CESM1 WACCM	CHASER	GFDL AM3	GFDL AM4	MERRA2-GMI	MOCAGE	MRI-ESM1r1	MRI-ESM2.0
2017	-	-	-	-	-	0.70	-	-	0.30
2016	-	-	-	-	0.86		0.14	-	
2015	-	-	-	-	0.54	0.33	0.13	-	
2014	-	-	-	0.51	0.07	0.28	0.03	-	0.11
2013	-	-	-	0.29	0.03	0.64	0.04	-	
2012	-	-	-	0.21	0.33	0.39	0.07	-	
2011	-	-	-	0.58	0.10	0.17	0.15	-	
2010				0.57	-	0.28	0.15		-
2009				0.43	-	0.56	0.01		-
2008				0.71	-	0.25	0.04		-
2007		0.06		0.78	-	0.11	0.05		-
2006				0.75	-	0.17	0.081		-
2005				0.61	-	0.39			-
2004				0.92	-		0.08		-
2003				0.51	-	0.49			-
2002				0.36	-	0.64			-
2001				0.84	-		0.16		-
2000			0.88		-	0.12			-
1999				0.64	-	0.35		0.01	-
1998				0.14	-	0.61	0.12	0.13	-
1997				0.39	-	0.61			-
1996				0.13	-	0.87			-
1995				0.21	-	0.79			-

1994				0.66	-	0.03	0.17	0.14	-
1993				0.89	-		0.11		-
1992				1.00	-				-
1991				0.89	-	0.03	0.01	0.07	-
1990				0.75	-		0.25		-

North America

	CESM1 CAM4-Chem	CESM1 WACCM	CHASER	GFDL AM3	GFDL AM4	MERRA2-GMI	MOCAGE	MRI-ESM1r1	MRI-ESM2.0
2017	-	-	-	-	-		-	-	1
2016	-	-	-	-	0.39			-	0.61
2015	-	-	-	-	0.35	0.41		-	0.24
2014	-	-	-		0.27	0.48		-	0.25
2013	-	-	-		0.91	0.09		-	
2012	-	-	-		0.42	0.43		-	0.15
2011	-	-	-		0.53	0.42		-	0.05
2010	0.32				-	0.64		0.04	-
2009	0.32		0.02		-	0.25		0.41	-
2008	0.38				-	0.34	0.07	0.21	-
2007	0.22		0.08		-	0.28	0.02	0.40	-
2006	0.35		0.02		-	0.25		0.38	-
2005	0.28	0.12			-	0.30	0.01	0.29	-
2004		0.37			-	0.39	0.24		-
2003	0.31		0.01		-	0.29		0.39	-
2002		0.53	0.01		-		0.08	0.38	-
2001		0.48	0.06		-			0.46	-
2000	0.13		0.13		-			0.74	-
1999		0.32	0.05		-		0.02	0.61	-
1998	0.15				-	0.16		0.69	-
1997		0.30	0.08		-		0.31	0.31	-
1996	0.52			0.17	-		0.23	0.08	-
1995	0.37		0.04		-		0.35	0.24	-
1994		0.71			-		0.29		-
1993	0.26			0.08	-		0.36	0.30	-
1992	0.23				-			0.77	-
1991	0.17	0.55		0.23	-		0.05		-
1990		0.53			-		0.47		-

Oceania

	CESM1 CAM4-Chem	CESM1 WACCM	CHASER	GFDL AM3	GFDL AM4	MERRA2-GMI	MOCAGE	MRI-ESM1r1	MRI-ESM2.0
2017	-	-	-	-	-	1	-	-	
2016	-	-	-	-		1		-	
2015	-	-	-	-		1		-	
2014	-	-	-		0.34	0.66		-	
2013	-	-	-			1		-	
2012	-	-	-			0.94	0.06	-	
2011	-	-	-			1		-	
2010			1		-				-
2009		0.06	0.88		-	0.06			-
2008			0.91		-	0.09			-
2007			0.97		-	0.01	0.02		-
2006		0.41	0.48		-	0.11			-
2005			0.59		-	0.41			-
2004			0.51		-	0.43	0.06		-
2003			0.84		-	0.16			-
2002			0.96		-	0.04			-
2001		0.49	0.14		-	0.37			-
2000			0.88		-	0.12			-
1999			0.76		-	0.24			-
1998			0.76		-	0.24			-
1997			0.76		-	0.24			-

1996			0.76		-	0.24			-
1995			0.76		-	0.24			-
1994			0.76		-	0.24			-
1993			0.76		-	0.24			-
1992			0.76		-	0.24			-
1991			0.76		-	0.24			-
1990			0.76		-	0.24			-

Russia

	CESM1 CAM4-Chem	CESM1 WACCM	CHASER	GFDL AM3	GFDL AM4	MERRA2-GMI	MOCAGE	MRI-ESM1r1	MRI-ESM2.0
2017	-	-	-	-	-		-	-	1
2016	-	-	-	-	0.91			-	0.09
2015	-	-	-	-	0.91			-	0.09
2014	-	-	-		0.63	0.22		-	0.15
2013	-	-	-		1			-	
2012	-	-	-		0.73	0.17	0.10	-	
2011	-	-	-		0.84		0.16	-	
2010			0.43		-		0.57		-
2009			0.32		-	0.38	0.27	0.03	-
2008	0.03		0.24		-	0.59	0.14		-
2007			0.38	0.37	-	0.02	0.23		-
2006			0.28	0.36	-		0.36		-
2005			0.24	0.63	-		0.13		-
2004			0.21		-	0.11	0.25	0.43	-
2003			0.01		-	0.99			-
2002		0.24	0.22	0.19	-		0.35		-
2001		0.04	0.46		-		0.50		-
2000		0.21	0.28	0.35	-		0.16		-
1999			0.41		-	0.16	0.43		-
1998			0.41		-	0.16	0.43		-
1997			0.41		-	0.16	0.43		-
1996			0.41		-	0.16	0.43		-
1995			0.41		-	0.16	0.43		-
1994			0.41		-	0.16	0.43		-
1993			0.41		-	0.16	0.43		-
1992			0.41		-	0.16	0.43		-
1991			0.41		-	0.16	0.43		-
1990			0.41		-	0.16	0.43		-

South America

	CESM1 CAM4-Chem	CESM1 WACCM	CHASER	GFDL AM3	GFDL AM4	MERRA2-GMI	MOCAGE	MRI-ESM1r1	MRI-ESM2.0
2017	-	-	-	-	-	0.34	-	-	0.66
2016	-	-	-	-	0.20	0.30		-	0.49
2015	-	-	-	-	0.21	0.30		-	0.49
2014	-	-	-		0.19	0.56	0.25	-	
2013	-	-	-		0.77			-	0.23
2012	-	-	-		0.19	0.22	0.05	-	0.54
2011	-	-	-	0.02		0.55		-	0.43
2010		0.39	0.51		-		0.10		-
2009		0.16		0.36	-	0.48			-
2008		0.41	0.15	0.44	-				-
2007		0.53	0.09	0.08	-		0.30		-
2006		0.30	0.67	0.03	-				-
2005		0.55	0.20	0.18	-		0.07		-
2004		0.42	0.03	0.23	-		0.32		-
2003				0.66	-		0.34		-
2002		0.11		0.39	-		0.50		-
2001				0.72	-	0.19	0.09		-
2000				0.55	-	0.17	0.28		-
1999		0.36		0.36	-		0.28		-

1998		0.36		0.36	-		0.28		-
1997		0.36		0.36	-		0.28		-
1996		0.36		0.36	-		0.28		-
1995		0.36		0.36	-		0.28		-
1994		0.36		0.36	-		0.28		-
1993		0.36		0.36	-		0.28		-
1992		0.36		0.36	-		0.28		-
1991		0.36		0.36	-		0.28		-
1990		0.36		0.36	-		0.28		-

South Central Asia

	CESM1 CAM4-Chem	CESM1 WACCM	CHASER	GFDL AM3	GFDL AM4	MERRA2-GMI	MOCAGE	MRI-ESM1r1	MRI-ESM2.0
2017	-	-	-	-	-	1	-	-	
2016	-	-	-	-	0.15	0.85		-	
2015	-	-	-	-	0.15	0.85		-	
2014	-	-	-	0.56		0.30		-	0.14
2013	-	-	-	0.34		0.66		-	
2012	-	-	-	0.42	0.06	0.52		-	
2011	-	-	-	0.60		0.40		-	
2010	0.39		0.55	0.06	-				-
2009	0.03	0.63	0.24	0.10	-				-
2008	0.69			0.31	-				-
2007	0.39	0.09	0.08	0.34	-			0.10	-
2006		0.36		0.64	-				-
2005	0.07		0.49	0.44	-				-
2004	0.53		0.01	0.46	-				-
2003	0.42		0.26	0.32	-				-
2002			0.41	0.59	-				-
2001	0.54			0.46	-				-
2000		0.43	0.15	0.43	-				-
1999	0.41		0.20	0.39	-				-
1998	0.41		0.20	0.39	-				-
1997	0.41		0.20	0.39	-				-
1996	0.41		0.20	0.39	-				-
1995	0.41		0.20	0.39	-				-
1994	0.41		0.20	0.39	-				-
1993	0.41		0.20	0.39	-				-
1992	0.41		0.20	0.39	-				-
1991	0.41		0.20	0.39	-				-
1990	0.41		0.20	0.39	-				-

(2) Spatial and Temporal Covariance Equations

The covariance derived from the offset removed observations can be described by the following equations. Let c_X = covariance, r = spatial lag in degrees, and τ = temporal lag in years.

Spatial Covariance:

$$c_X(r, \tau = 0) = 59.9938 \left(0.70 \exp\left(-\frac{3r}{1.20}\right) + 0.3 \exp\left(-\frac{3r}{25}\right)\right) \quad \text{(S1)}$$

Temporal Covariance:

$$c_X(r = 0, \tau) = 59.9938 \left(0.75 \exp\left(-\frac{3\tau}{80}\right) + 0.25 \exp\left(-\frac{3\tau}{1.5}\right)\right) \quad \text{(S2)}$$

Spatiotemporal Covariance:

$$\begin{aligned} c_X(r, \tau) = 59.9938 \Bigg(&0.70 \exp\left(-\frac{3r}{1.20}\right) \exp\left(-\frac{3\tau}{80}\right) + 0.25 \exp\left(-\frac{3r}{25}\right) \exp\left(-\frac{3\tau}{1.5}\right) \\ &+ 0.05 \exp\left(-\frac{3r}{25}\right) \exp\left(-\frac{3\tau}{80}\right) + \Bigg) \end{aligned} \quad \text{(S3)}$$

(3) Fine Resolution Addition

To change the resolution of our output from 0.5° to 0.1°, we use output from the NASA G5NR-Chem model, which was run at 0.125° resolution and regridded to 0.1° resolution. Figure S2 displays the theoretical addition of fine resolution to a 0.5° grid cell, with Figure S3 showing an example from our final output. The average of each 0.5° grid cell is the same before and after the fine resolution addition.

Figure S2: Theoretical addition of fine resolution to our BME estimations at 0.5°.

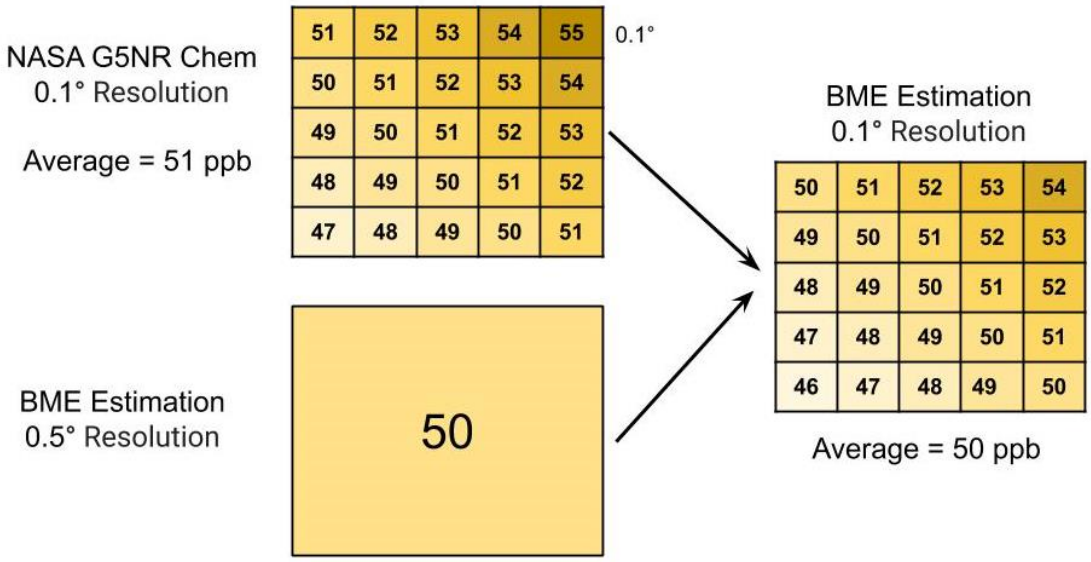

Figure S3: Example of fine resolution addition in a 0.5° grid cell over Charlotte, NC: BME Coarse Resolution with average 55.832 ppb (left), NASA Fine Resolution with average 59.4874 ppb (center), and BME Fine Resolution with average 55.832 ppb (right).

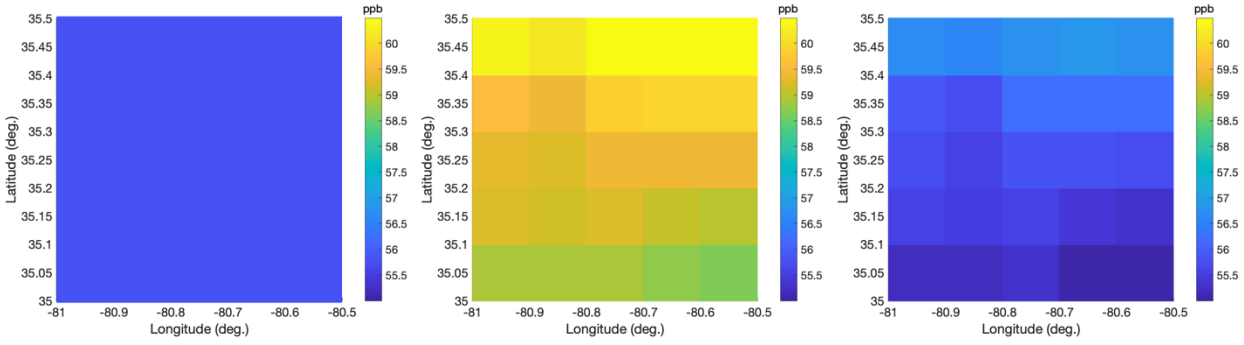

(4) Yearly Maps

For each year, the following maps are displayed in figures below:

1. Observations:
   TOAR and CNEMC data, as OSDMA8.

2. Multi-model Mean:
   Average of all model output available in the given year, as OSDMA8.

3. Multi-model Composite:
   Combination of model output using M^3Fusion method, as OSDMA8.

4. Space Only:
   BME corrected M^3Fusion composite where observations can only influence across space in the year they were measured, as OSDMA8.

5. Space Time:
   BME corrected M^3Fusion composite where observations can influence across space and time, as OSDMA8.

6. Space Time Variance:
   Variance of BME corrected M^3Fusion composite where observations can influence across space and time.

7. Space Time – Model Composite:
   Difference between Space Time and Multi-model Composite methods, as OSDMA8.

8. Fine Resolution:
   Space time corrected output with fine resolution from the NASA G5NR-Chem model, as OSDMA8.

Figure S4: Yearly Maps for 1990

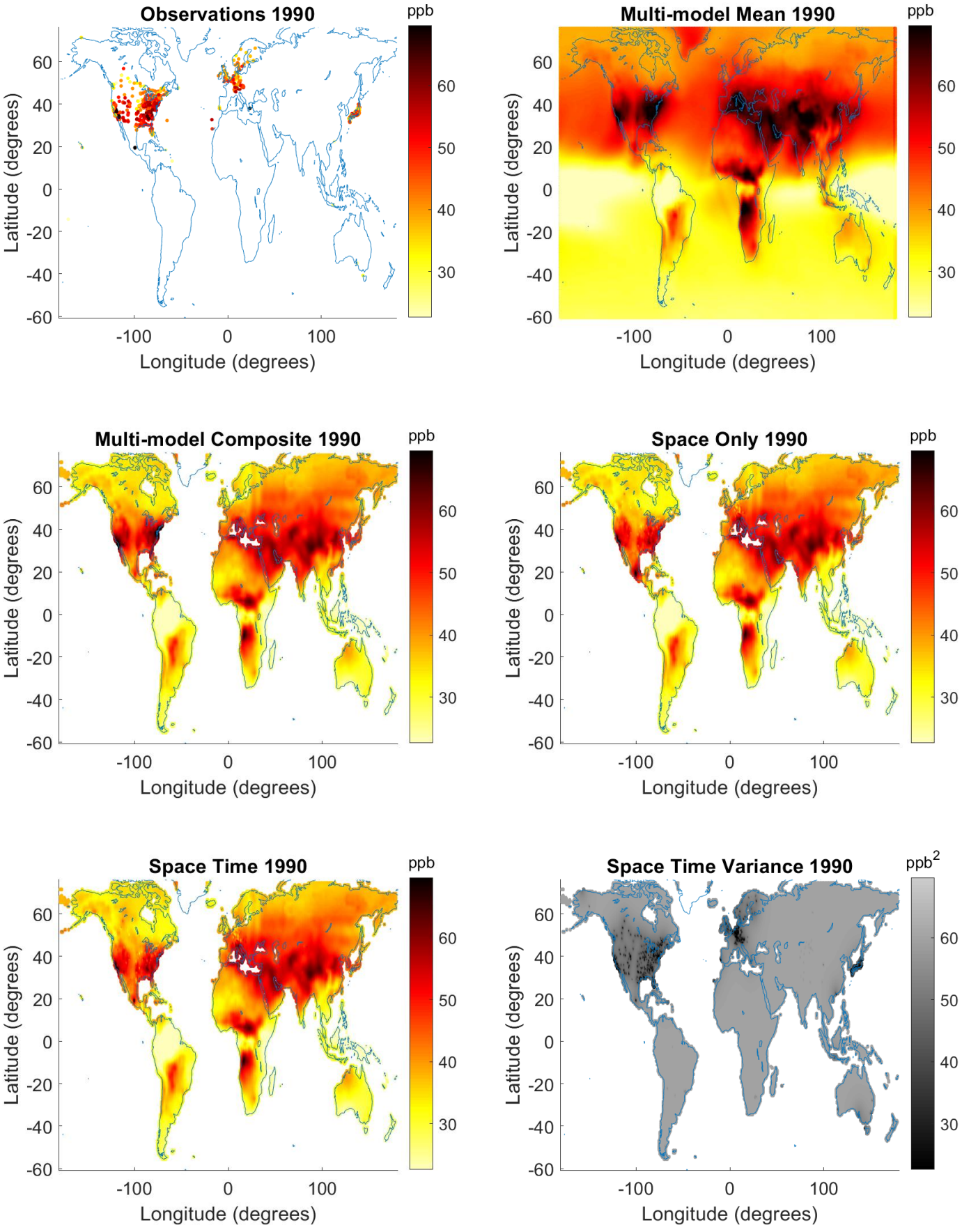

Figure S4: (continued)

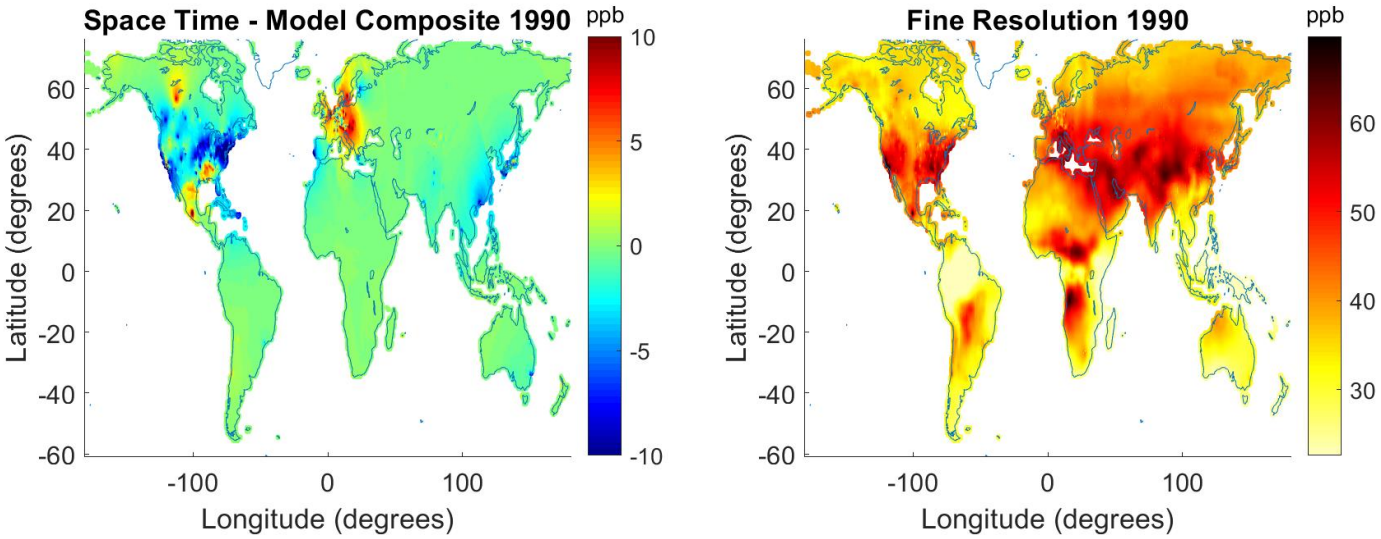

Figure S5: Yearly Maps for 1991

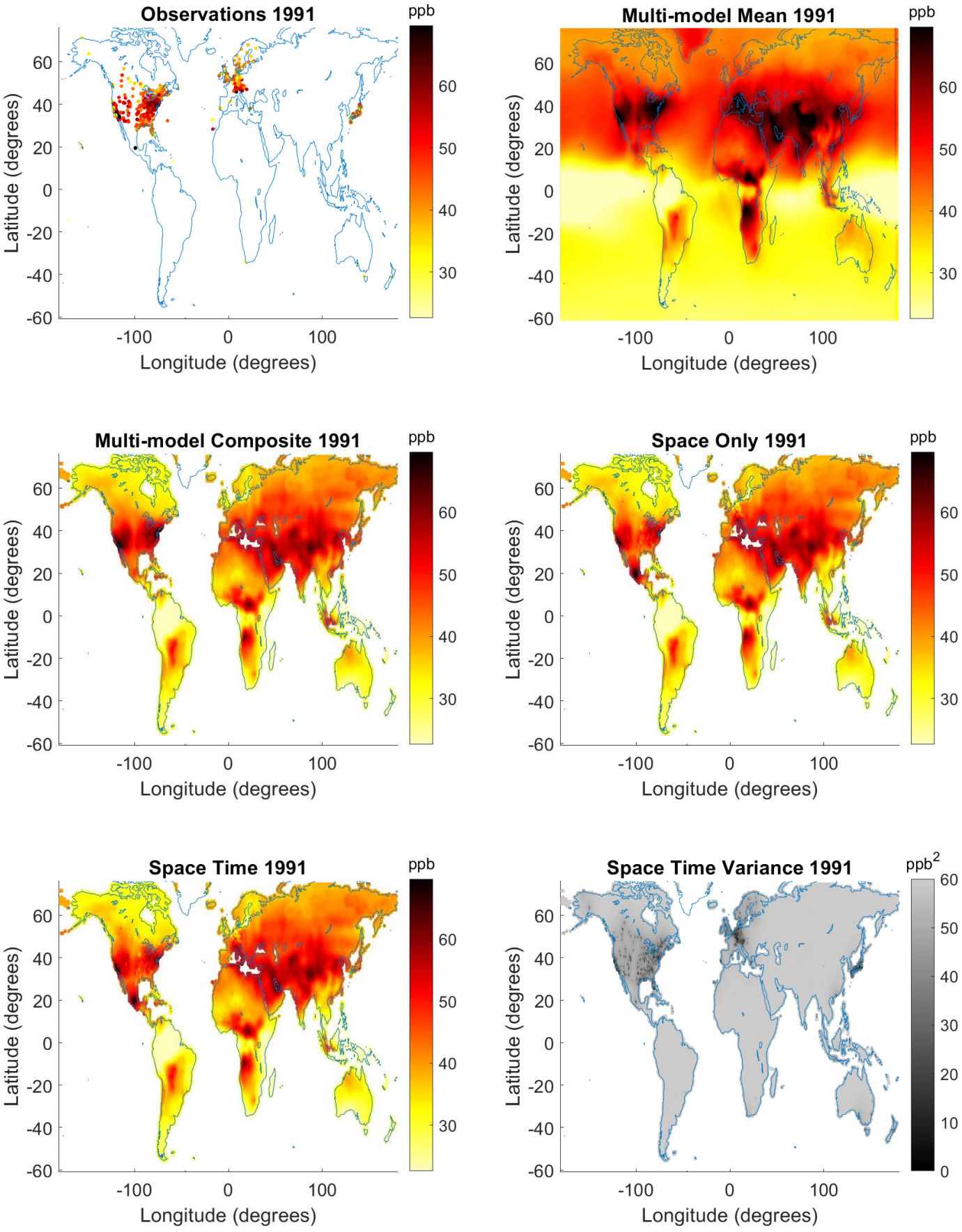

Figure S5: (continued)

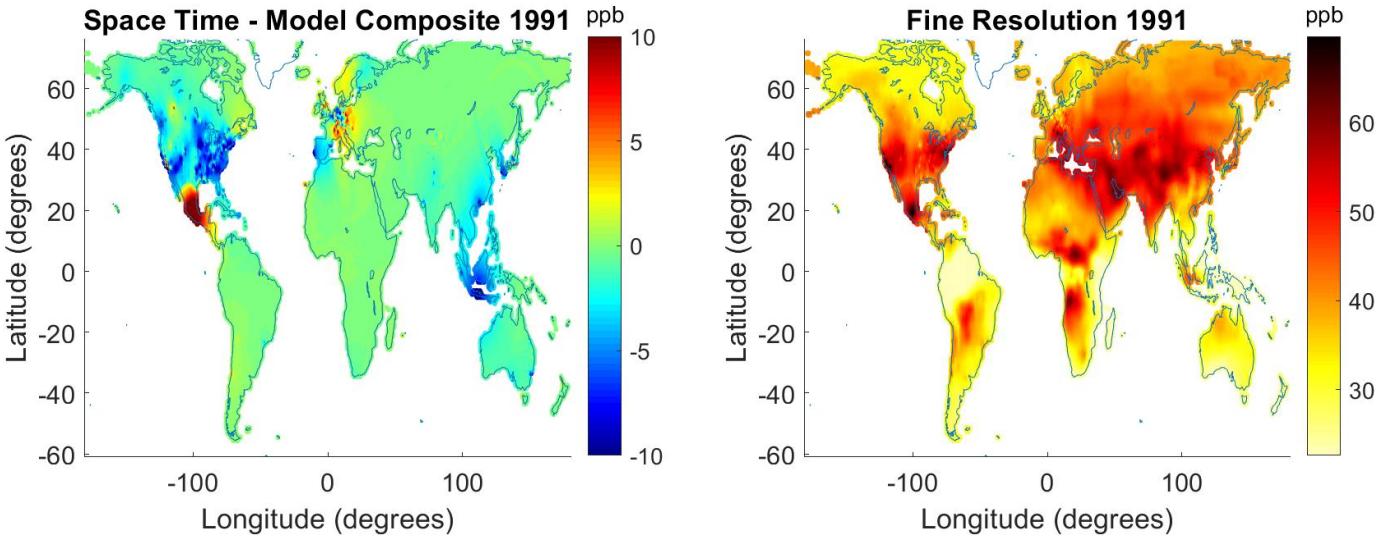

Figure S6: Yearly Maps for 1992

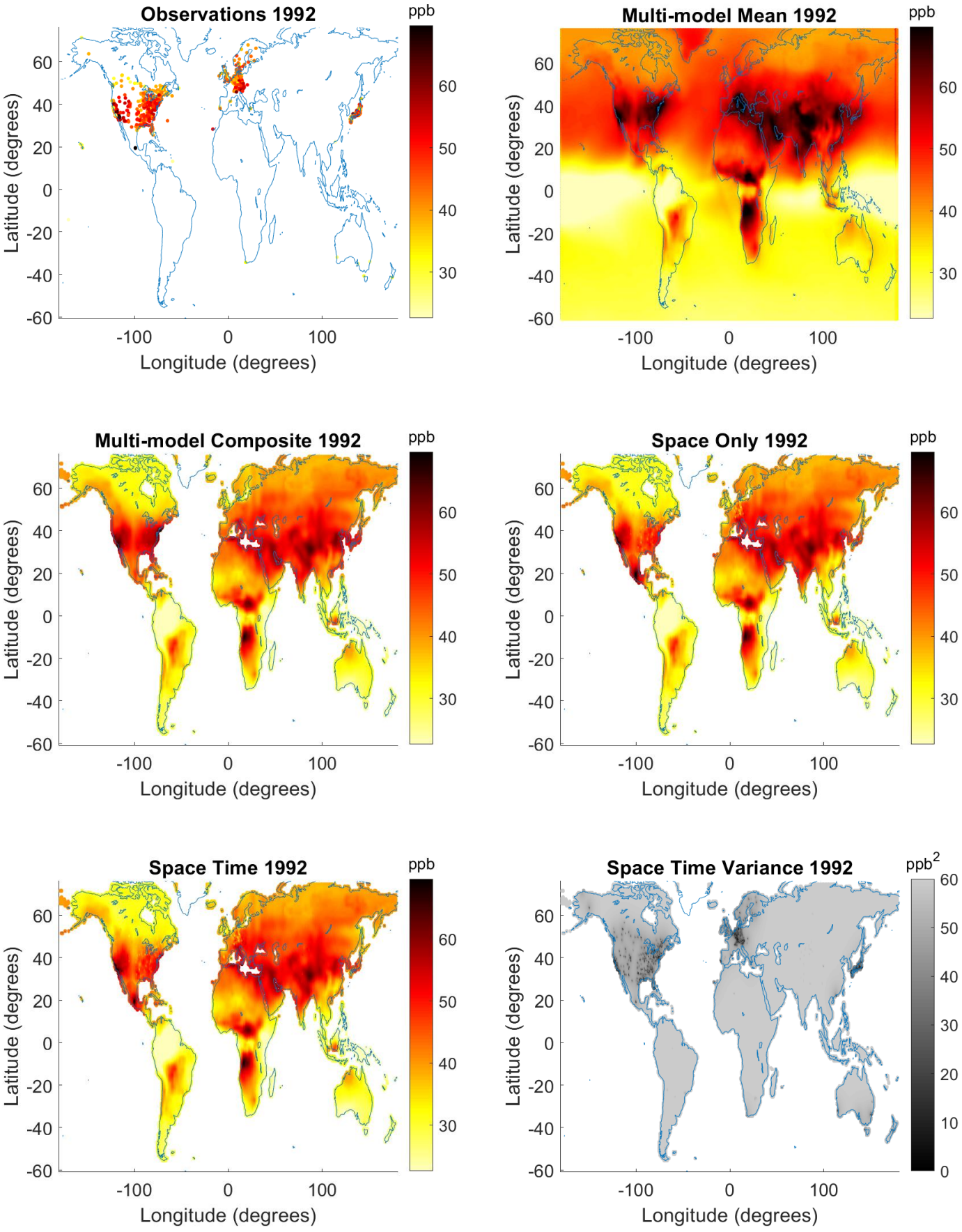

Figure S6: (continued)

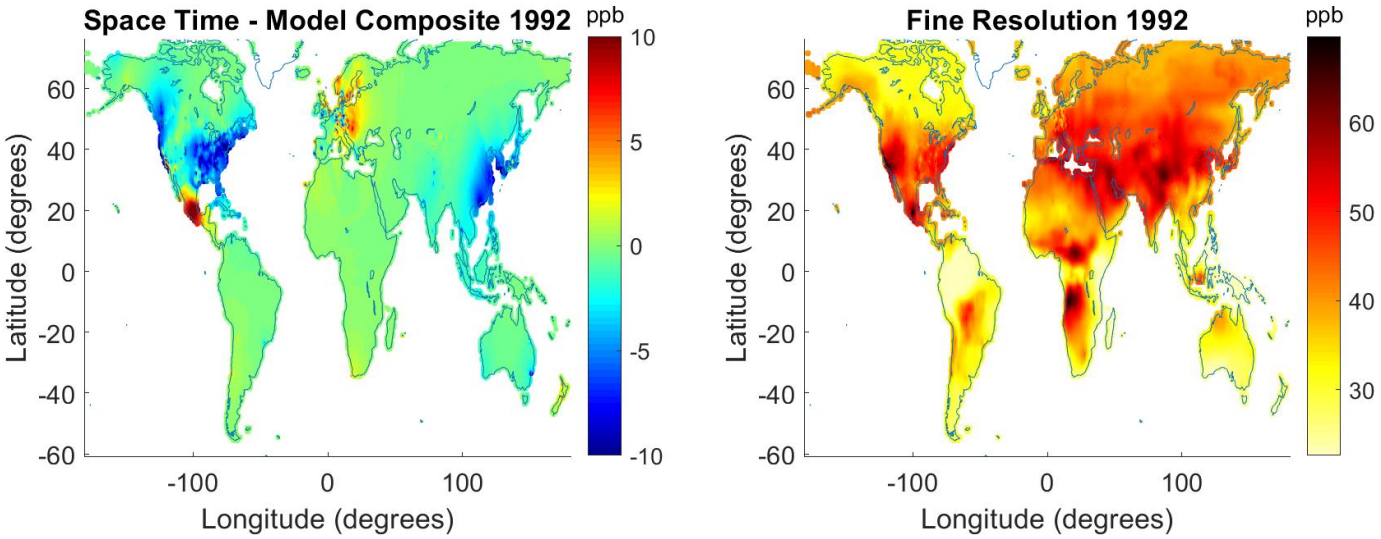

Figure S7: Yearly Maps for 1993

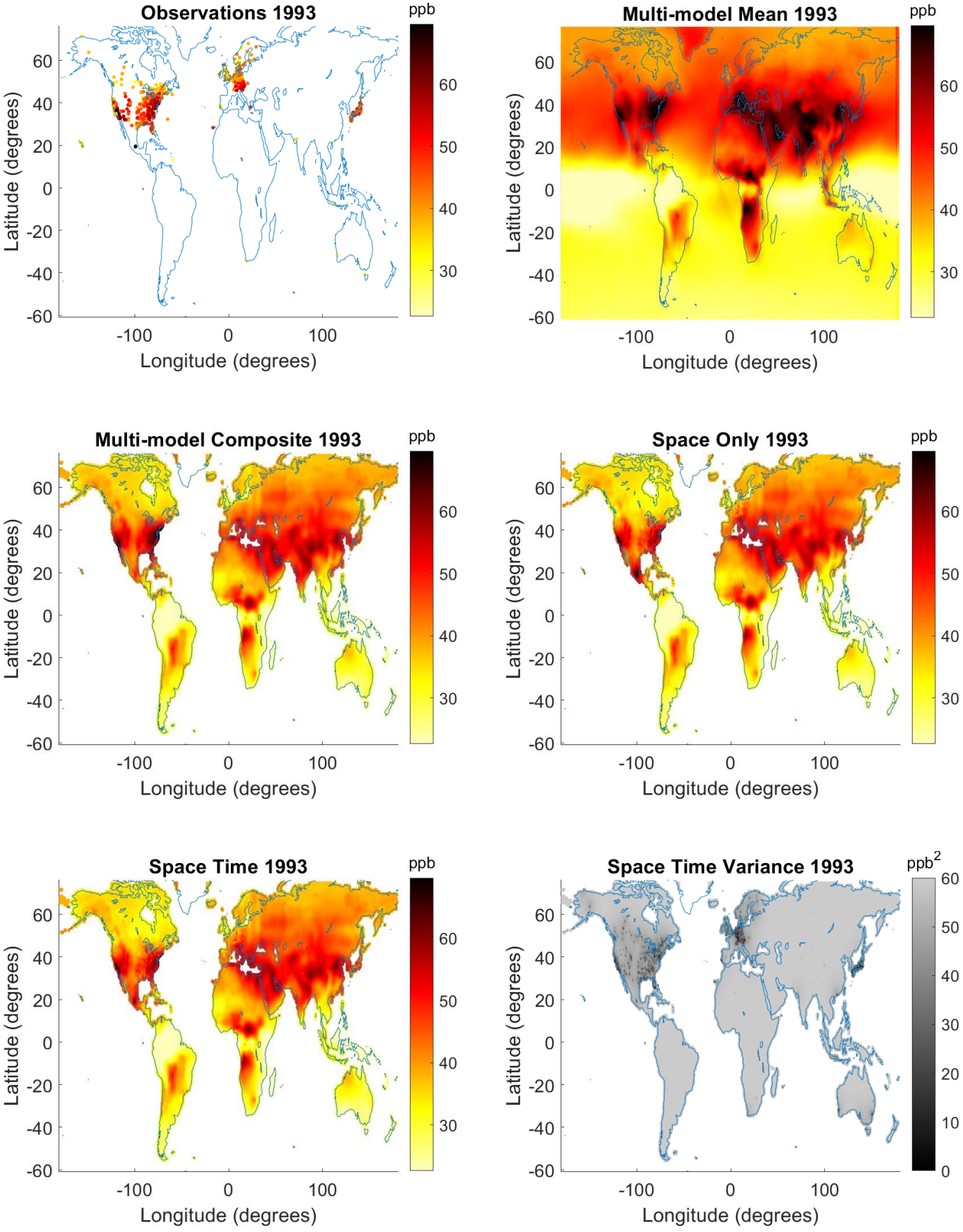

Figure S7: (continued)

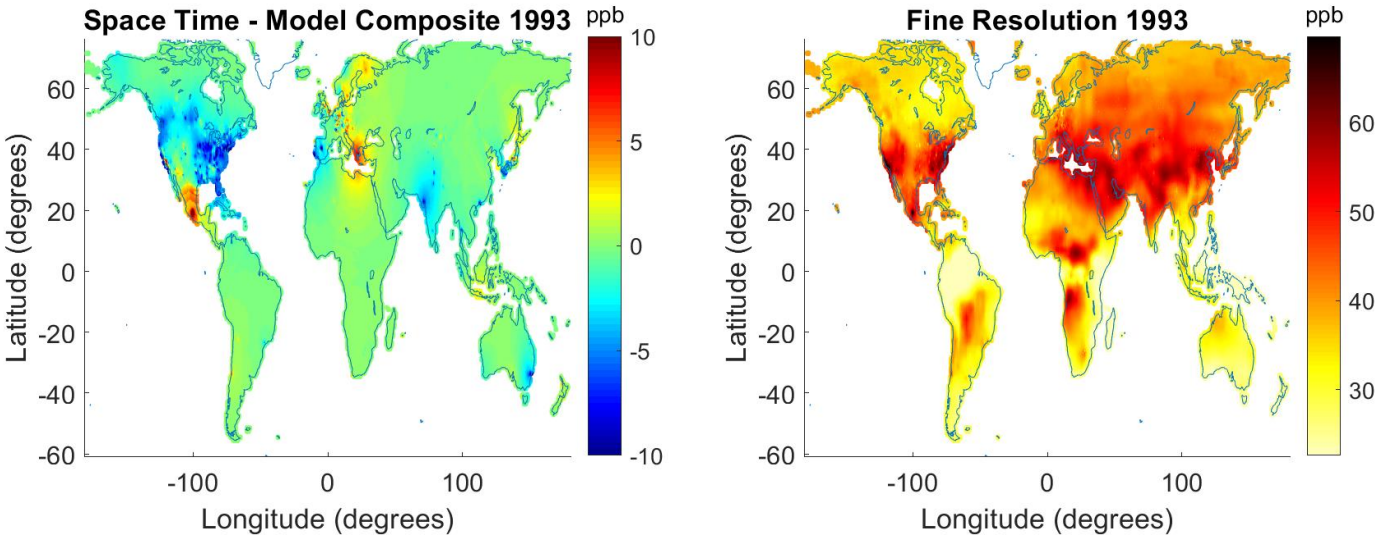

Figure S8: Yearly Maps for 1994

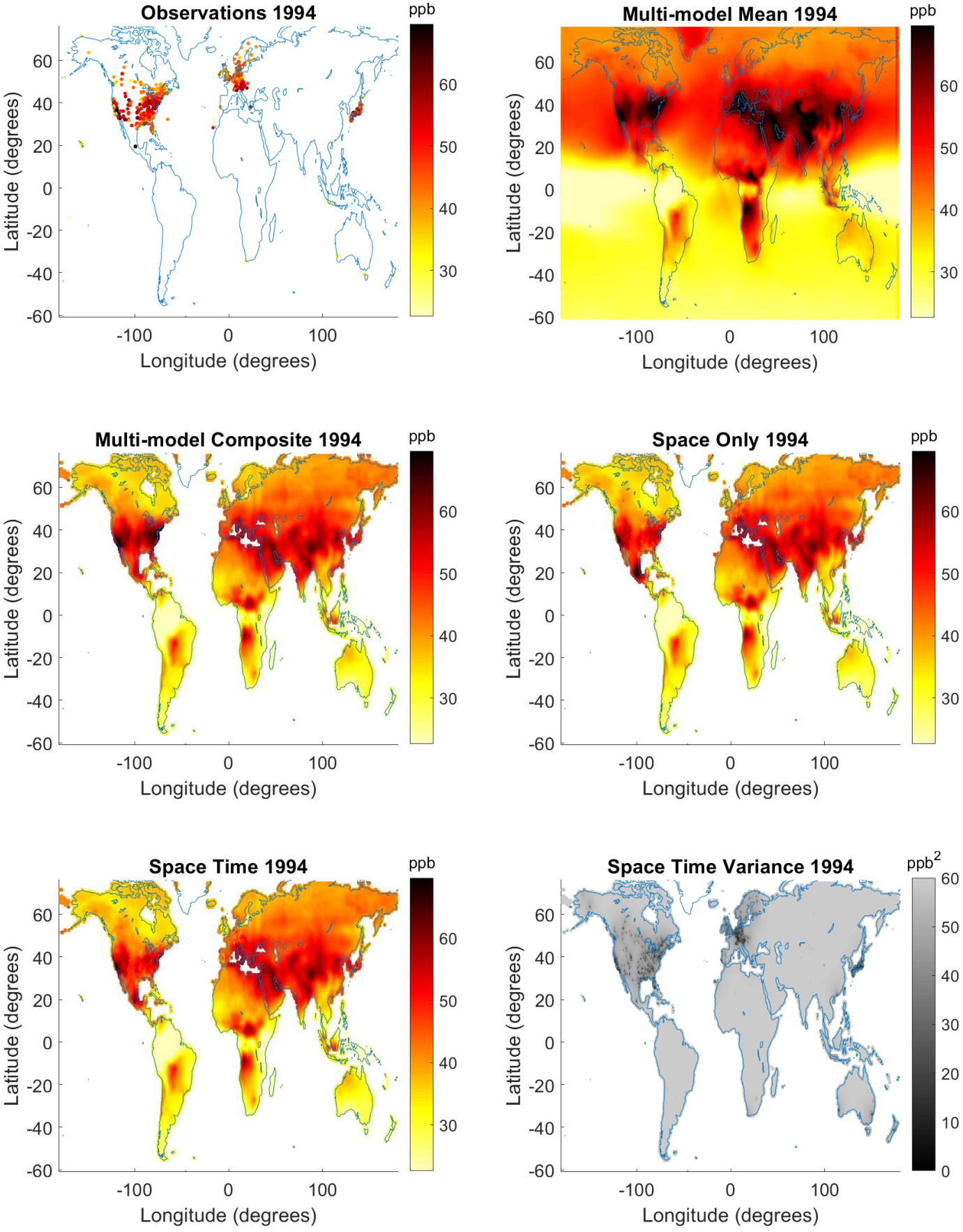

Figure S8: (continued)

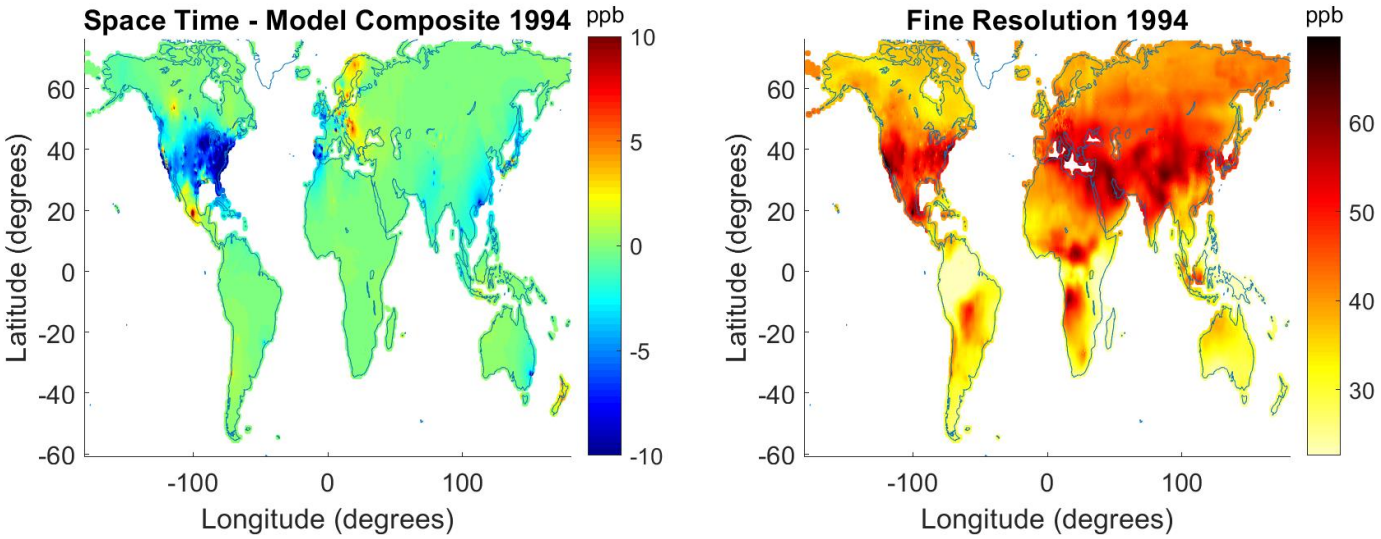

Figure S9: Yearly Maps for 1995

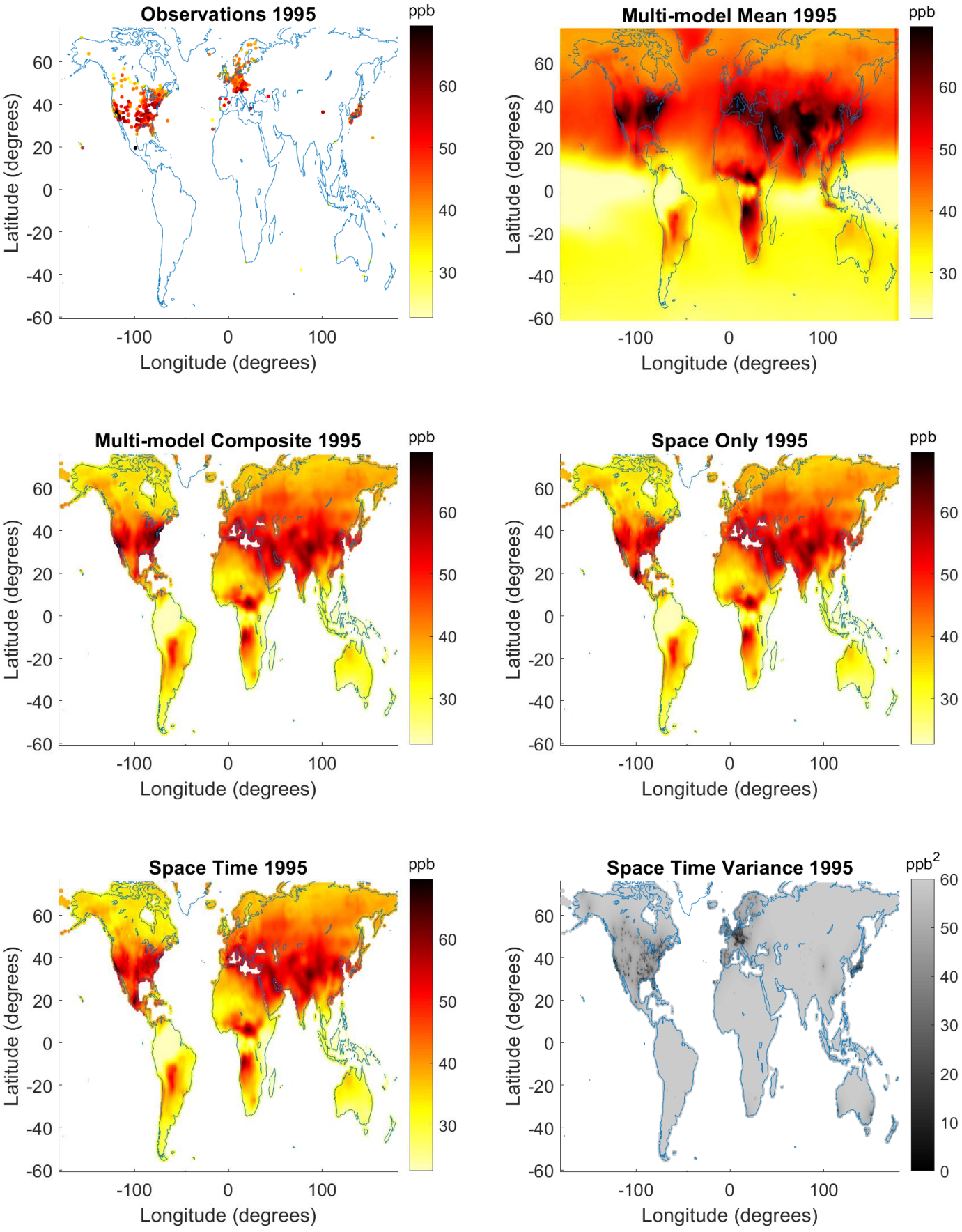

Figure S9: (continued)

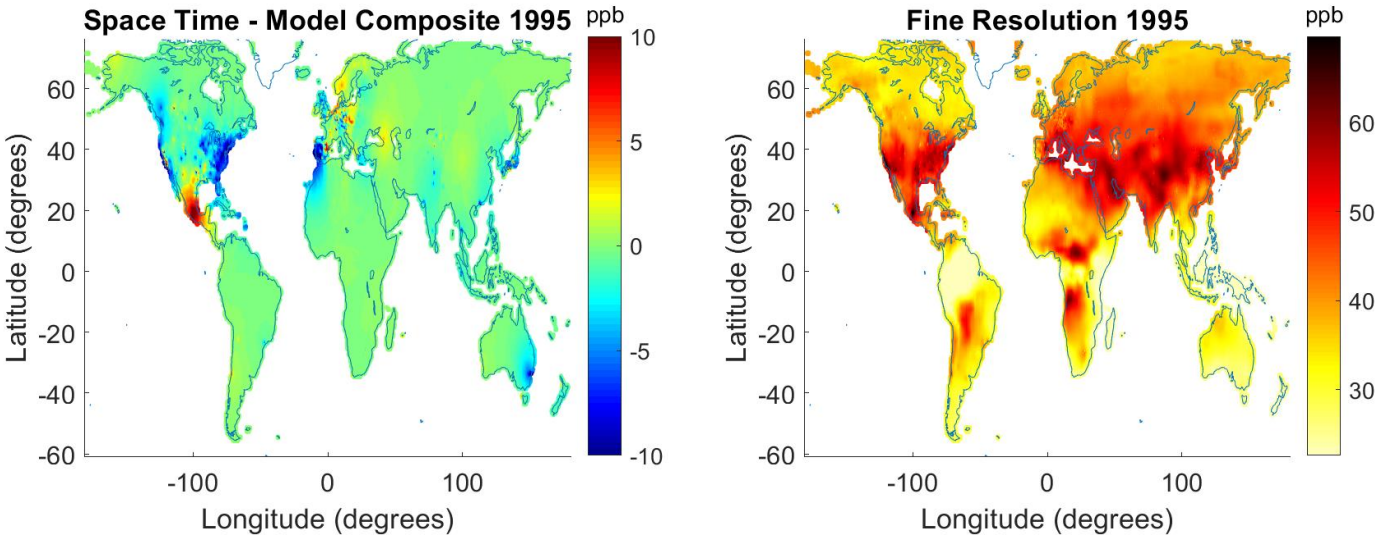

Figure S10: Yearly Maps for 1996

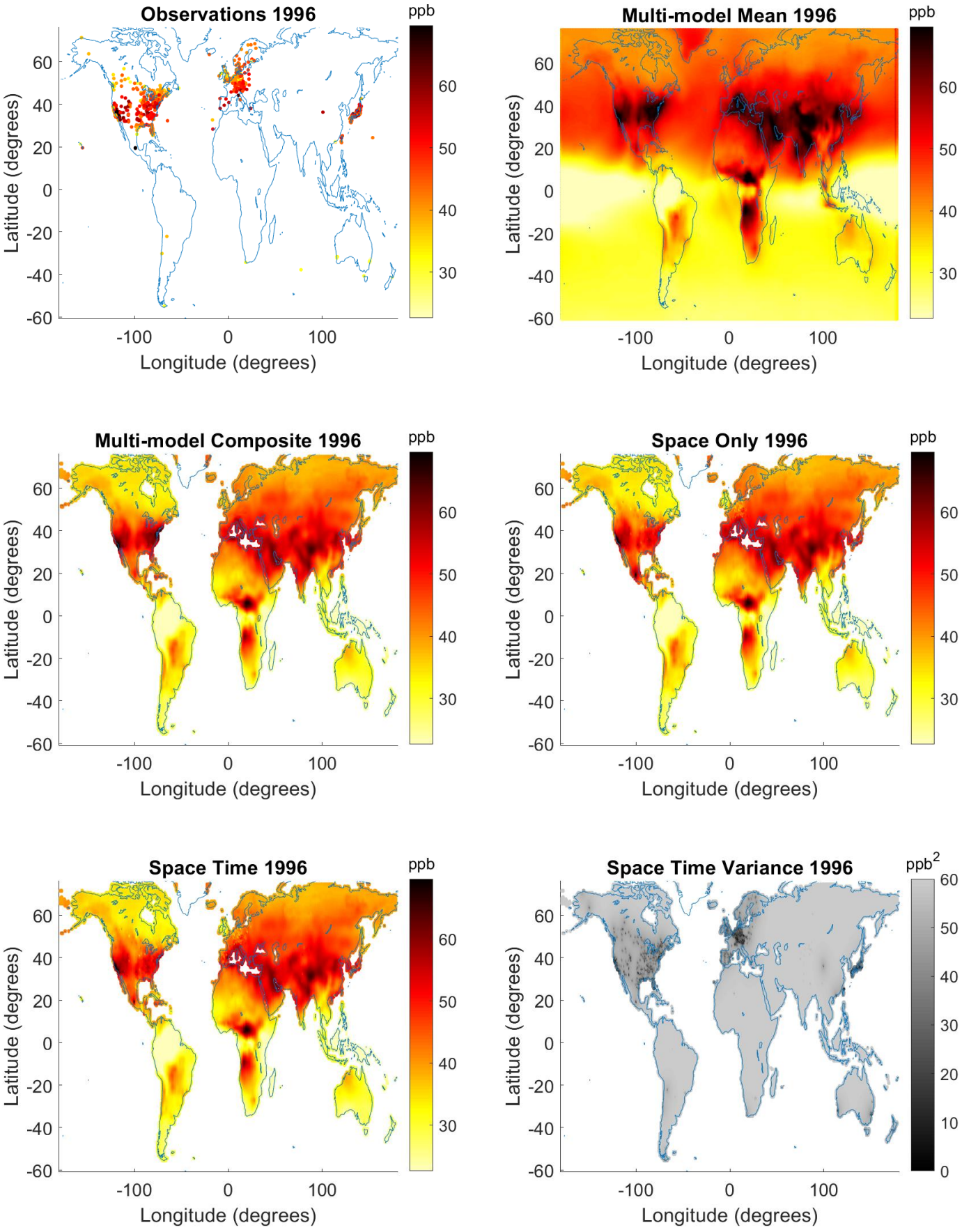

Figure S10: (continued)

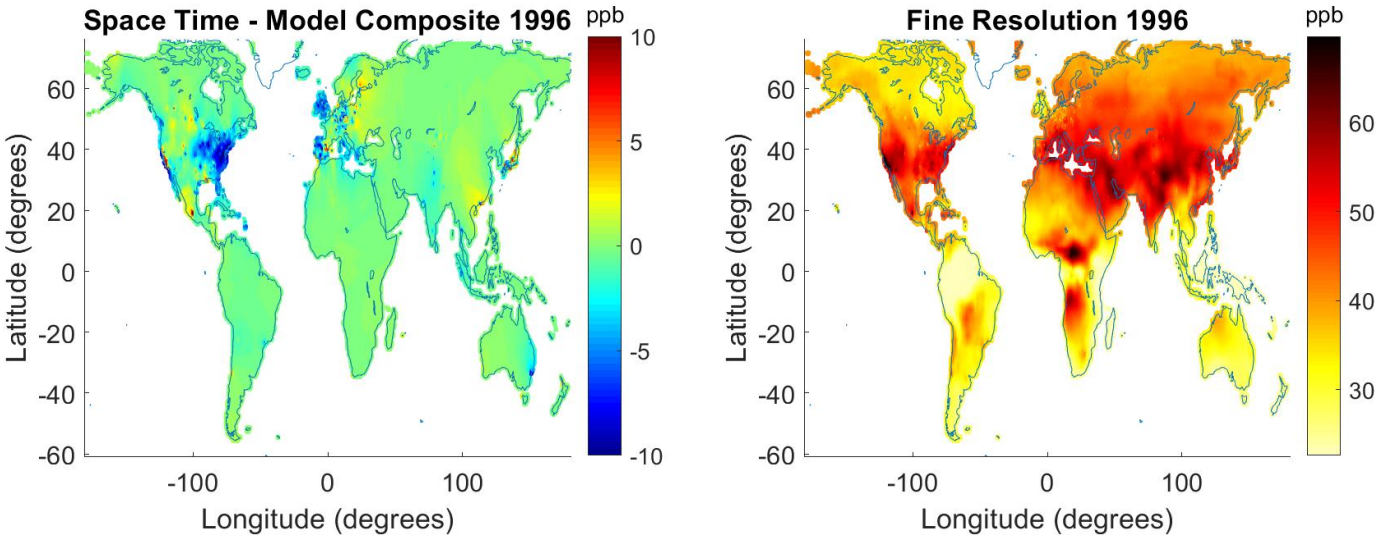

Figure S11: Yearly Maps for 1997

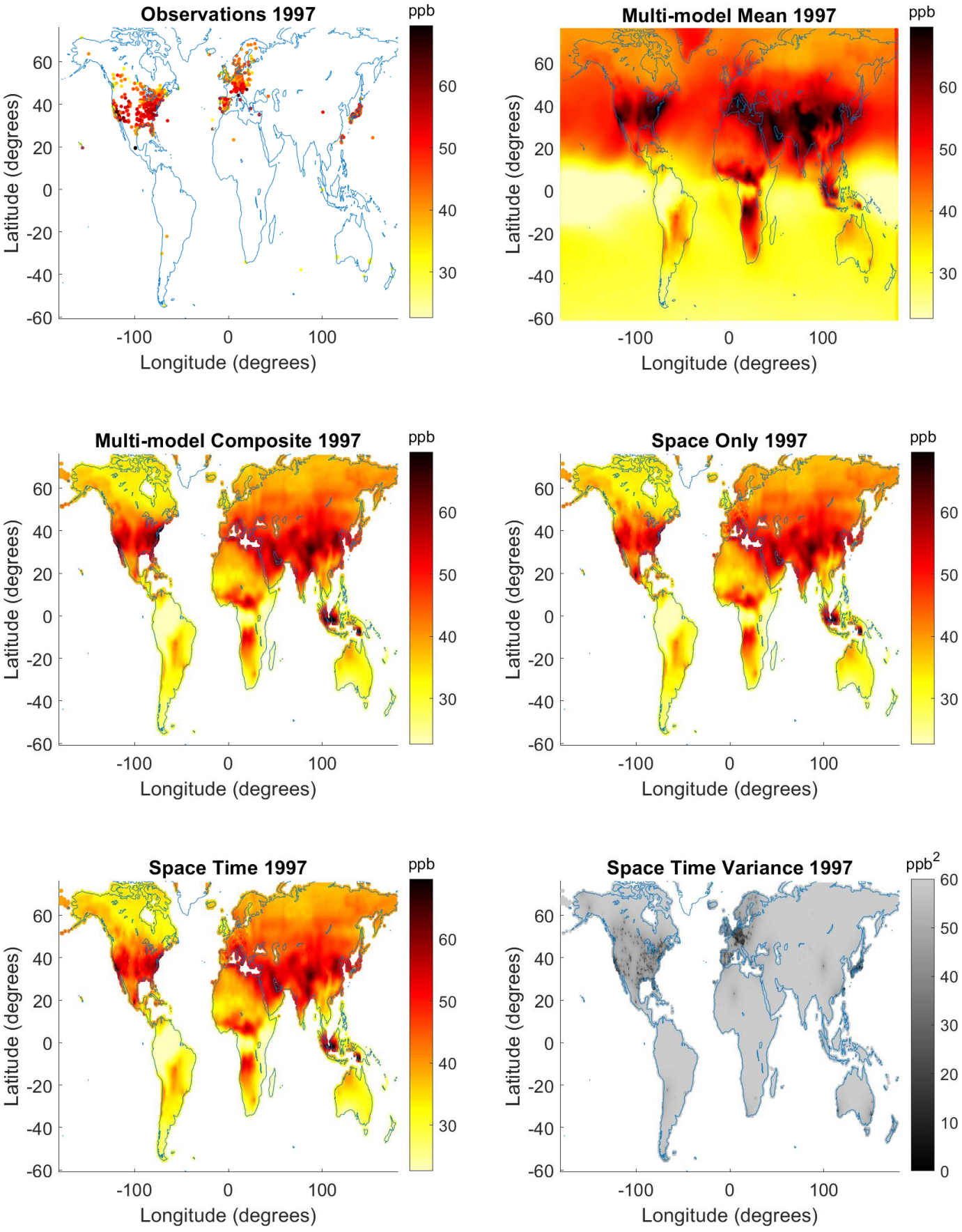

Figure S11: (continued)

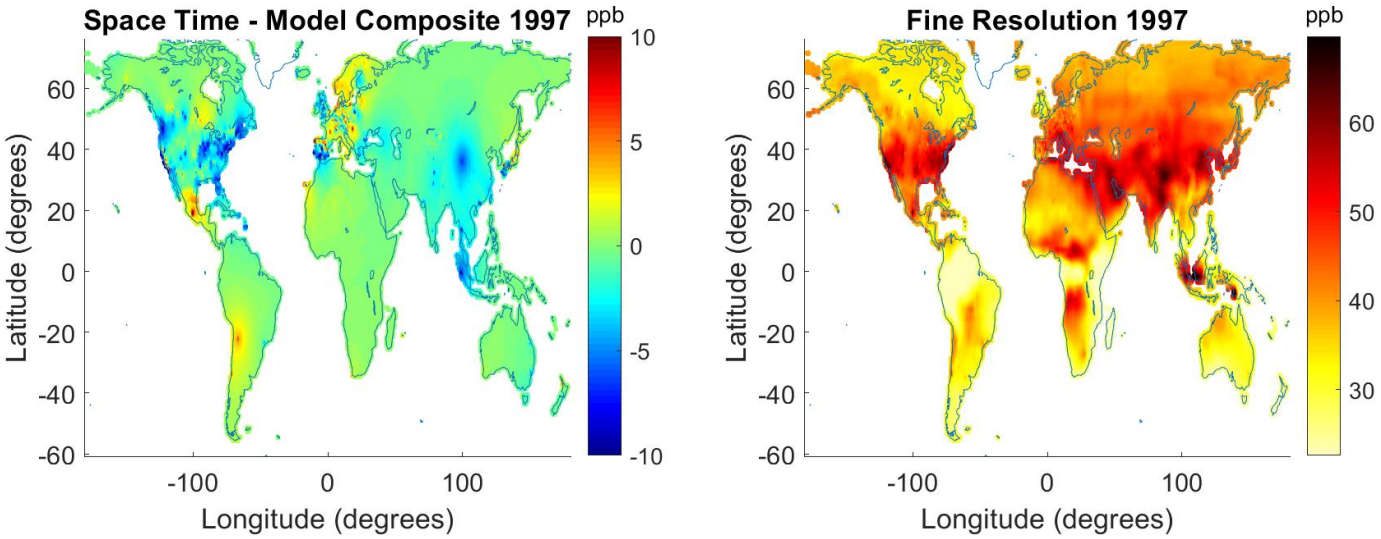

Figure S12: Yearly Maps for 1998

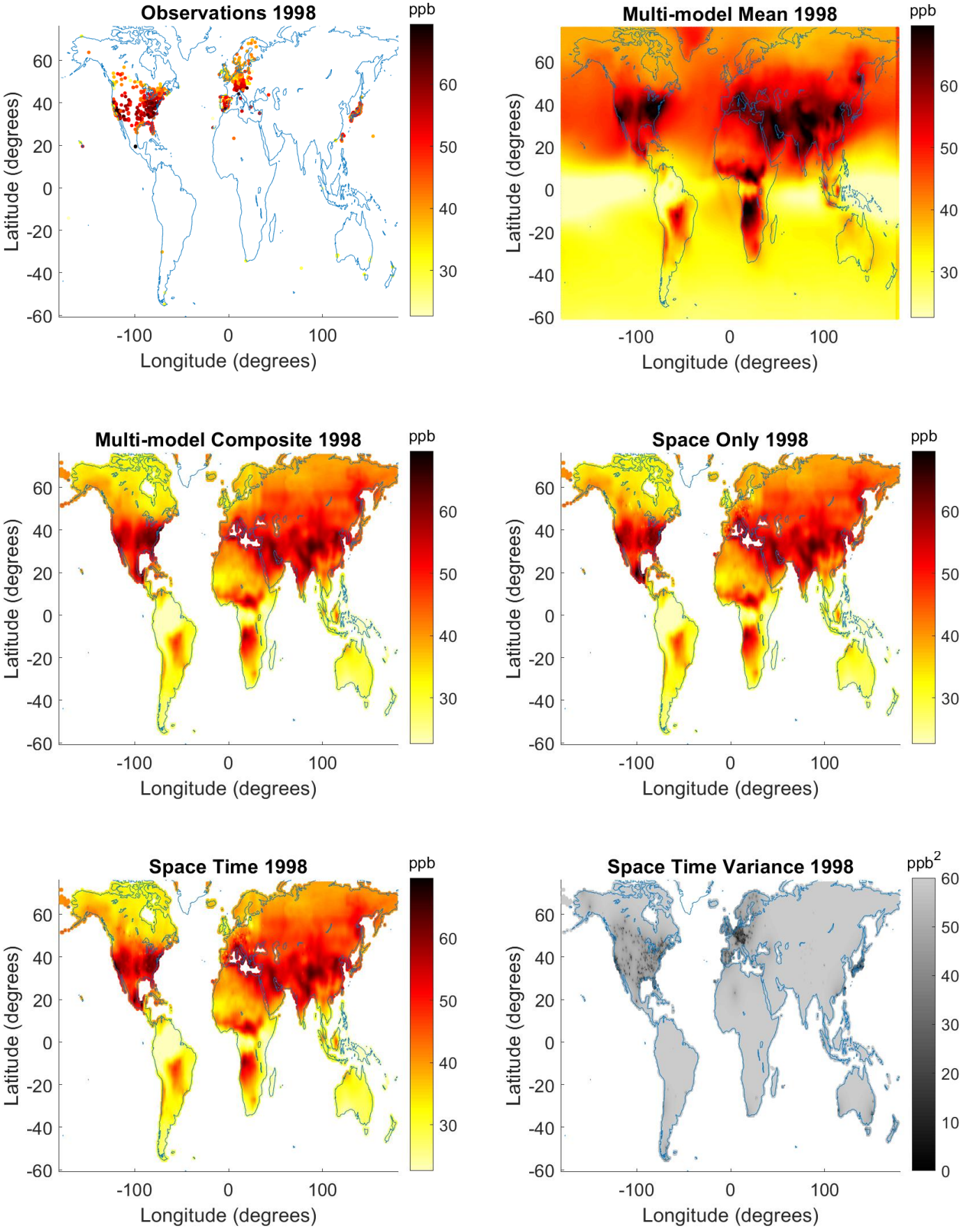

Figure S12: (continued)

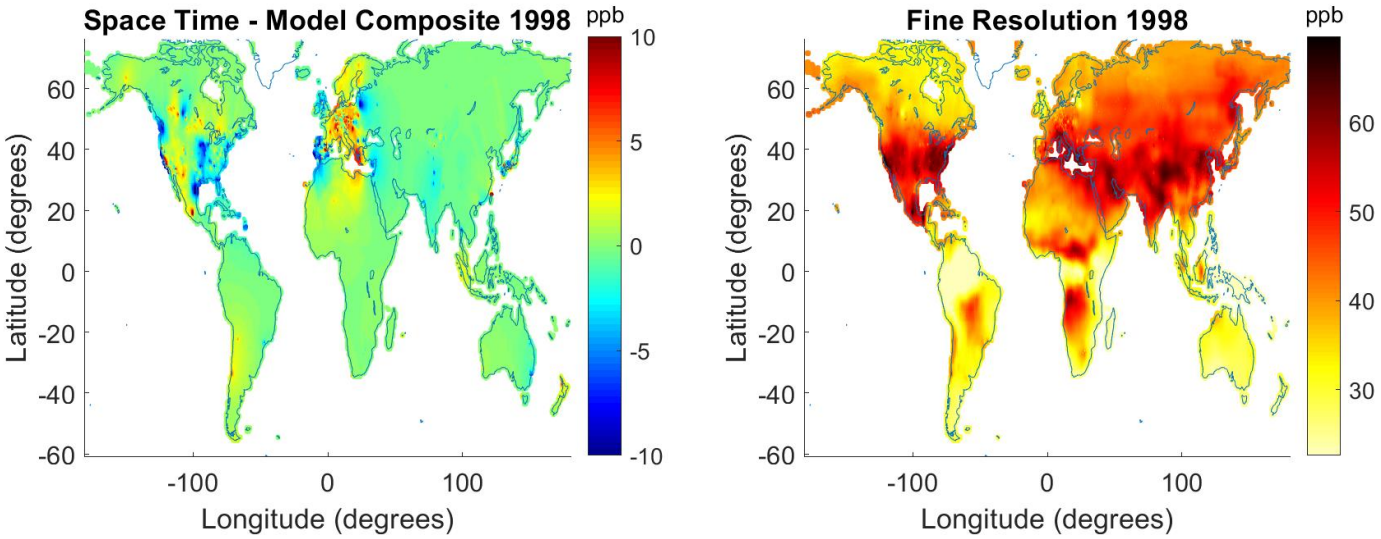

Figure S13: Yearly Maps for 1999

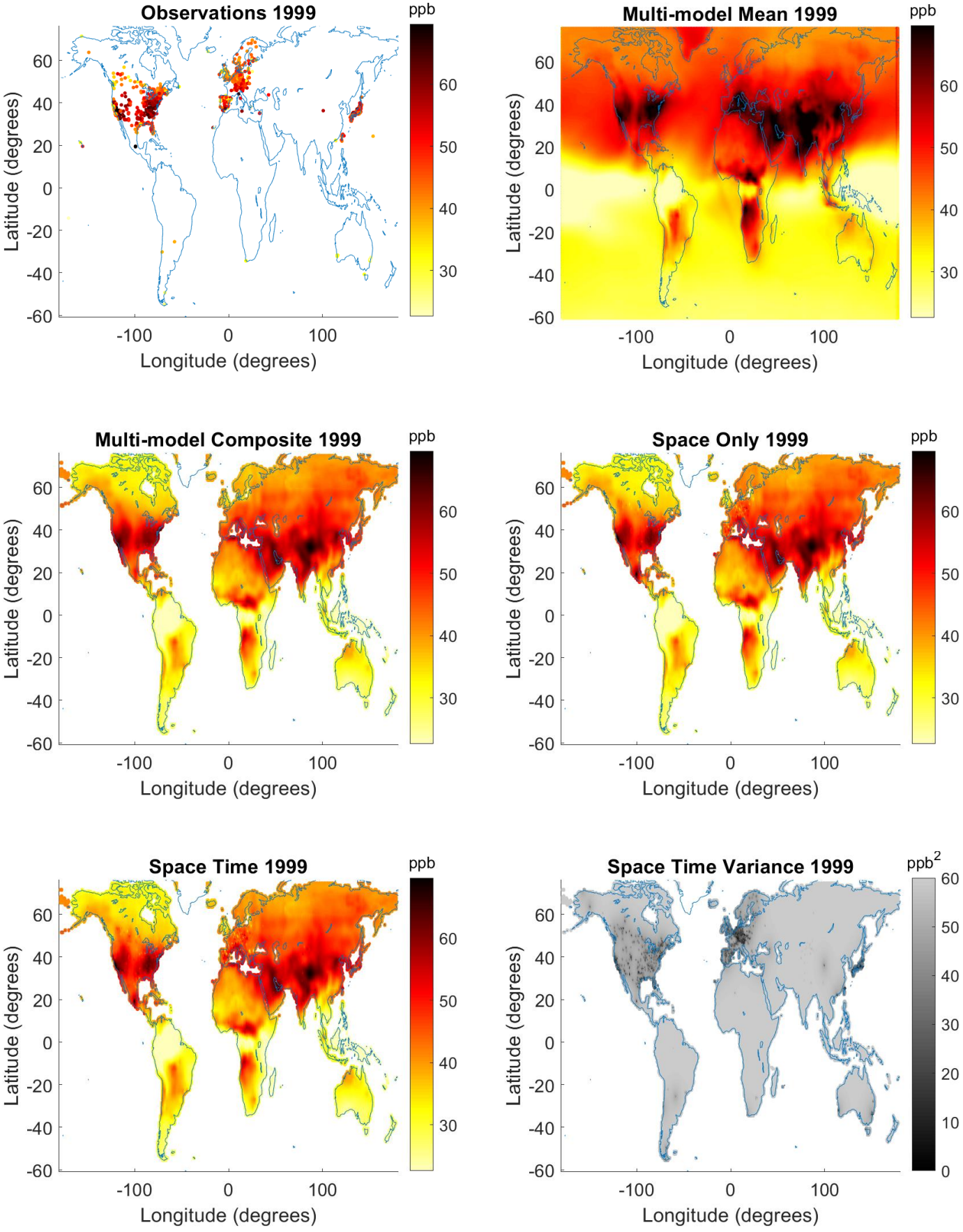

Figure S13: (continued)

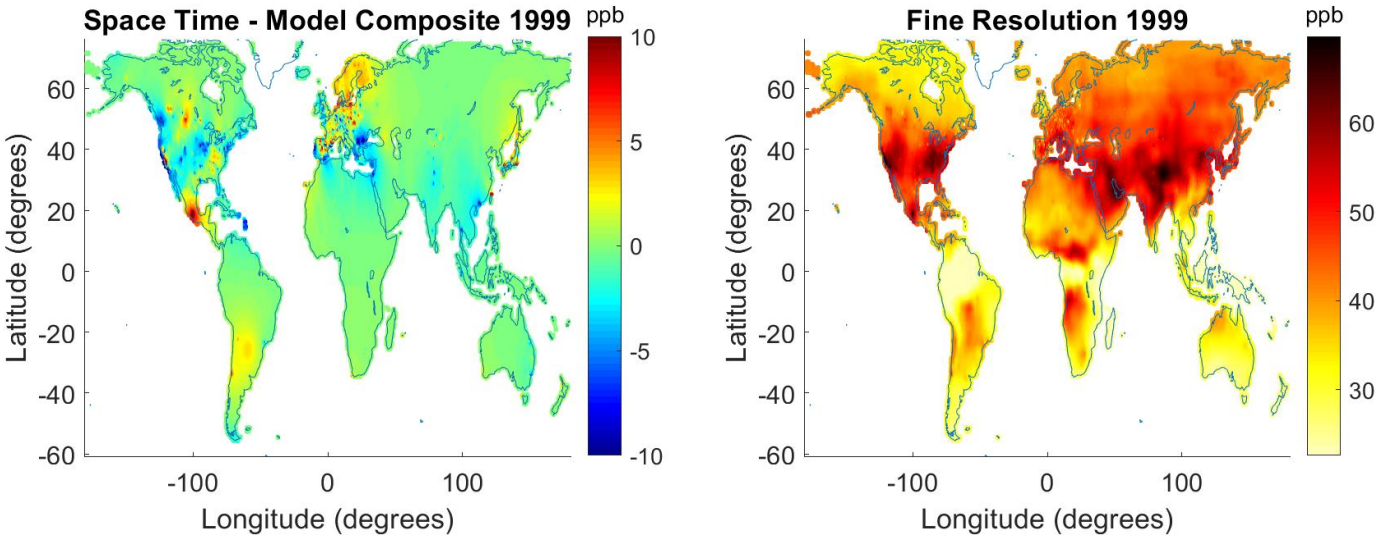

Figure S14: Yearly Maps for 2000

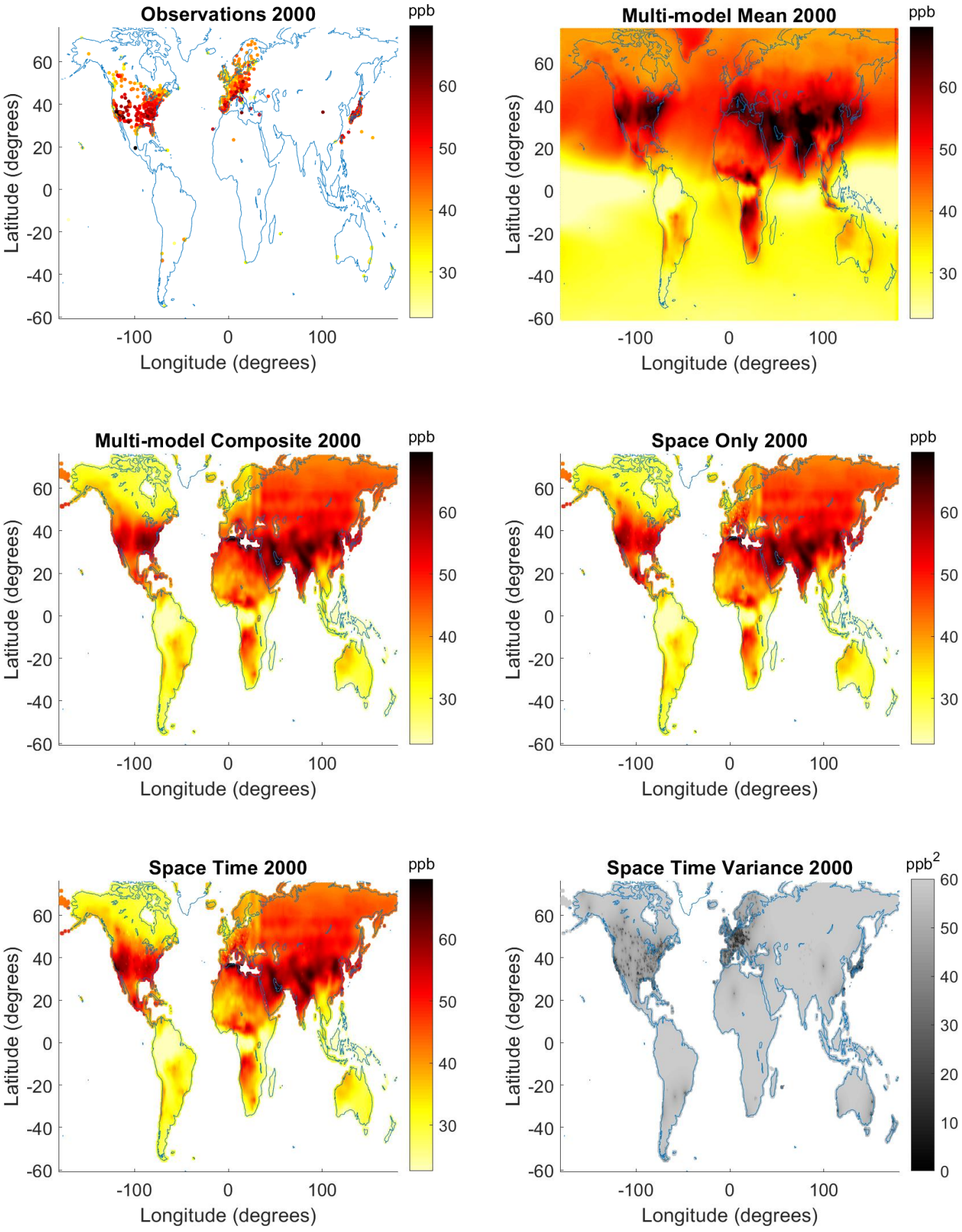

Figure S14: (continued)

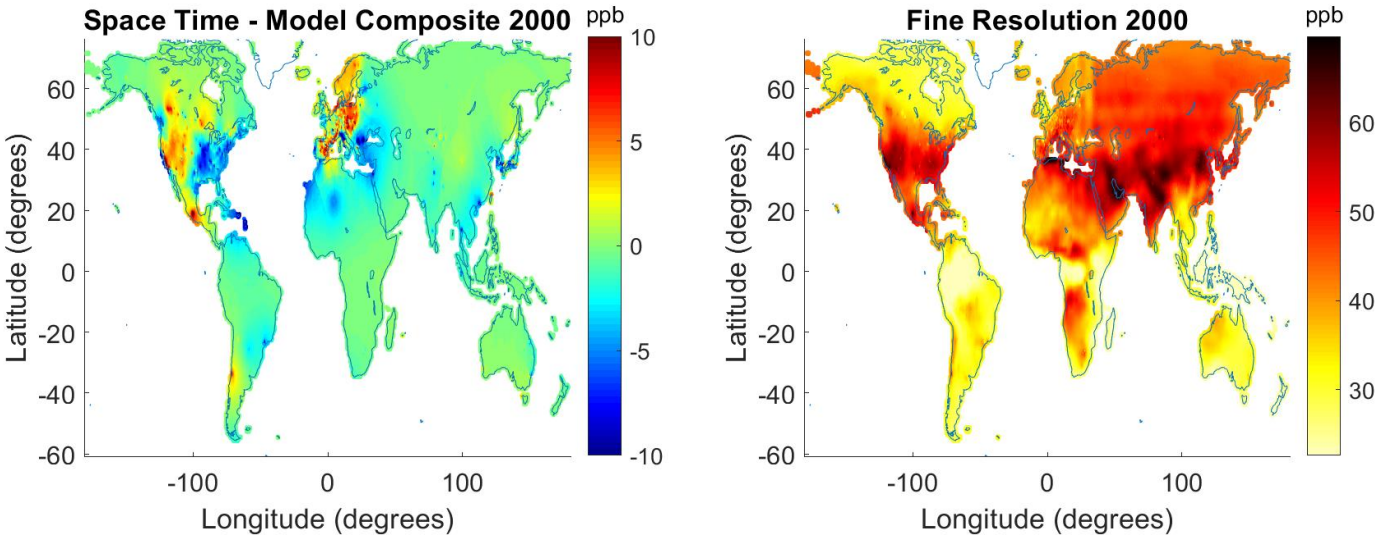

Figure S15: Yearly Maps for 2001

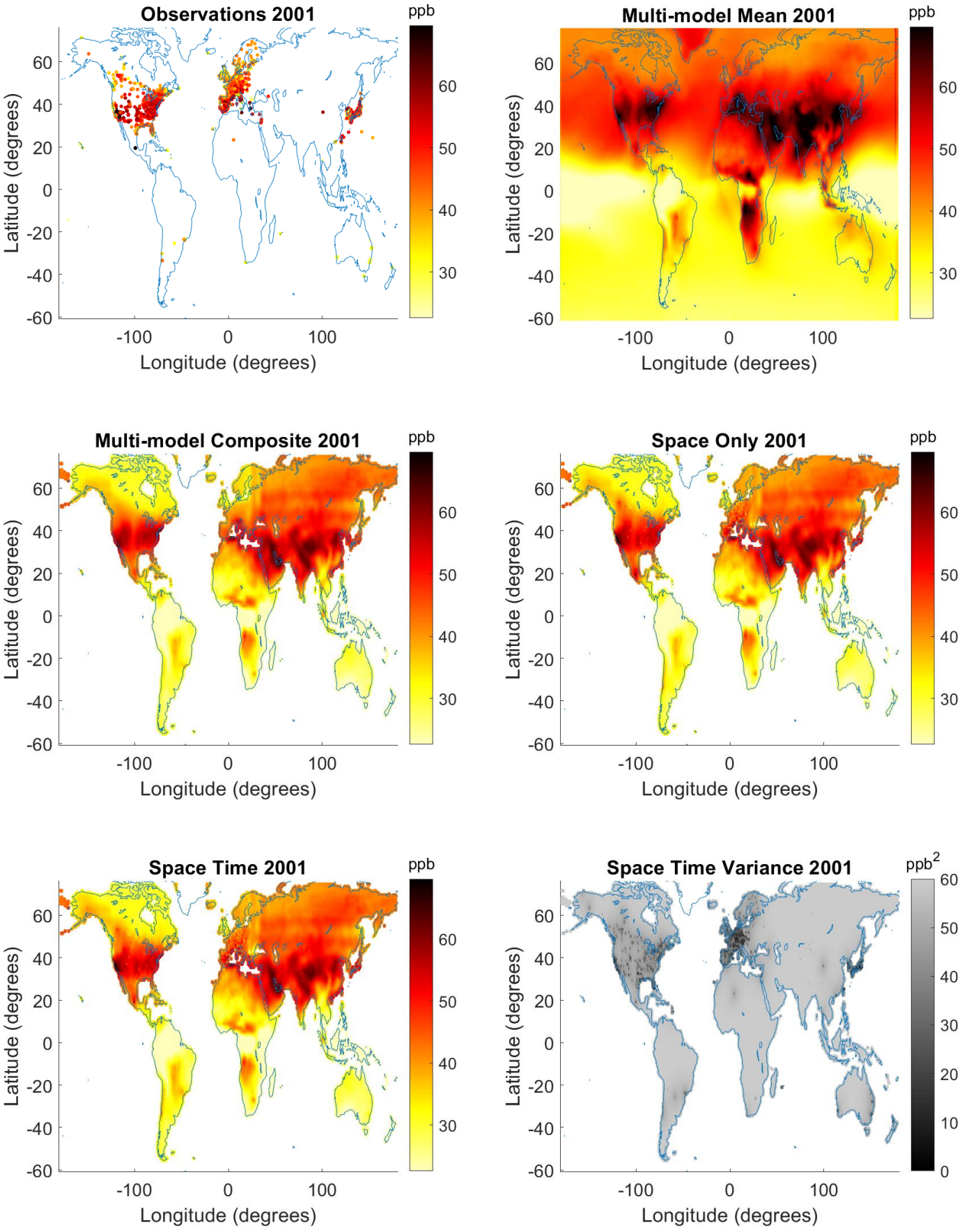

Figure S15: (continued)

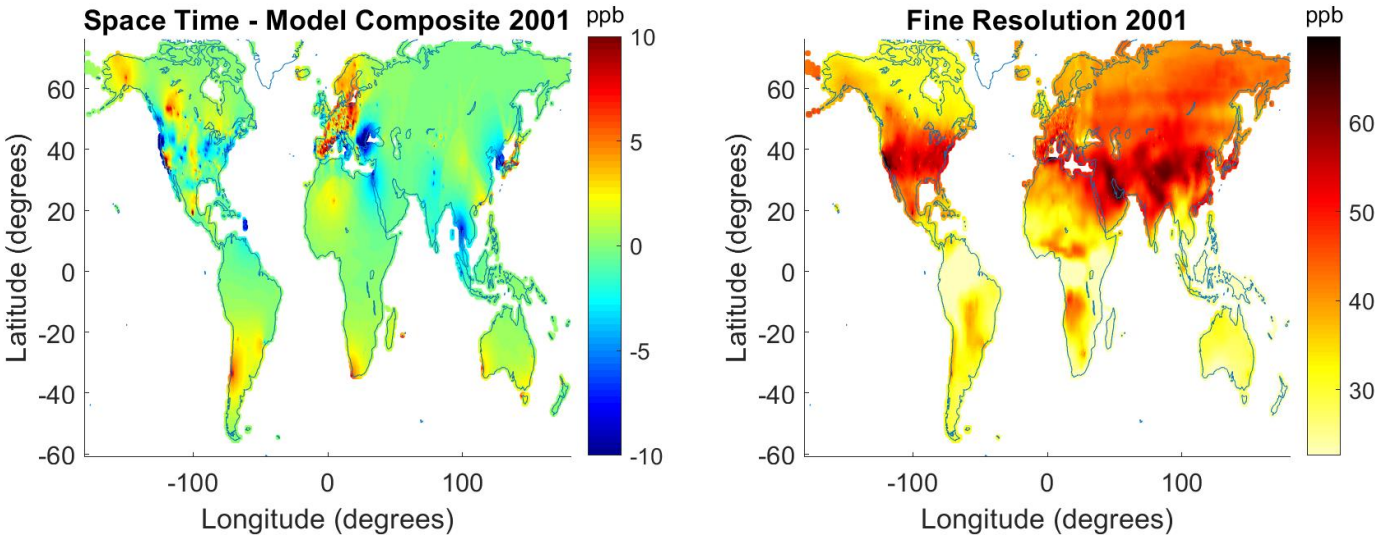

Figure S16: Yearly Maps for 2002

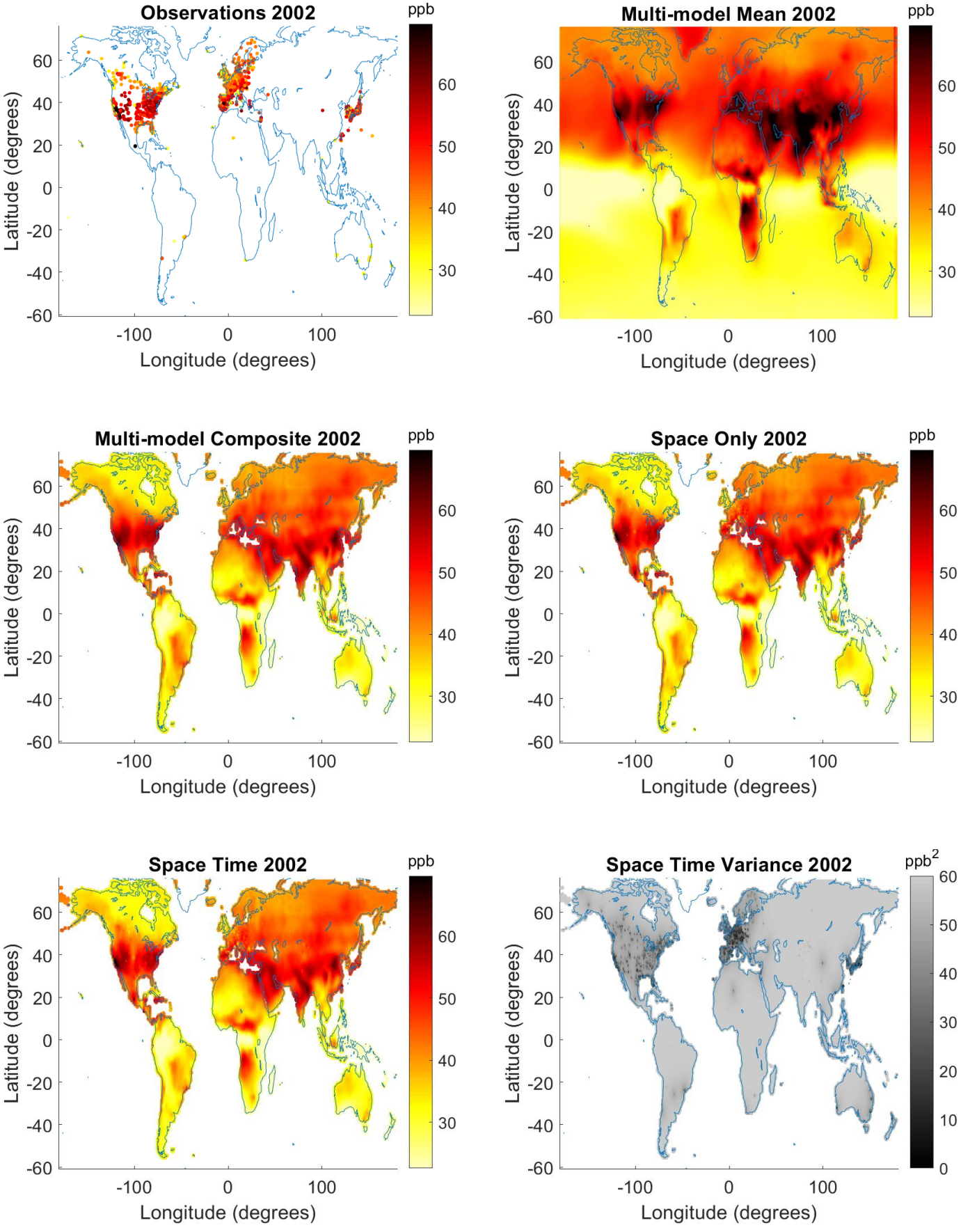

Figure S16: (continued)

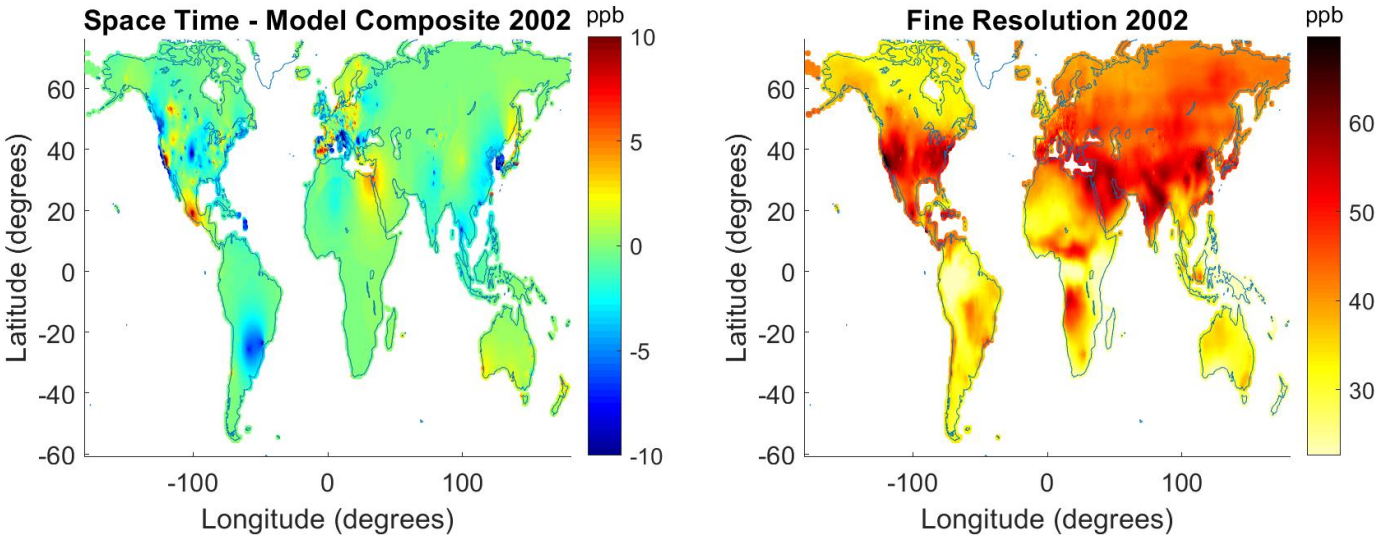

Figure S17: Yearly Maps for 2003

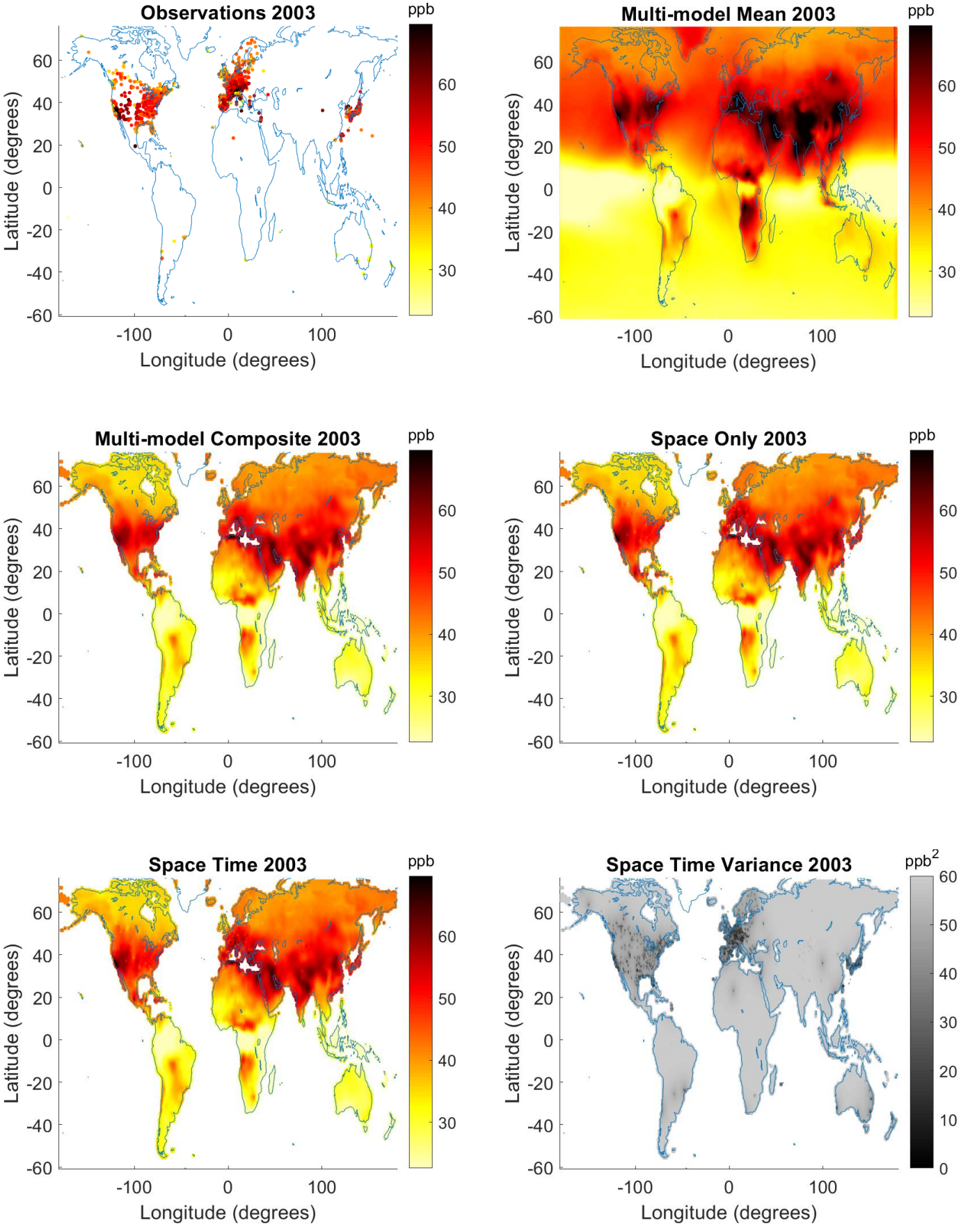

Figure S17: (continued)

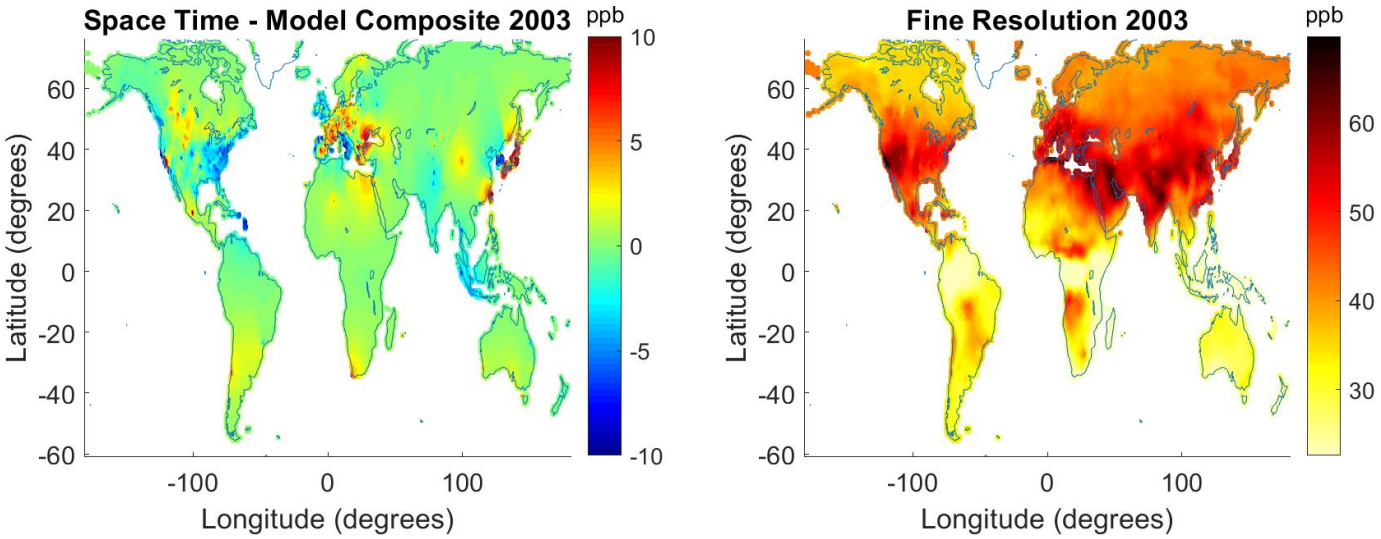

Figure S18: Yearly Maps for 2004

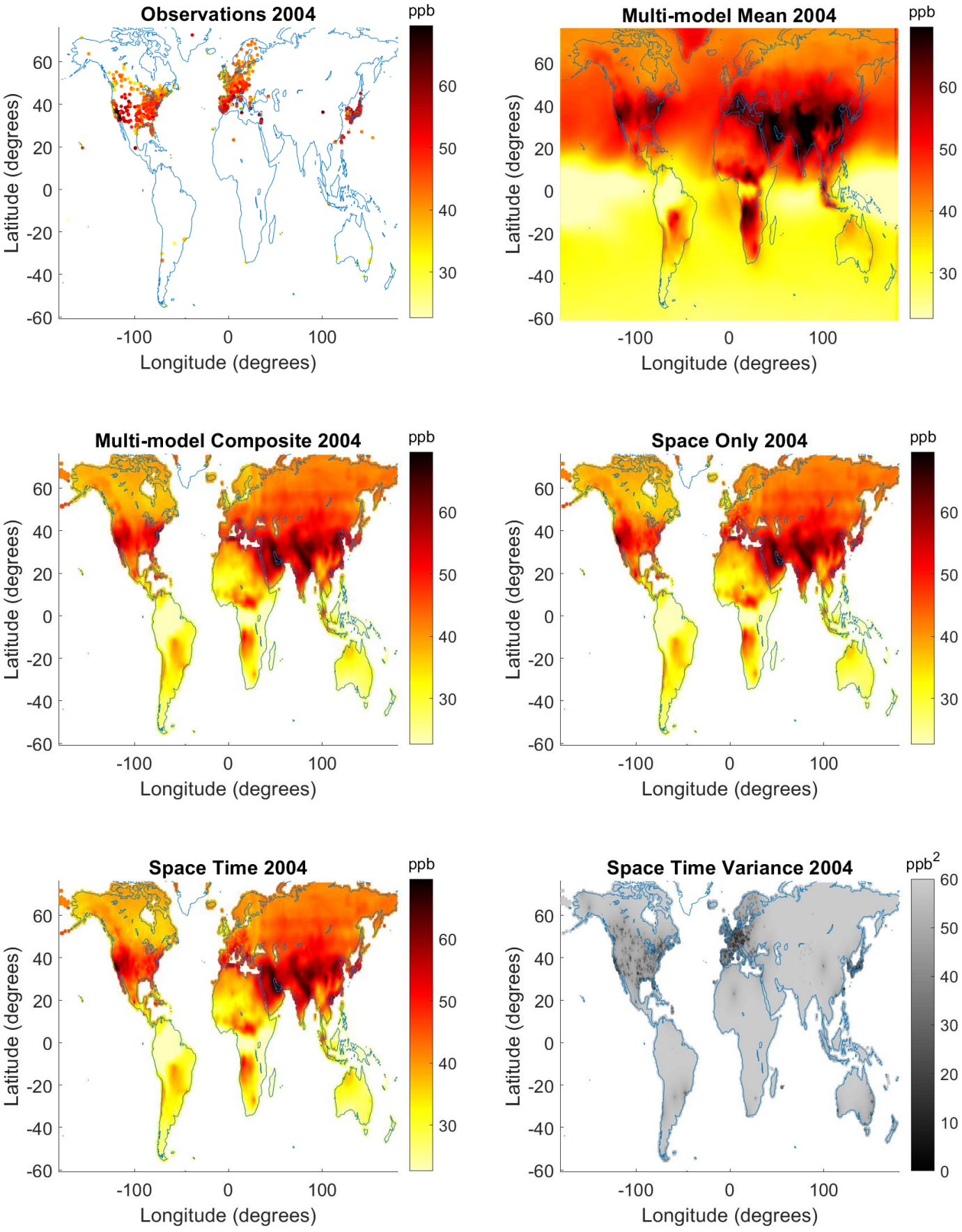

Figure S18: (continued)

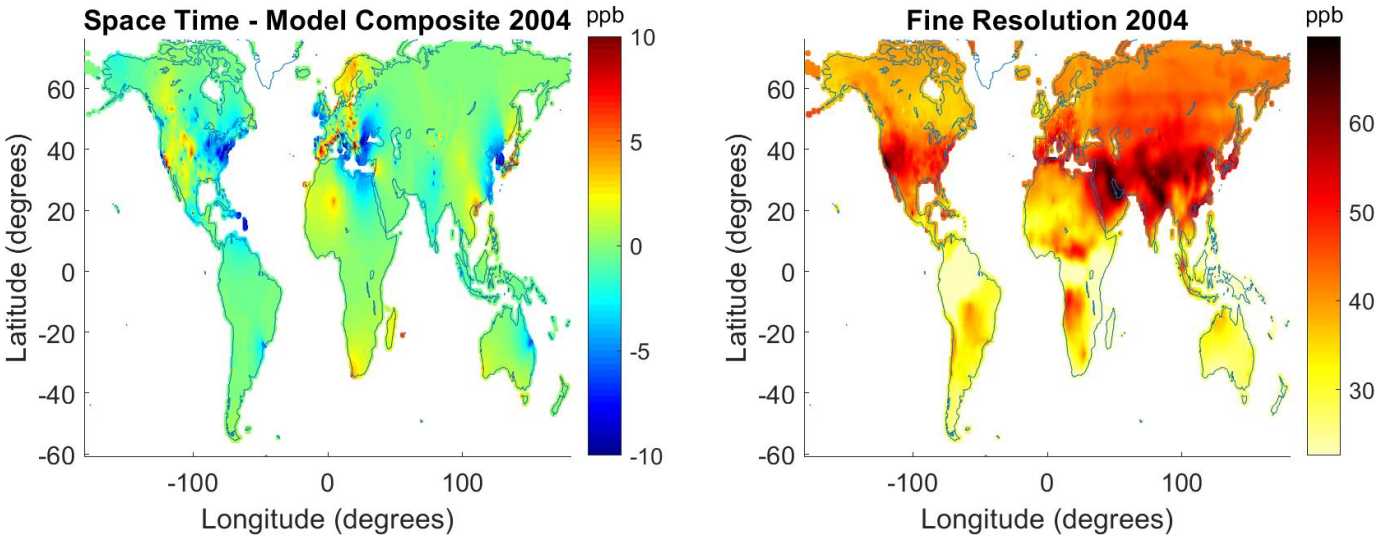

Figure S19: Yearly Maps for 2002

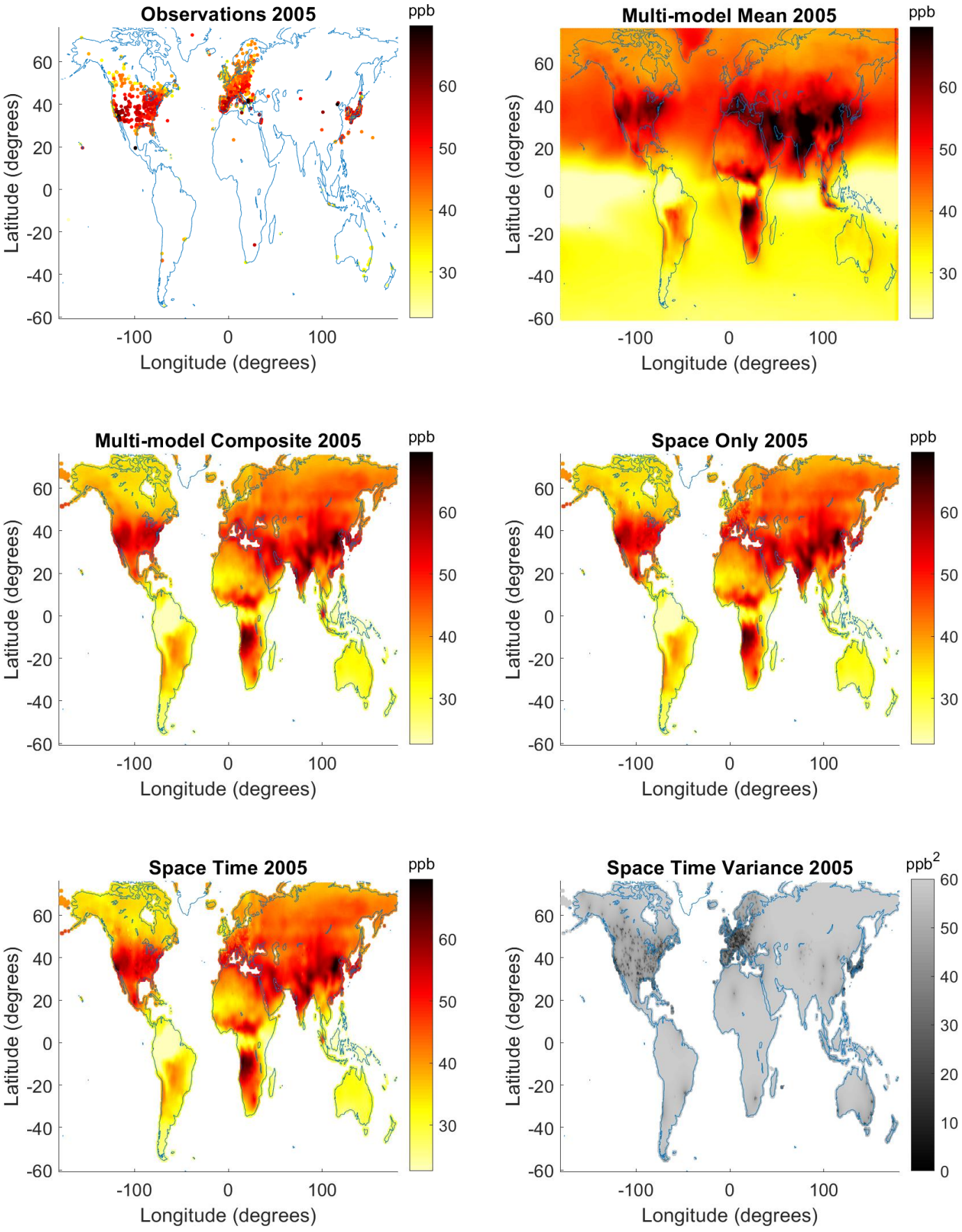

Figure S19: (continued)

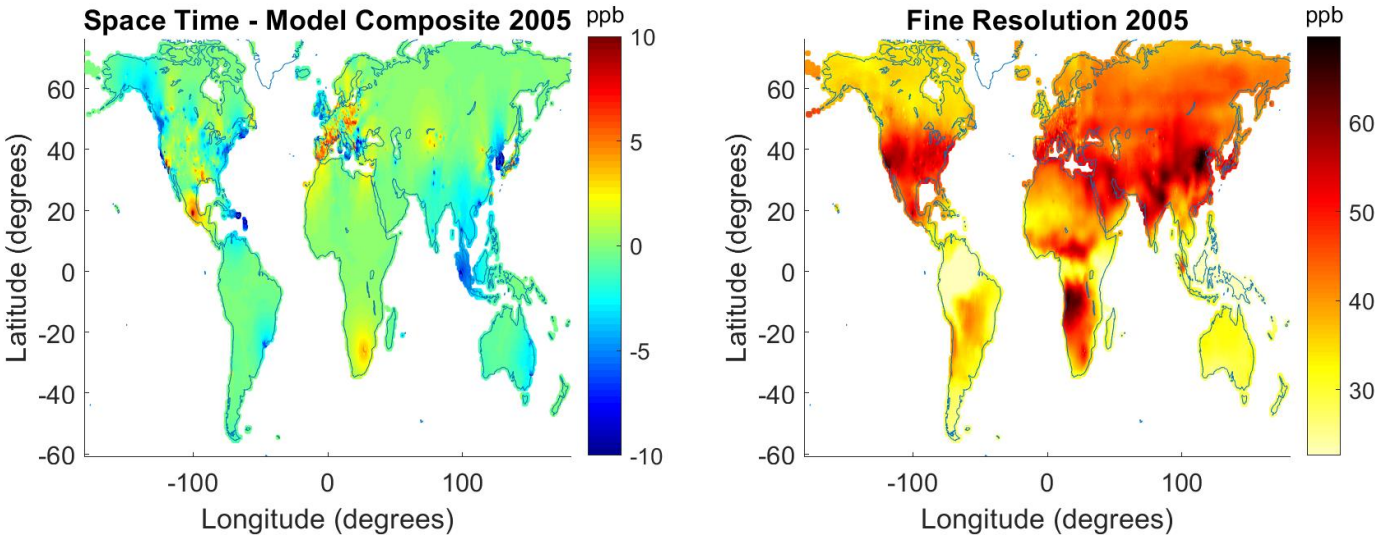

Figure S20: Yearly Maps for 2006

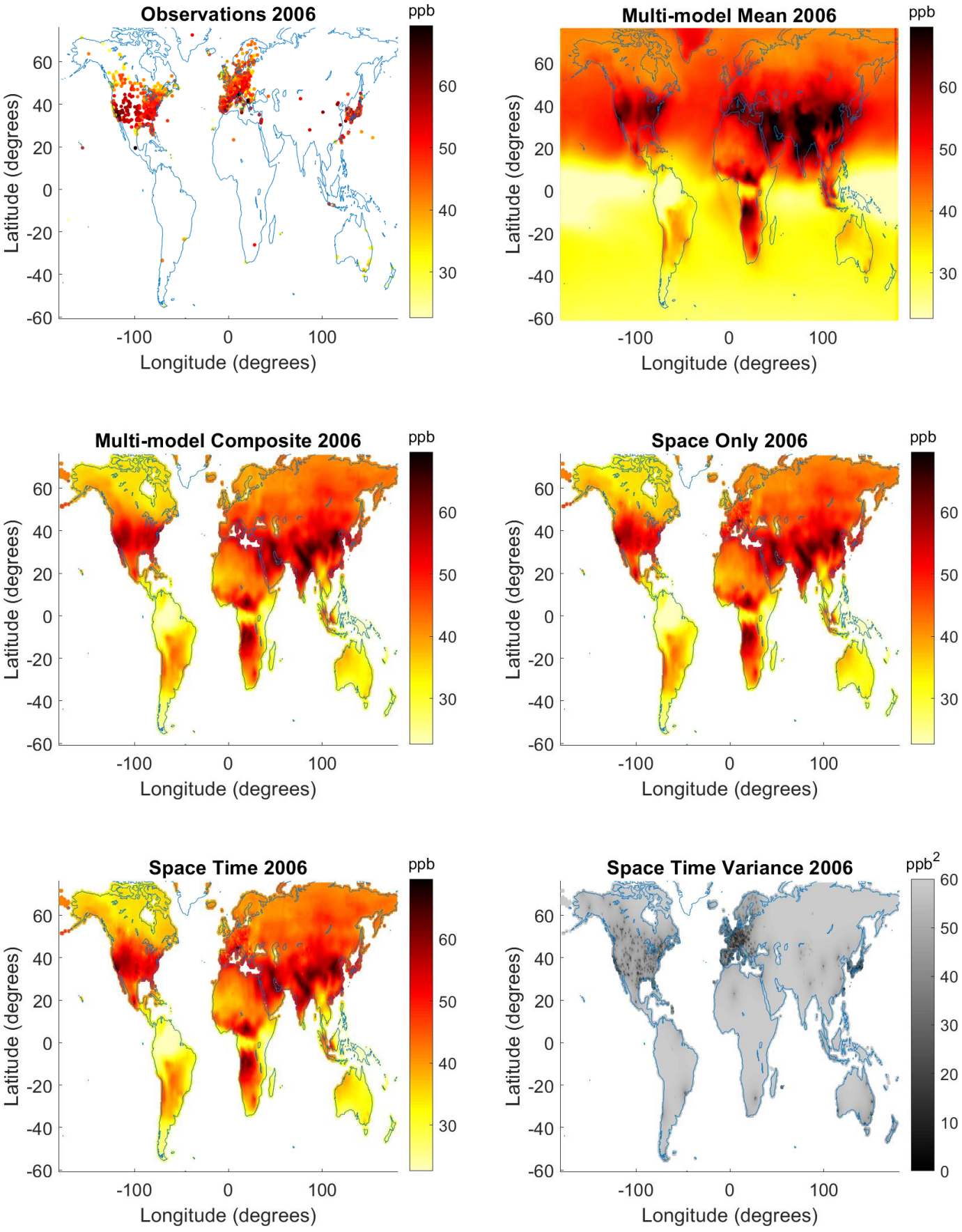

Figure S20: (continued)

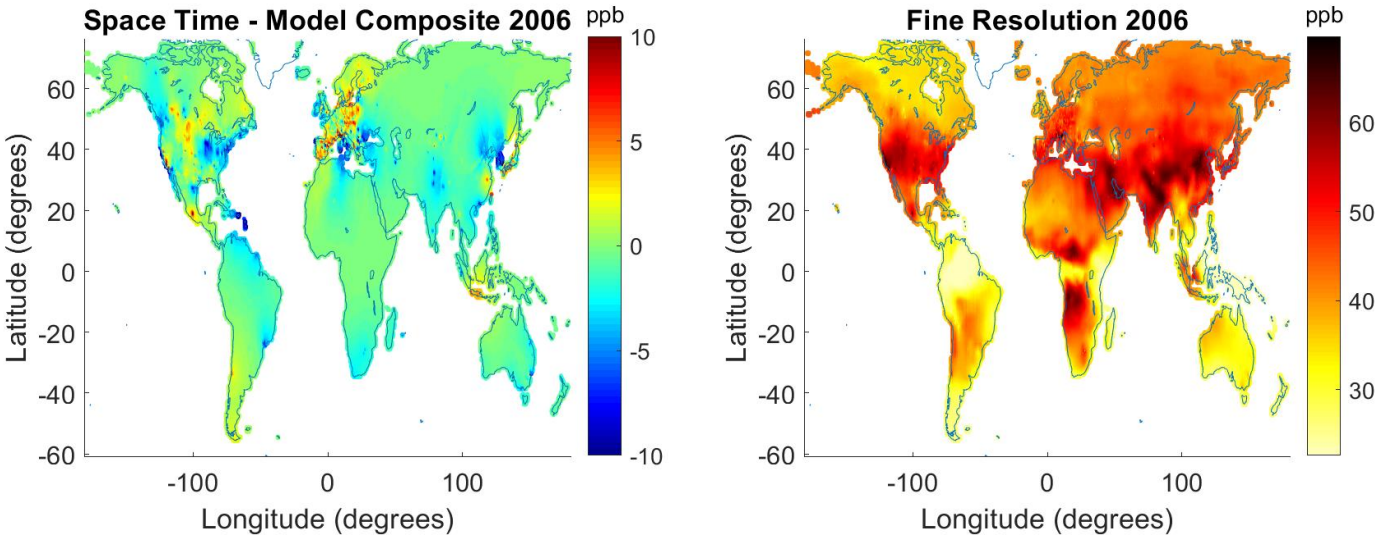

Figure S21: Yearly Maps for 2007

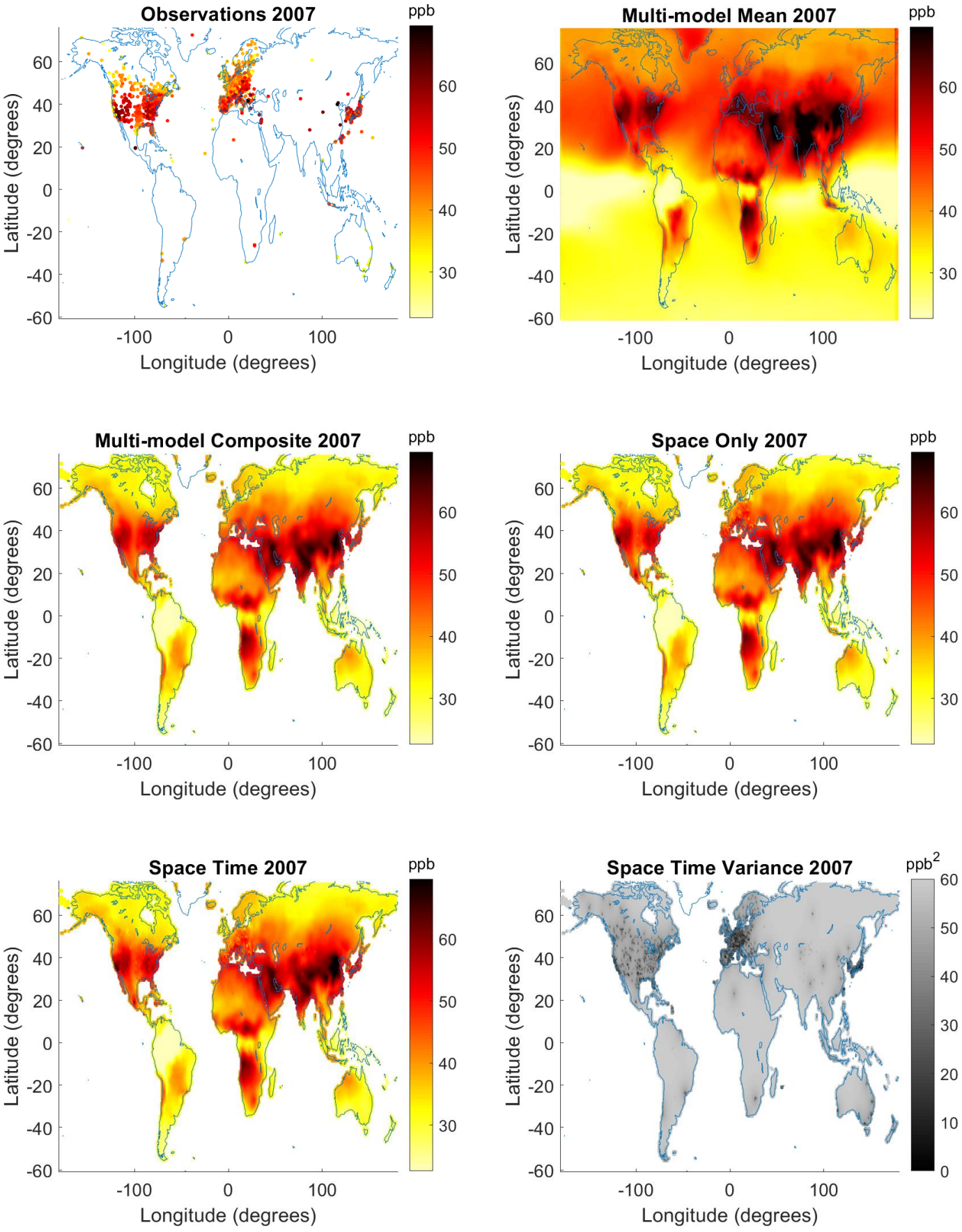

Figure S21: (continued)

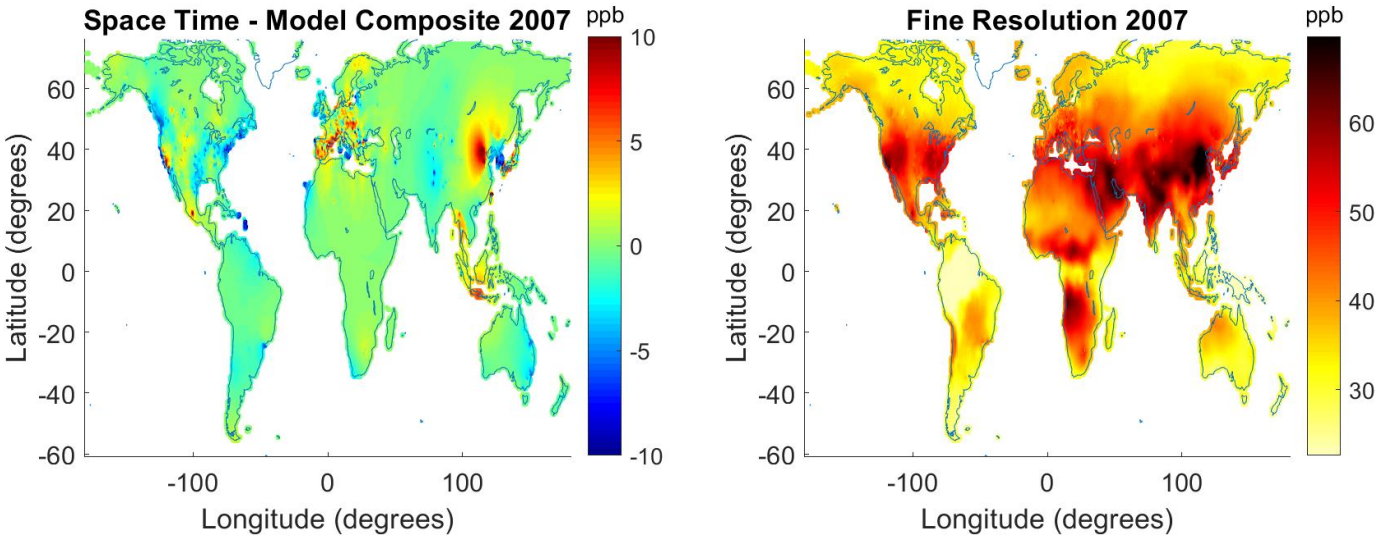

Figure S22: Yearly Maps for 2008

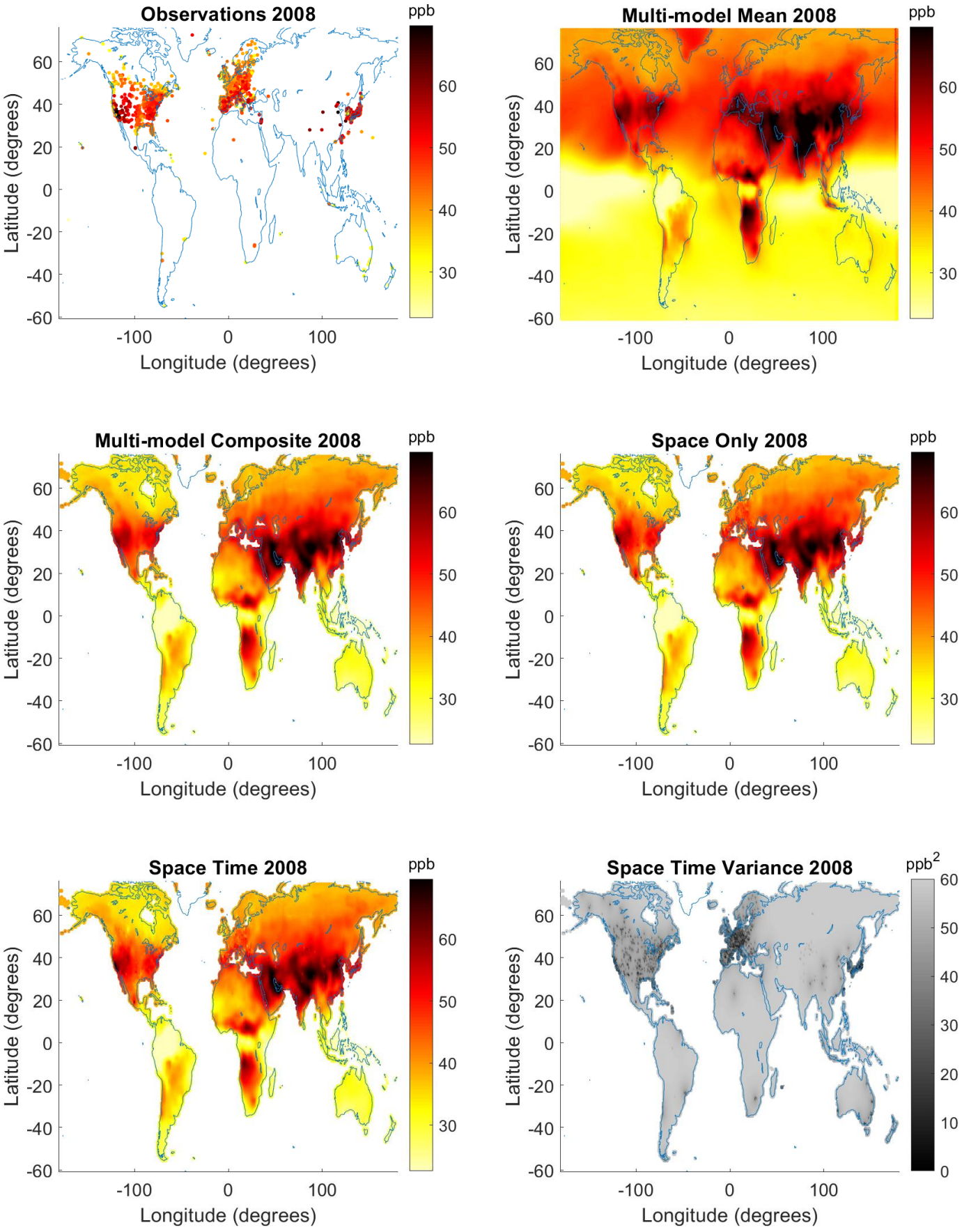

Figure S22: (continued)

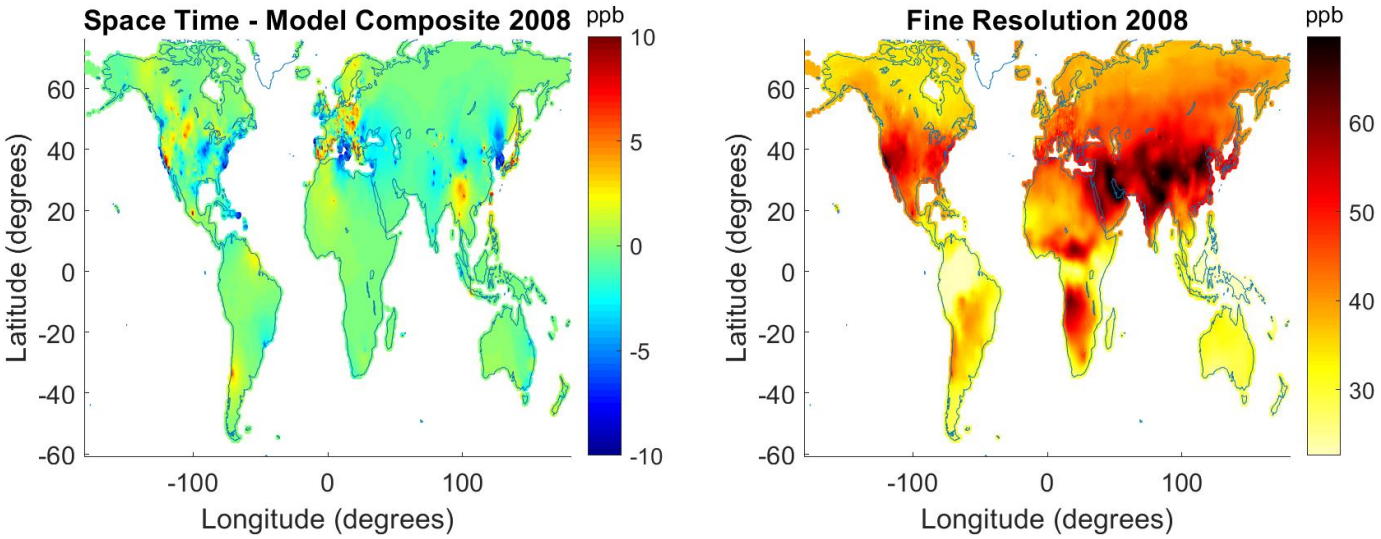

Figure S23: Yearly Maps for 2009

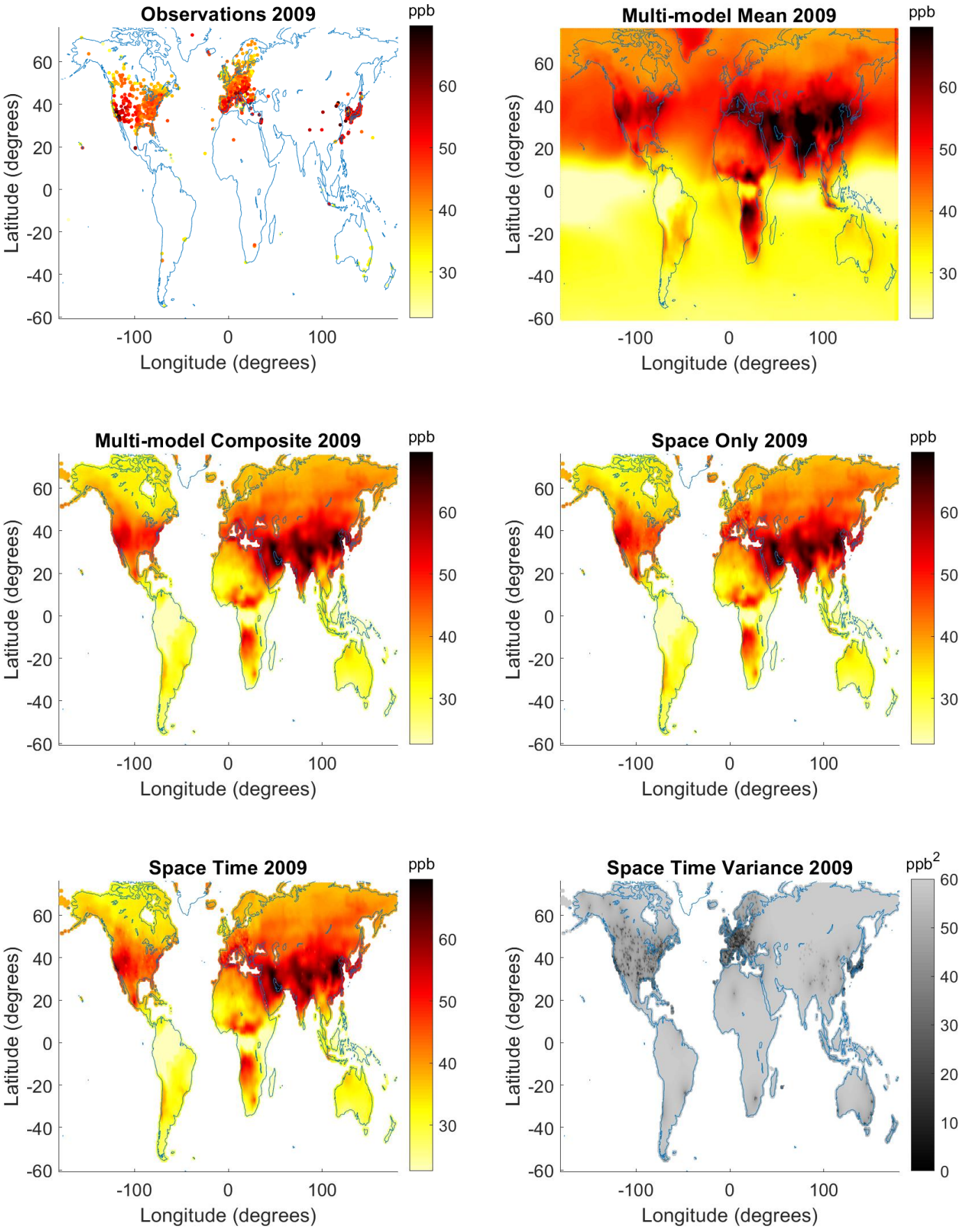

Figure S23: (continued)

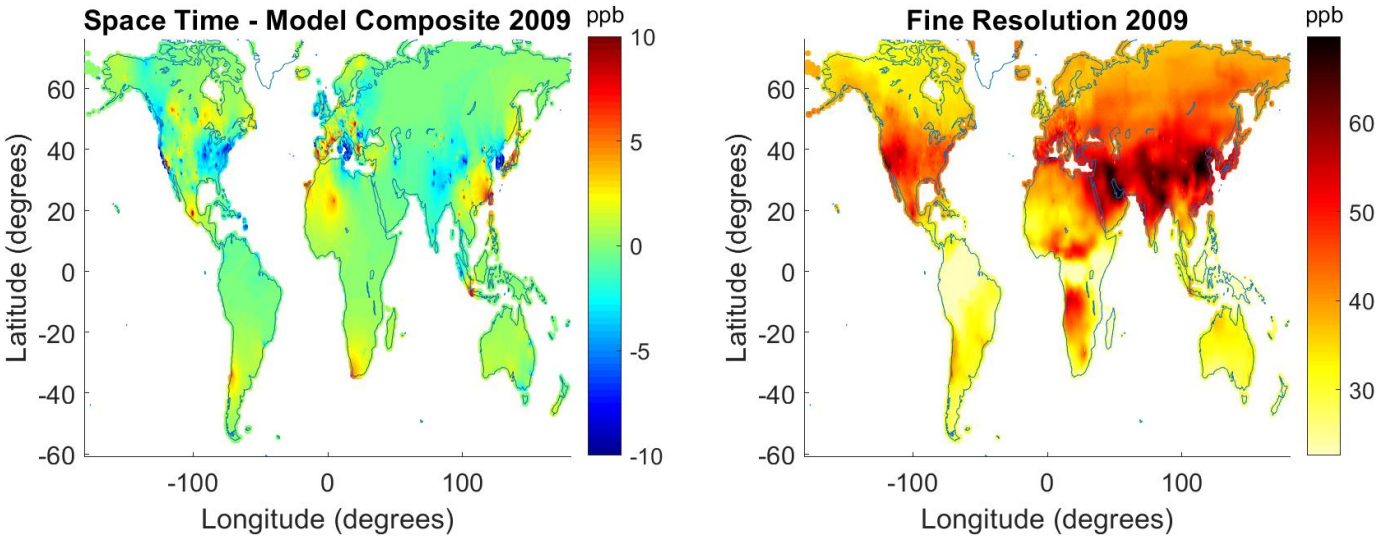

Figure S24: Yearly Maps for 2010

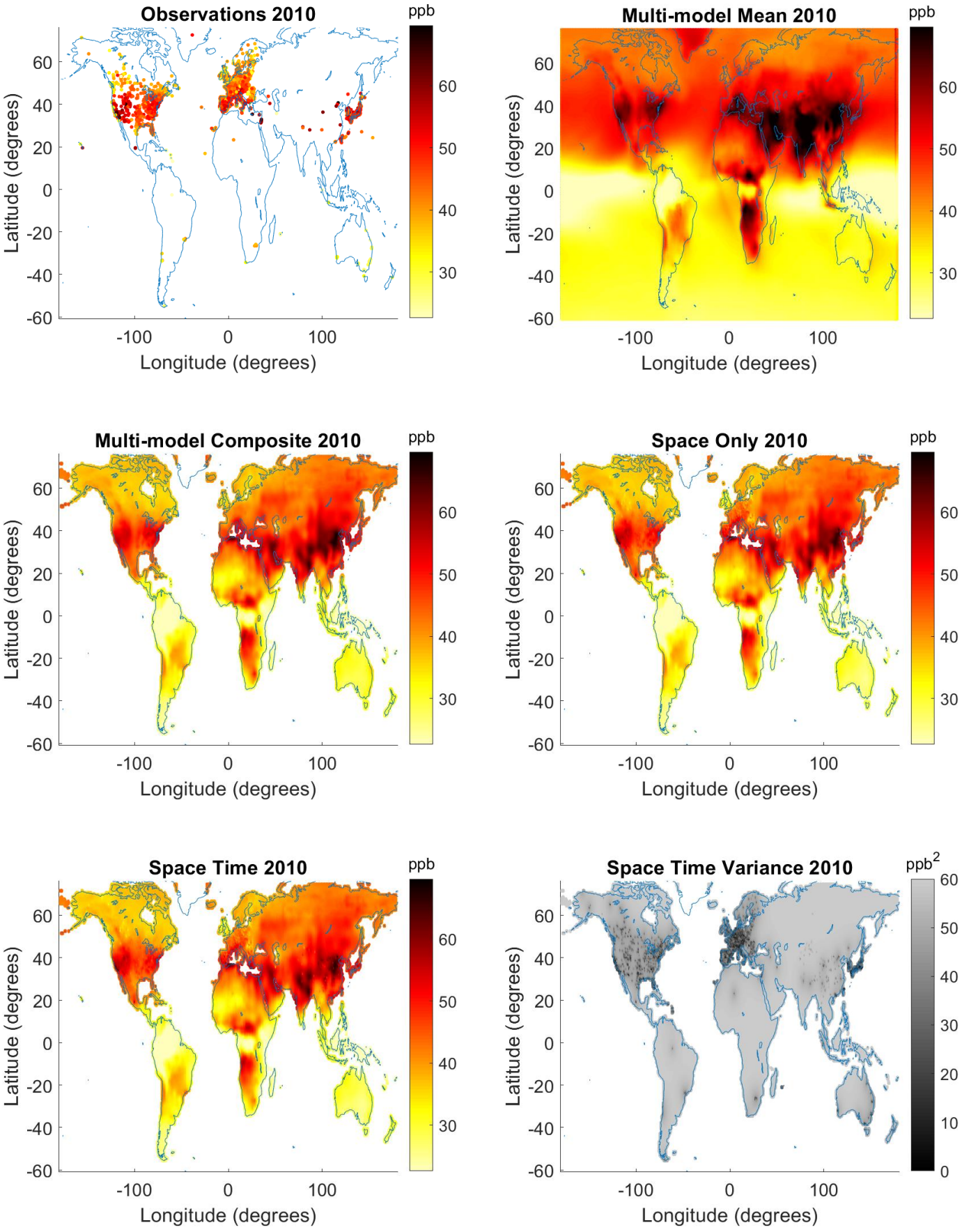

Figure S24: (continued)

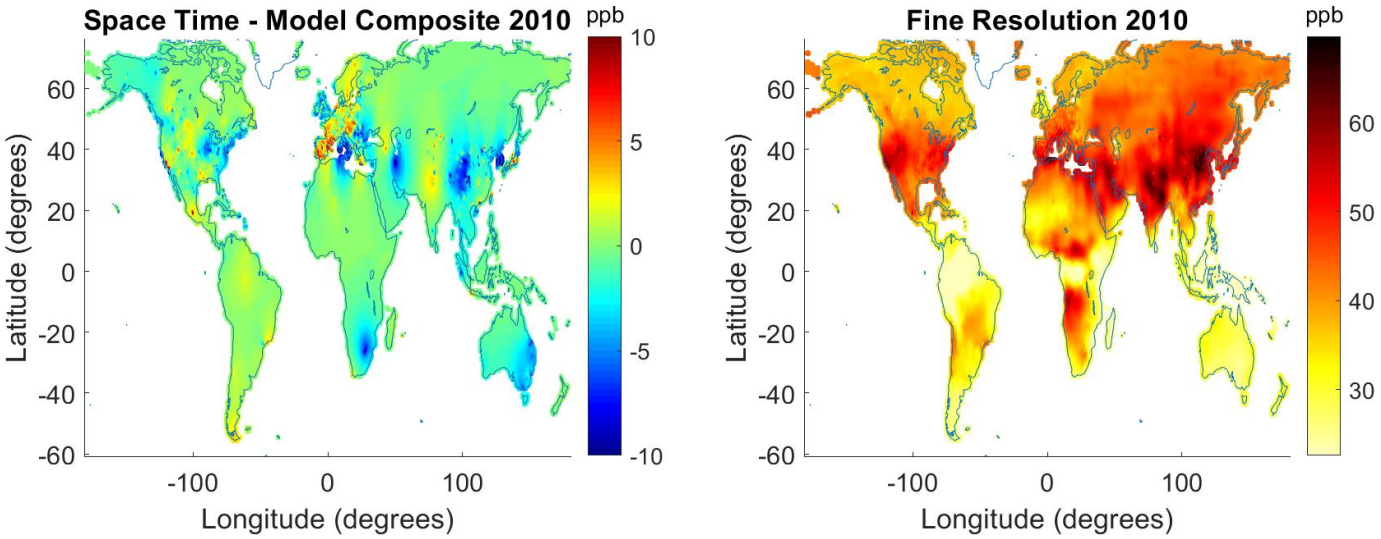

Figure S25: Yearly Maps for 2011

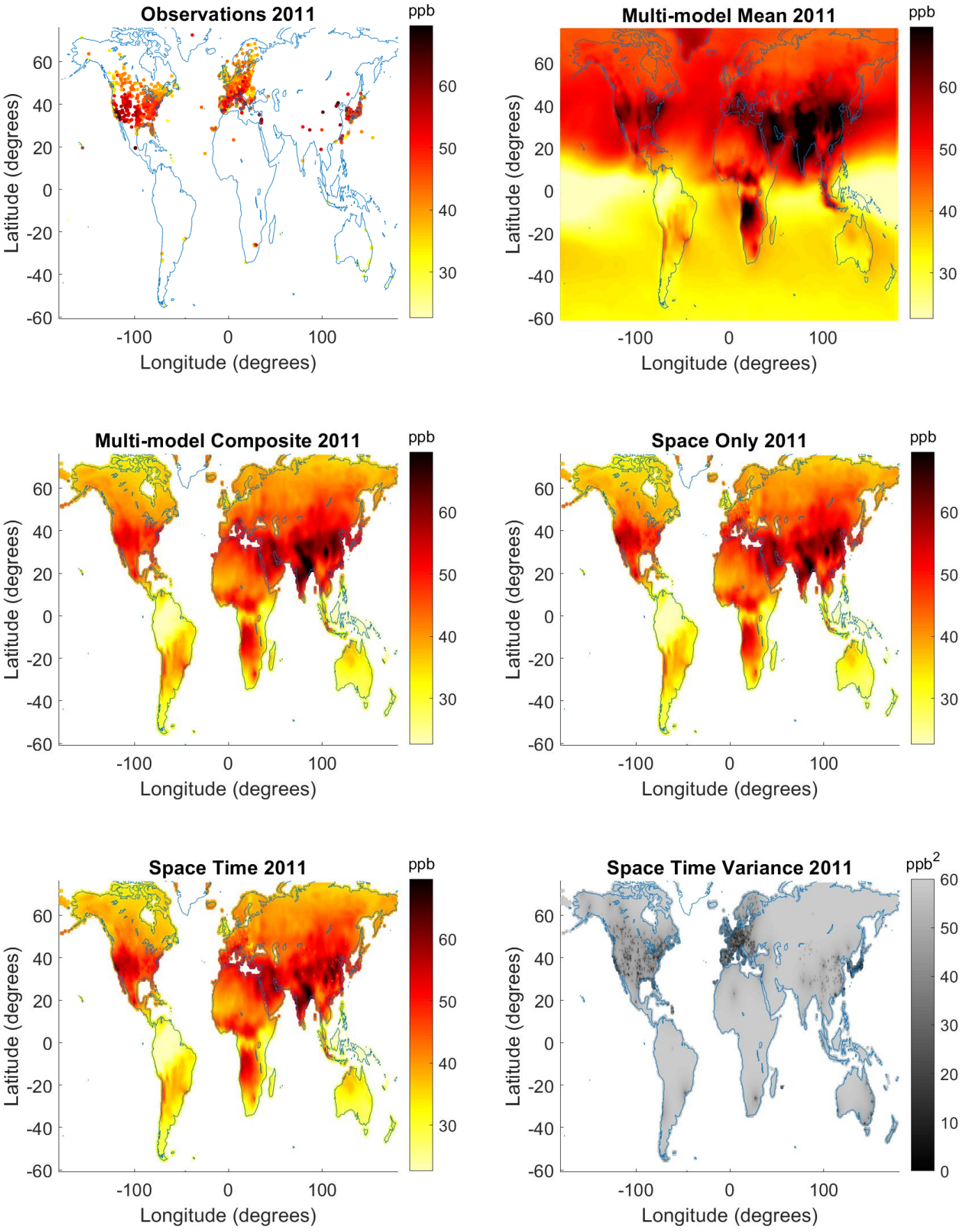

Figure S25: (continued)

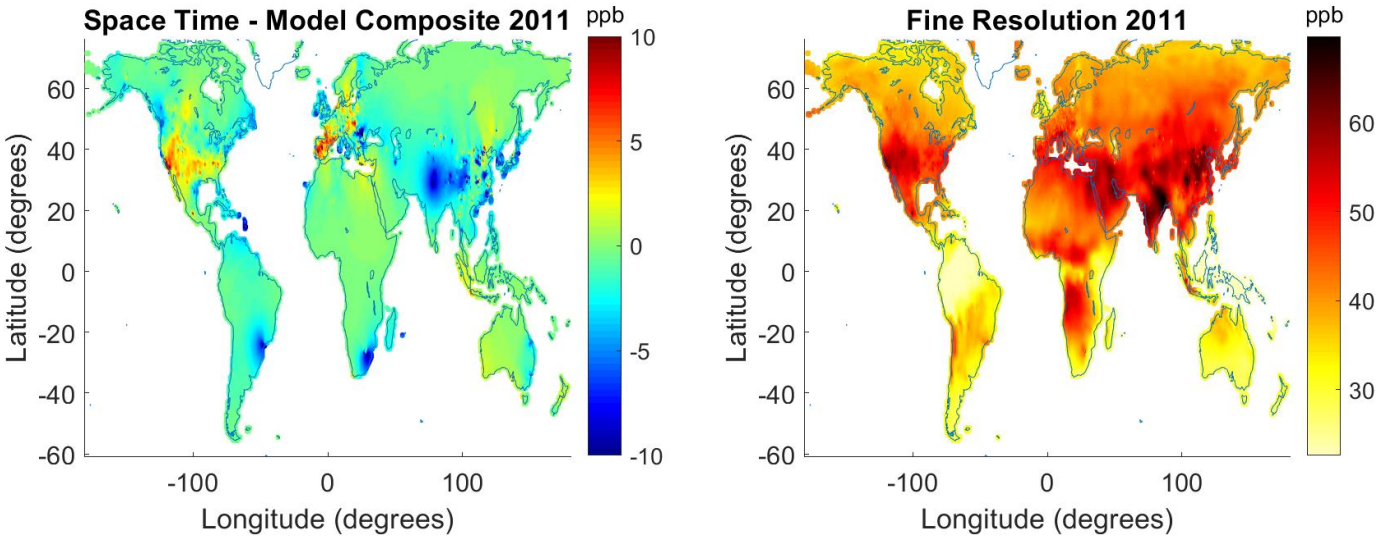

Figure S26: Yearly Maps for 2012

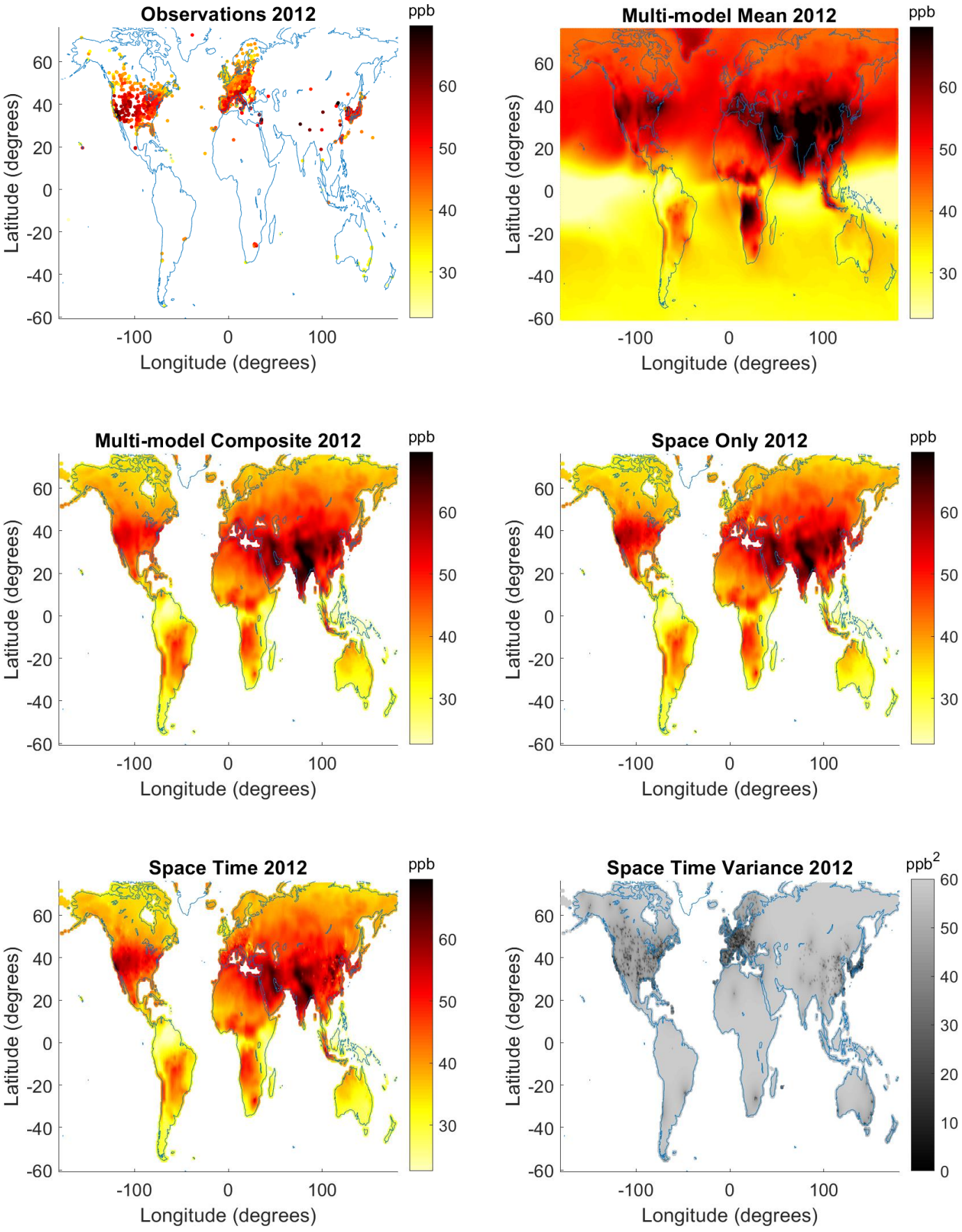

Figure S26: (continued)

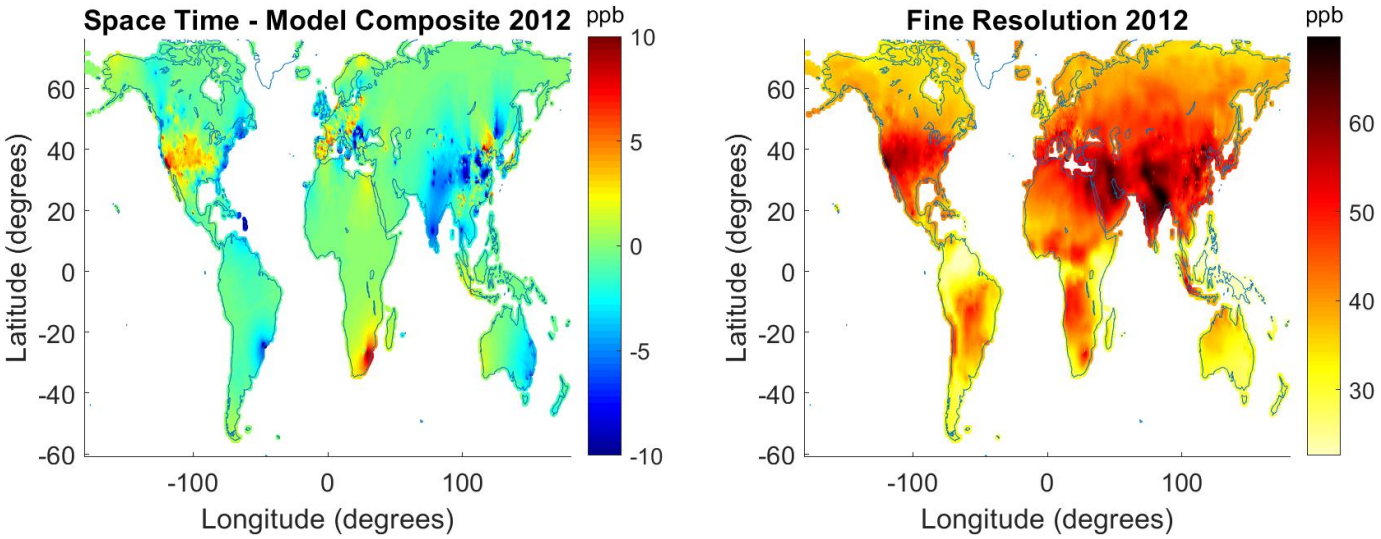

Figure S27: Yearly Maps for 2013

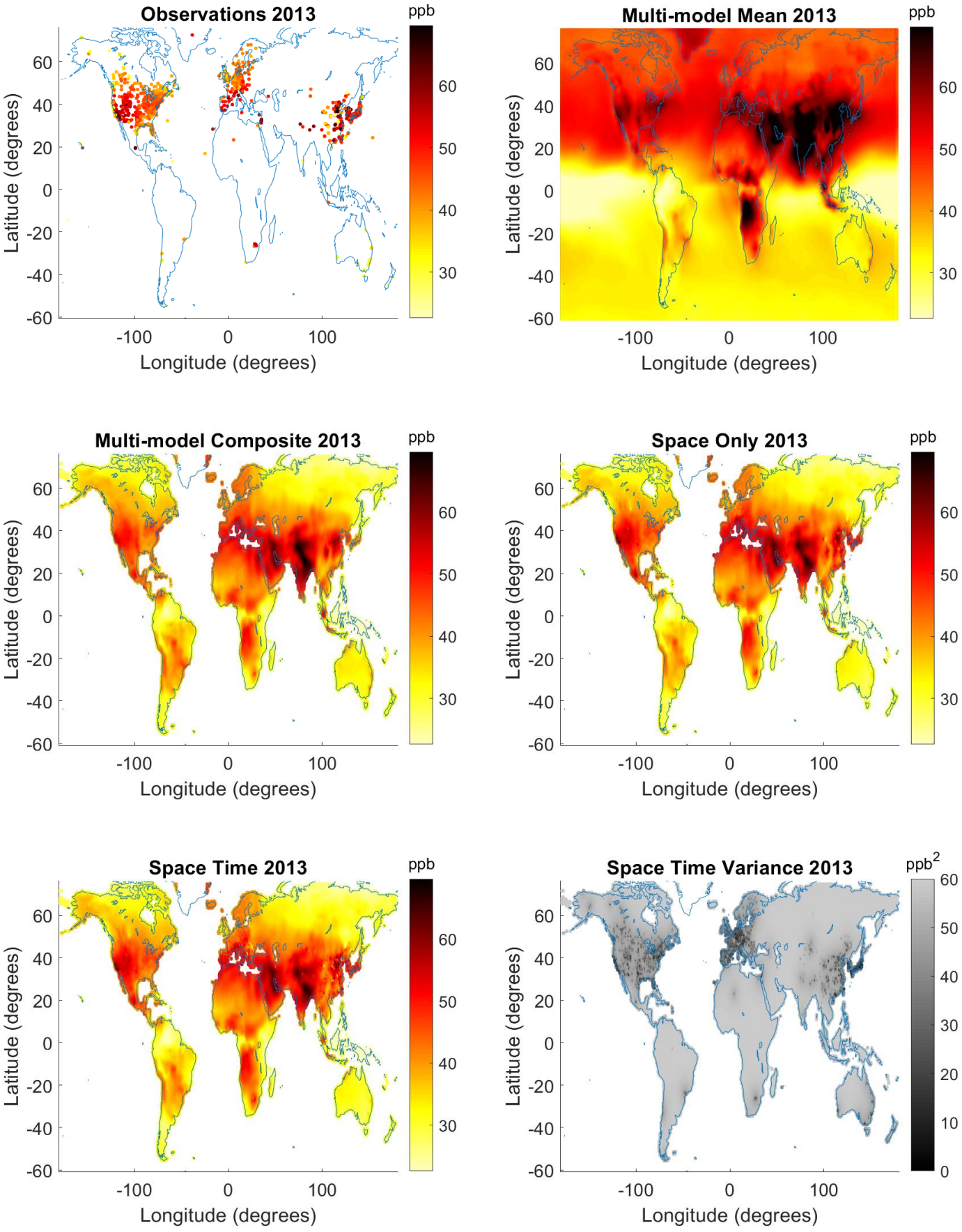

Figure S27: (continued)

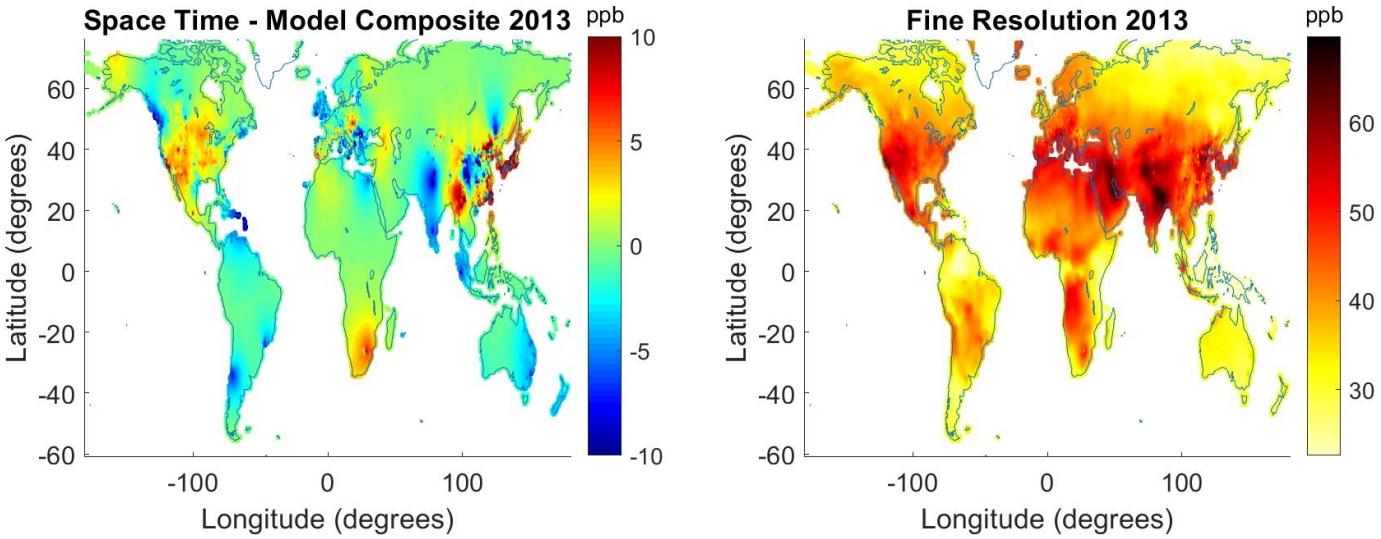

Figure S28: Yearly Maps for 2014

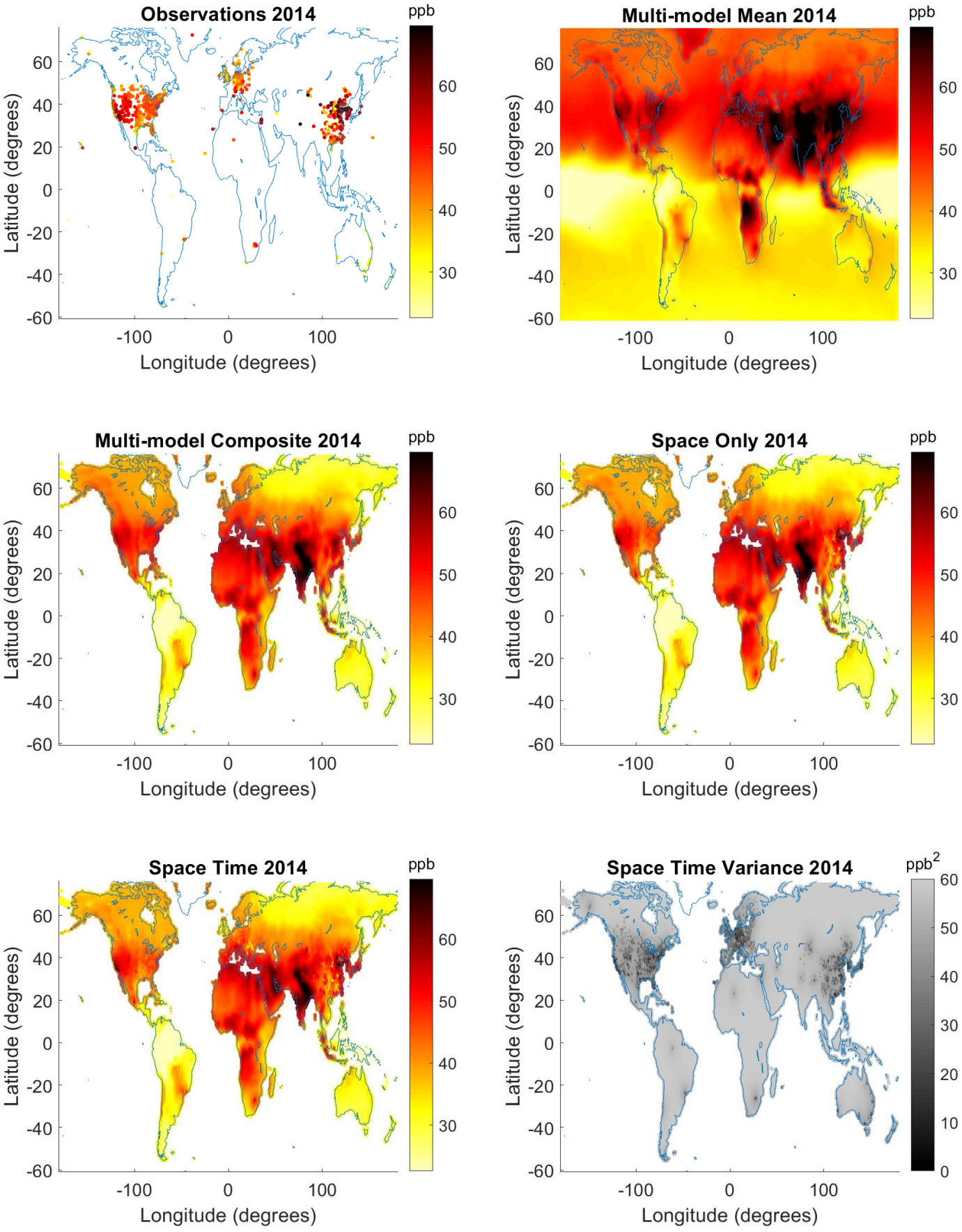

Figure S28: (continued)

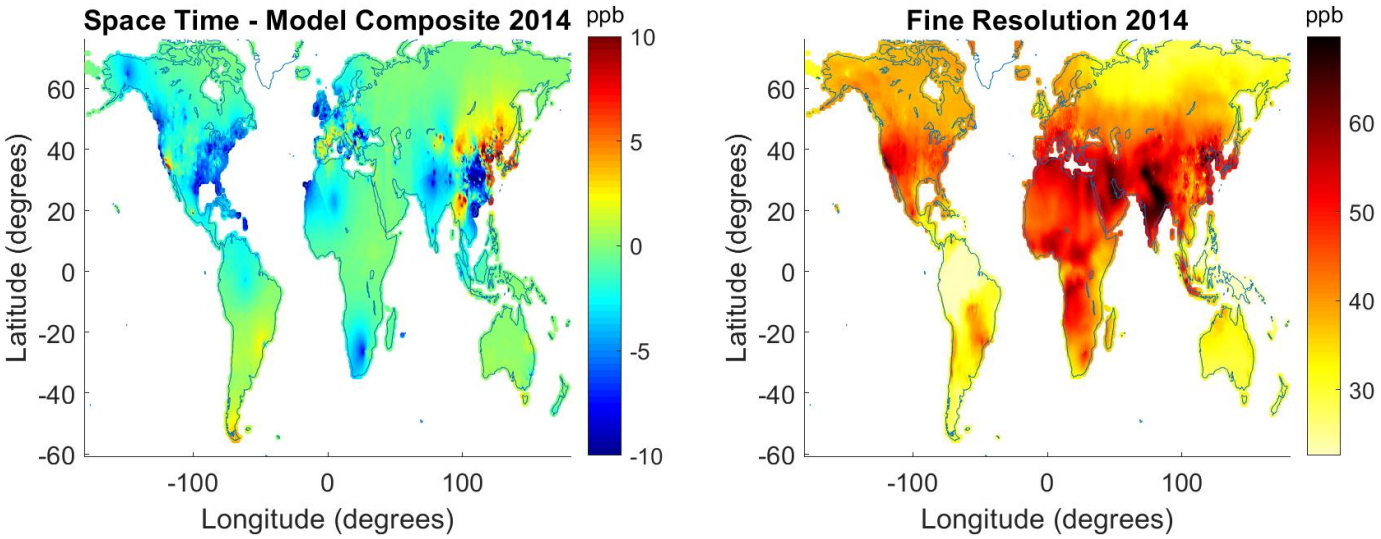

Figure S29: Yearly Maps for 2015

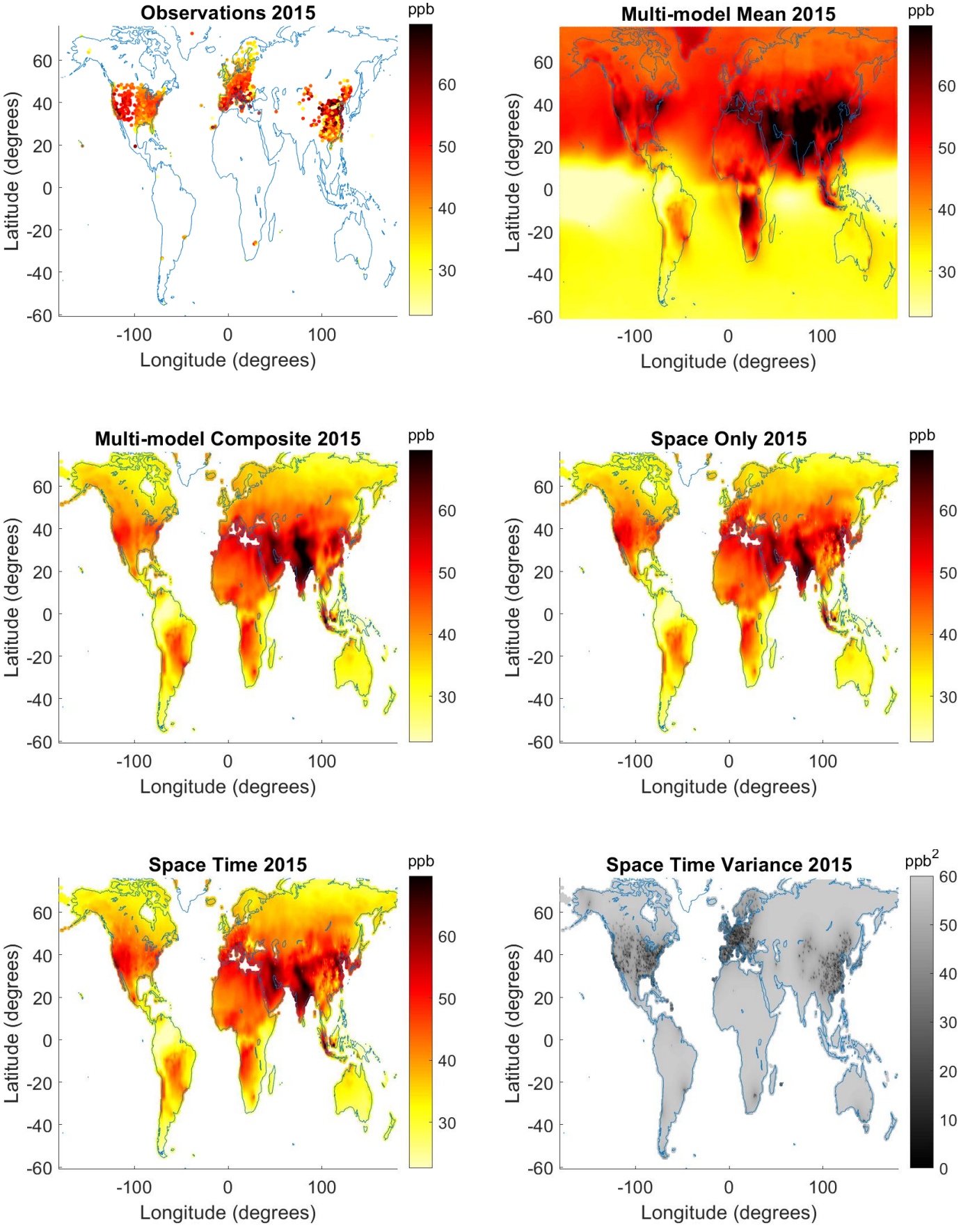

Figure S29: (continued)

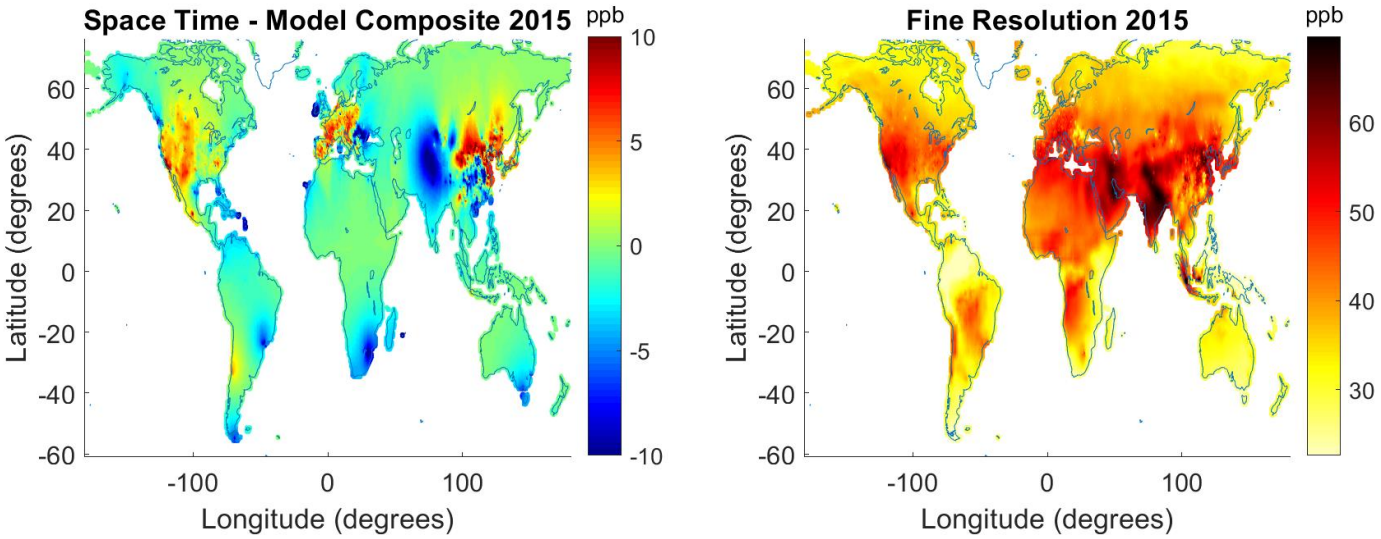

Figure S30: Yearly Maps for 2016

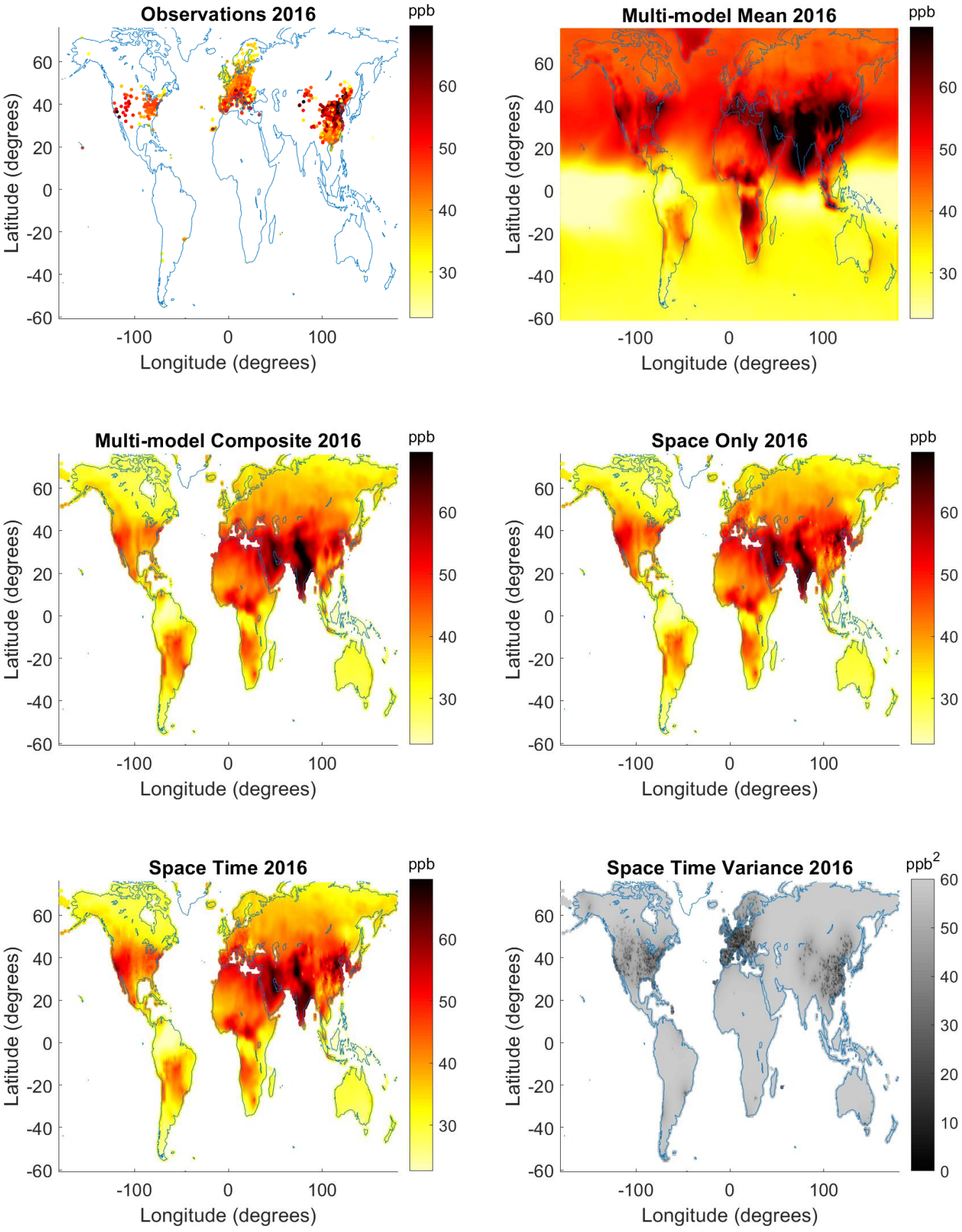

Figure S30: (continued)

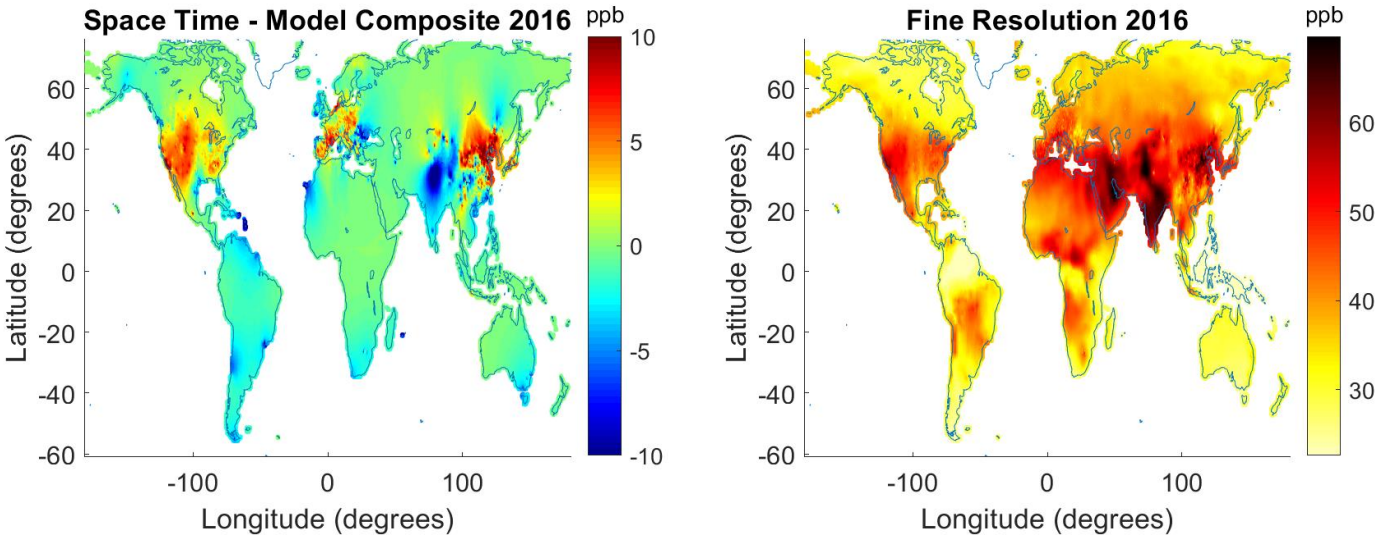

Figure S31: Yearly Maps for 2017

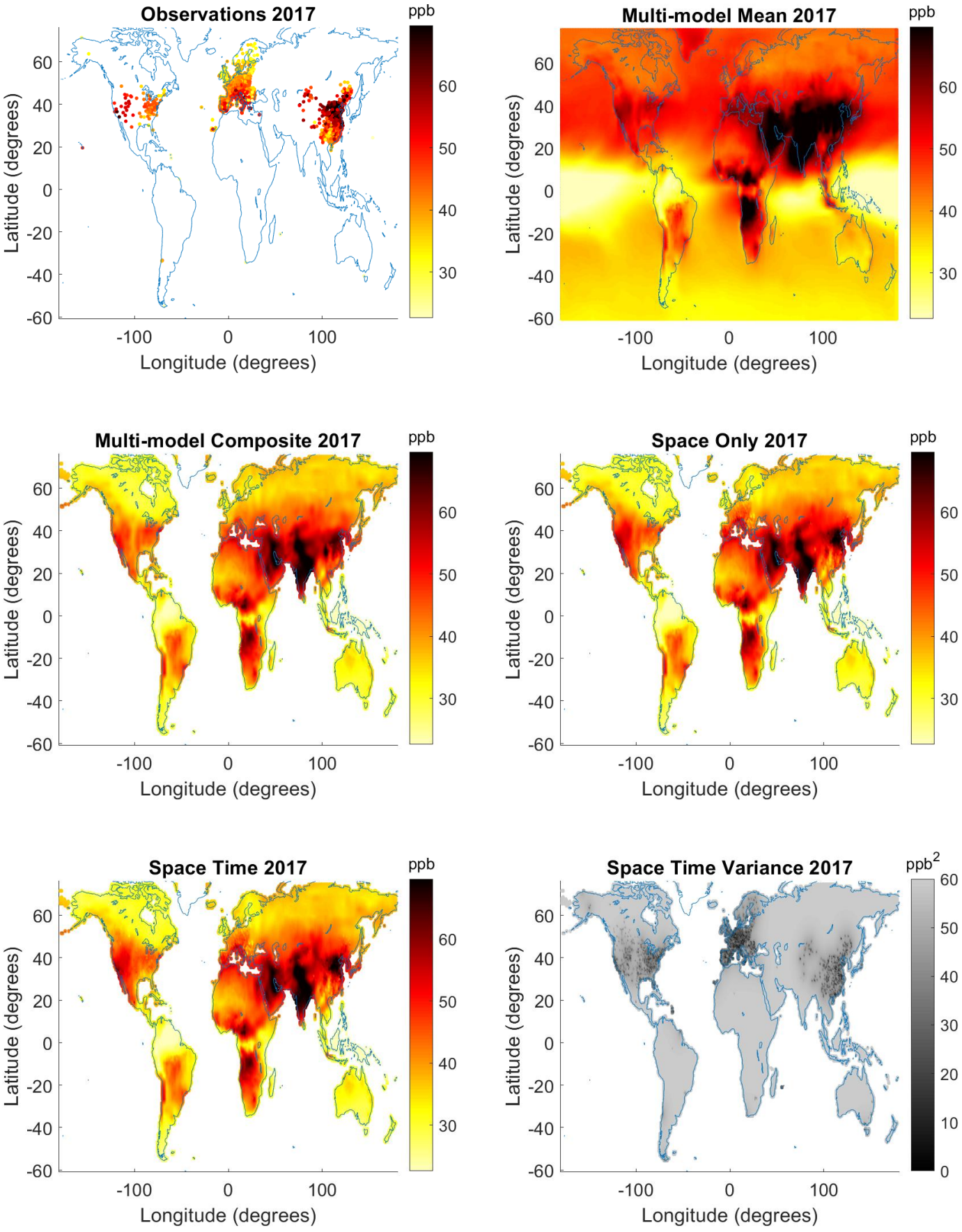

Figure S31: (continued)

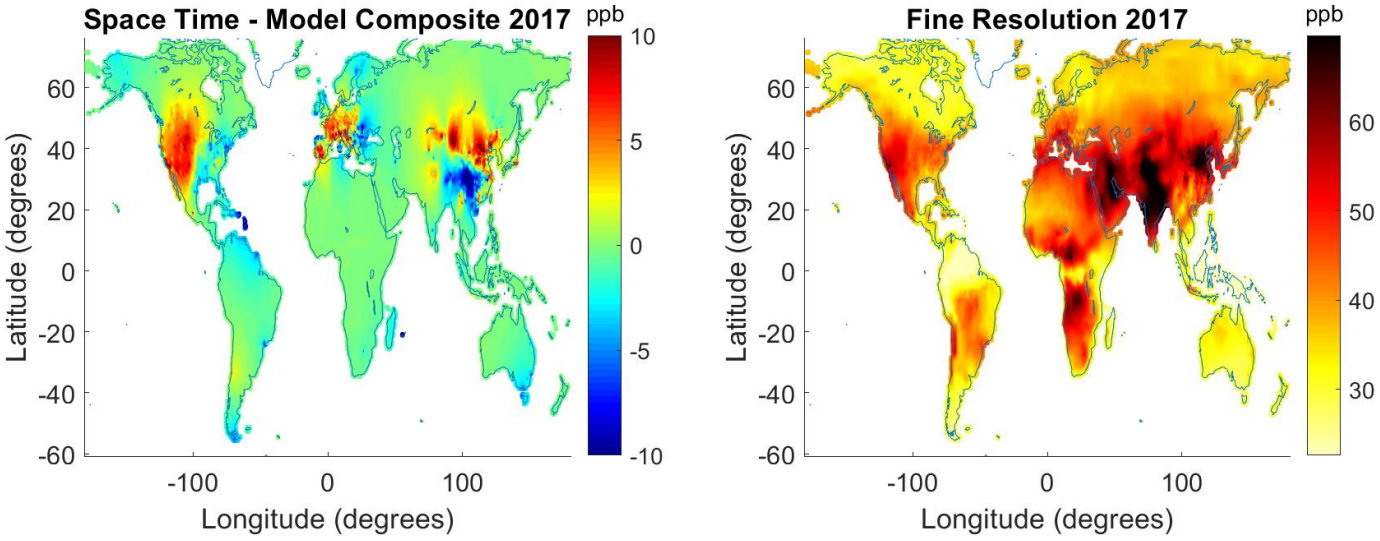

(5) Cross Validation Statistics

Table S2. Cross validation statistic equations.

Statistic	Equation	Variable Definitions
Error (E)	$E(\boldsymbol{p}_i) = Z(\boldsymbol{p}_i) - z_0(\boldsymbol{p}_i)$	$Z(\boldsymbol{p_i}) = estimated\ ozone\ at\ \boldsymbol{p_i}$ $z_o(\boldsymbol{p_i}) = observed\ ozone\ at\ \boldsymbol{p_i}$
Root mean square error (RMSE)	$RMSE = \sqrt{\frac{\sum_{i=1}^{n}\left(Z(\boldsymbol{p}_i) - z_0(\boldsymbol{p}_i)\right)^2}{n}}$	$Z(\boldsymbol{p}_i) = estimated\ ozone\ at\ \boldsymbol{p}_i$ $z_o(\boldsymbol{p}_i) = observed\ ozone\ at\ \boldsymbol{p}_i$ $n = number\ of\ observations$
Mean error (ME)	$ME = \frac{\sum_{i=1}^{n}\left(Z(\boldsymbol{p}_i) - z_0(\boldsymbol{p}_i)\right)}{n}$	$Z(\boldsymbol{p}_i) = estimated\ ozone\ at\ \boldsymbol{p}_i$ $z_o(\boldsymbol{p}_i) = observed\ ozone\ at\ \boldsymbol{p}_i$ $n = number\ of\ observations$
R-squared (R^2)	$R^2 = 1 - \frac{\sum_{i=1}^{n}(Z(\boldsymbol{p}_i) - f_i)^2}{\sum_{i=1}^{n}(Z(\boldsymbol{p}_i) - \mu)^2}$	$Z(\boldsymbol{p}_i) = estimated\ ozone\ at\ \boldsymbol{p}_i$ $f_i = linear\ model\ prediction$ $\mu = mean\ of\ Z(\boldsymbol{p}) = \frac{(\sum_{i=1}^{n} Z(\boldsymbol{p}_i))}{n}$
Variance of error (varE)	$varE = \frac{\left(\sum_{i=1}^{n}(E(\boldsymbol{p}_i) - \mu)^2\right)}{n-1}$	$E(\boldsymbol{p}_i) = error\ at\ \boldsymbol{p}_i$ $\mu = mean\ of\ E(\boldsymbol{p}) = \frac{(\sum_{i=1}^{n} E(\boldsymbol{p}_i))}{n}$ $n = number\ of\ observations$
Variance of estimated ozone (varZ)	$varZ = \frac{\left(\sum_{i=1}^{n}(Z(\boldsymbol{p}_i) - \mu)^2\right)}{n-1}$	$Z(\boldsymbol{p}_i) = estimated\ ozone\ at\ \boldsymbol{p}_i$ $\mu = mean\ of\ Z(\boldsymbol{p}) = \frac{(\sum_{i=1}^{n} Z(\boldsymbol{p}_i))}{n}$ $n = number\ of\ observations$

(6) Output Comparison to M^{3}Fusion Method

In the M^{3}Fusion method described by Chang et al. (2019), the ozone output created is the seven-year average of 2008 to 2014. To compare our results, we averaged our fine resolution output over the years 2008 to 2014.

Figure S32: Fine resolution average 2008-2014.

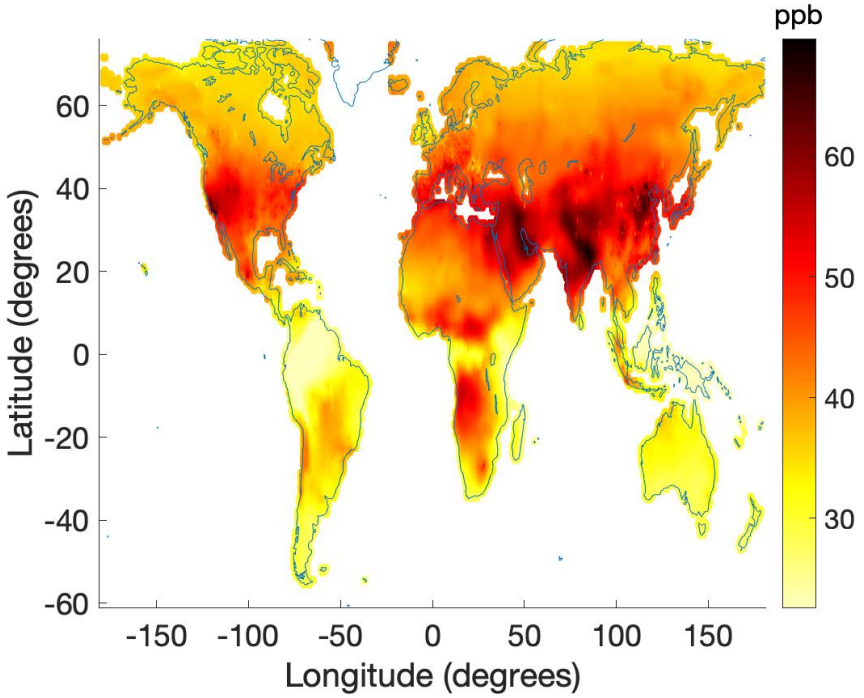

Figure S33: Fine resolution – Chang et al. (2019) for 2008-2014 average.

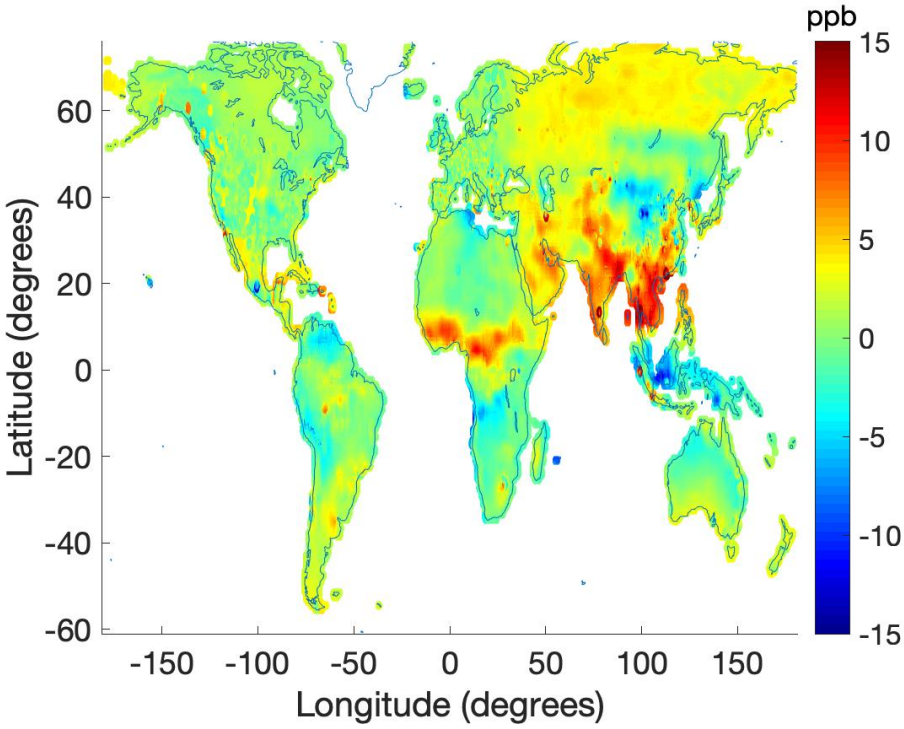

(7) Population Weight Ozone by Region Statistical Analysis

Table S3. Regional Ozone Trends Slope Statistical Analysis.

Region	Slope	P-value
Africa	0.21	0.0072
East Asia	0.29	0.0000057
Europe	-0.049	0.18
North America	-0.27	0.000000059
Oceania	0.22	0.0041
Russia	-0.23	0.0000099
South America	0.03	0.41
South Central Asia	0.36	0.0000000026
Global	0.21	0.000000017

(8) Population Weighted Ozone by Country

Figure S34: Ozone trend for the most populous countries as population weighted OSDMA8.

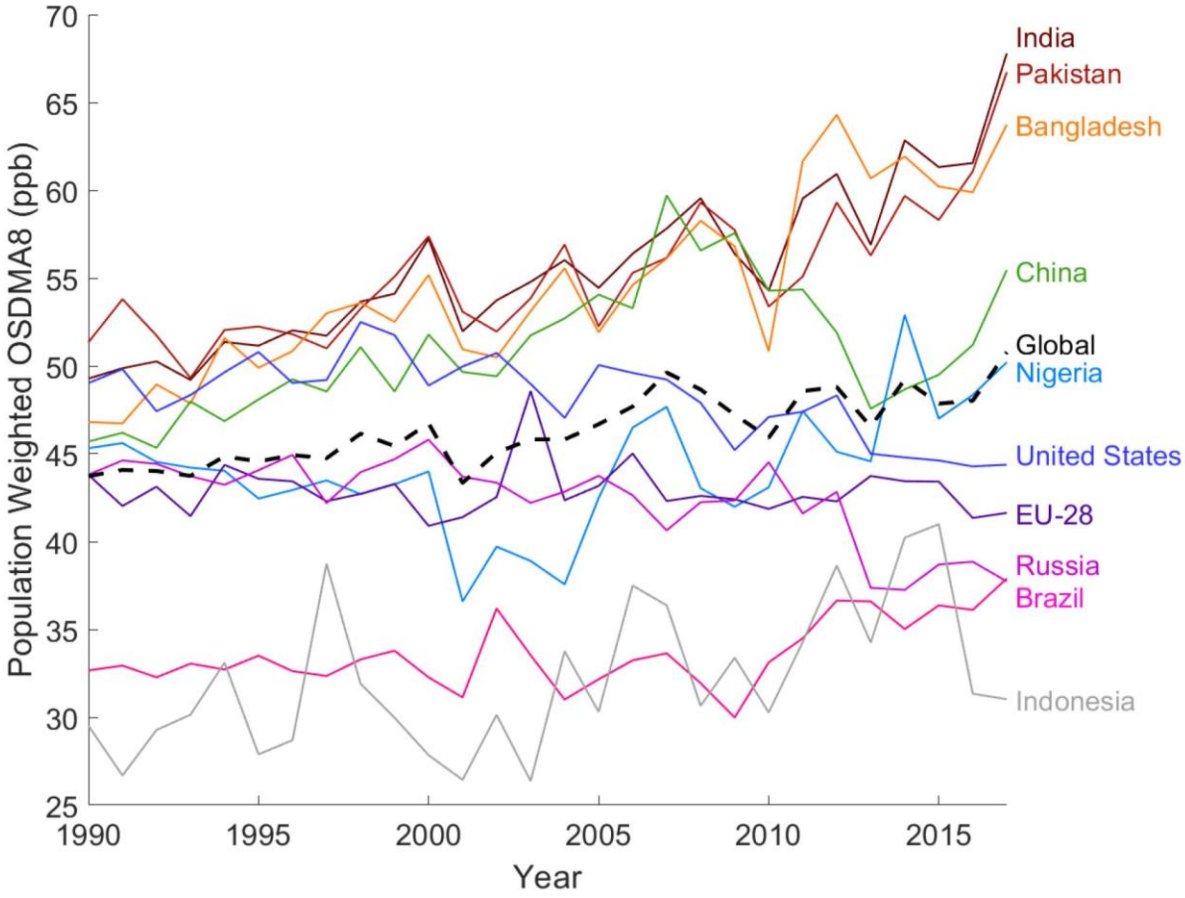

Table S4. Ozone Trends by Country Slope Statistical Analysis.

Country	Slope	P-value
Bangladesh	0.55	0.00000000040
Brazil	0.13	0.0022
China	0.26	0.0011
EU-28	-0.018	0.61
India	0.51	0.000000000026
Indonesia	0.26	0.0048
Nigeria	0.17	0.03
Pakistan	0.37	0.00000048
Russia	-0.22	0.0000029
United States	-0.19	0.000038
Global	0.21	0.000000017

(9) Ozone Trends with Uncertainty

Uncertainty intervals are shown as the population weighted lower and upper bound of ozone as OSDMA8.

Figure S35: Global ozone trend with uncertainty interval.

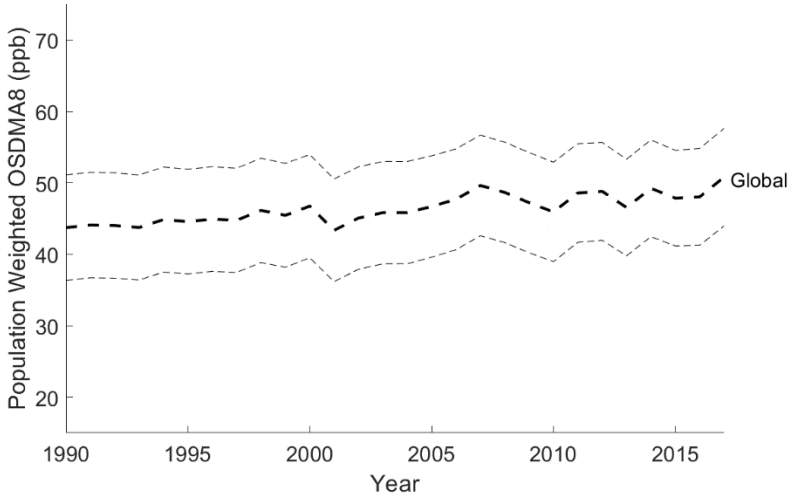

Figure S36: South Central Asia ozone trend with uncertainty interval.

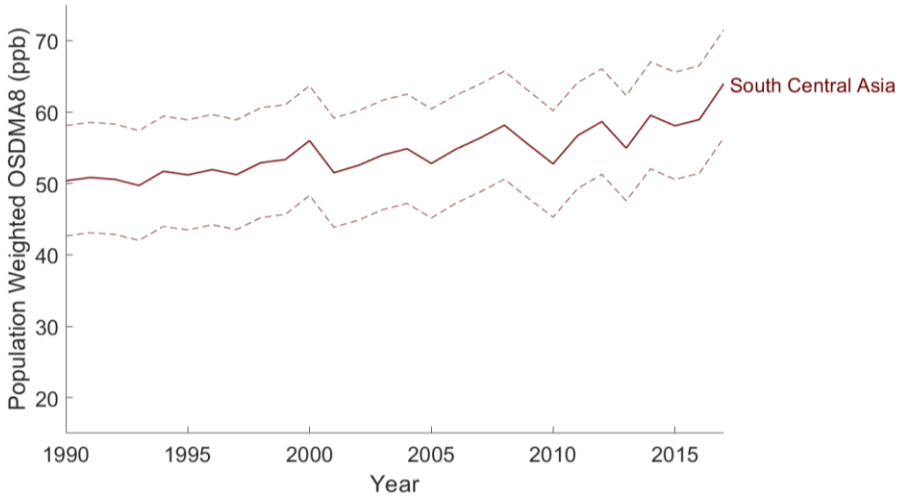

Figure S37: East Asia ozone trend with uncertainty interval.

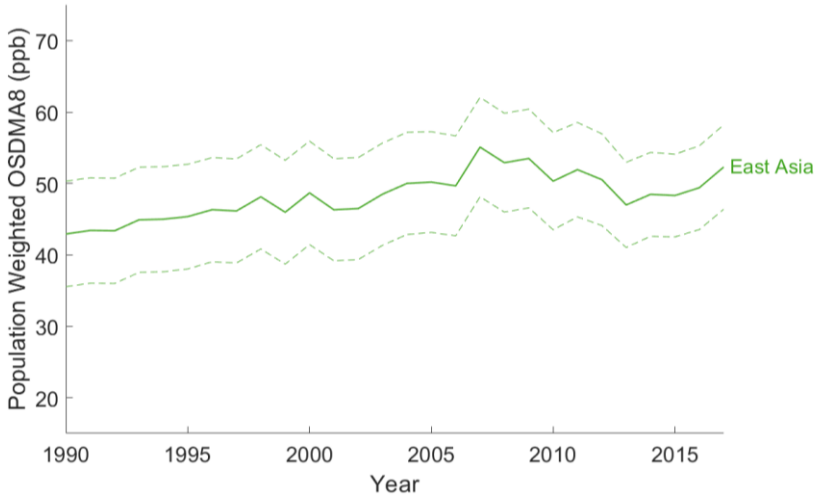

Figure S38: North America ozone trend with uncertainty interval.

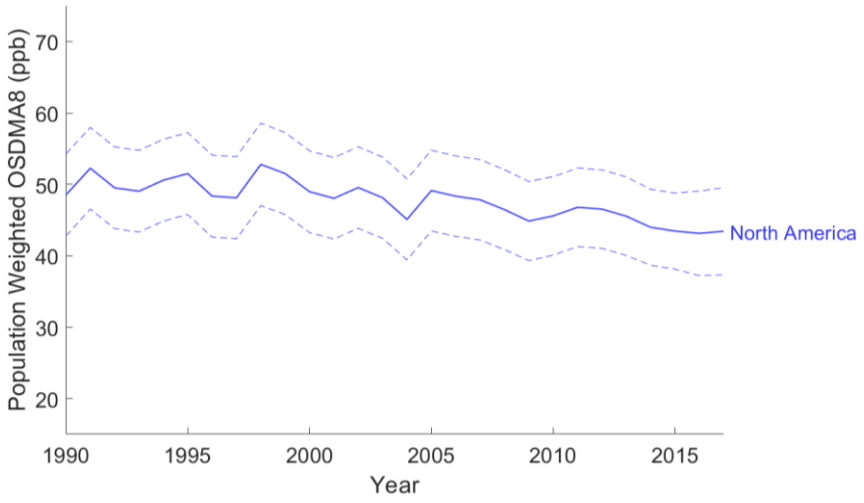

Figure S39: Europe ozone trend with uncertainty interval.

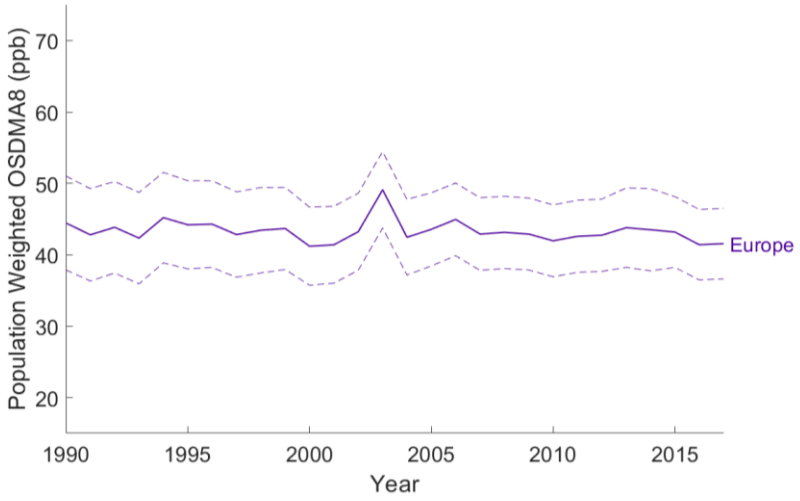

Figure S40: Africa ozone trend with uncertainty interval.

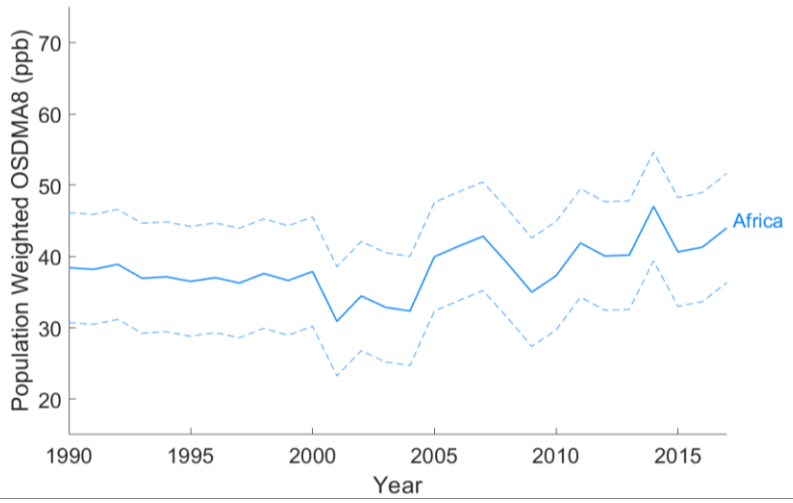

Figure S41: Russia ozone trend with uncertainty interval.

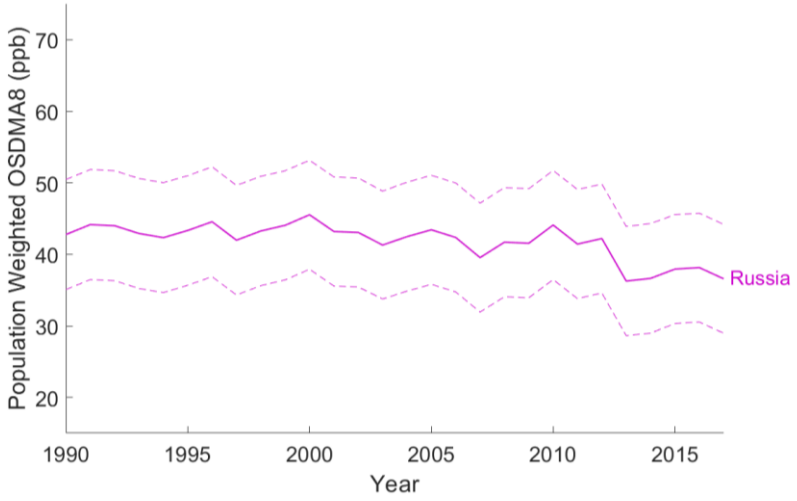

Figure S42: South America ozone trend with uncertainty interval.

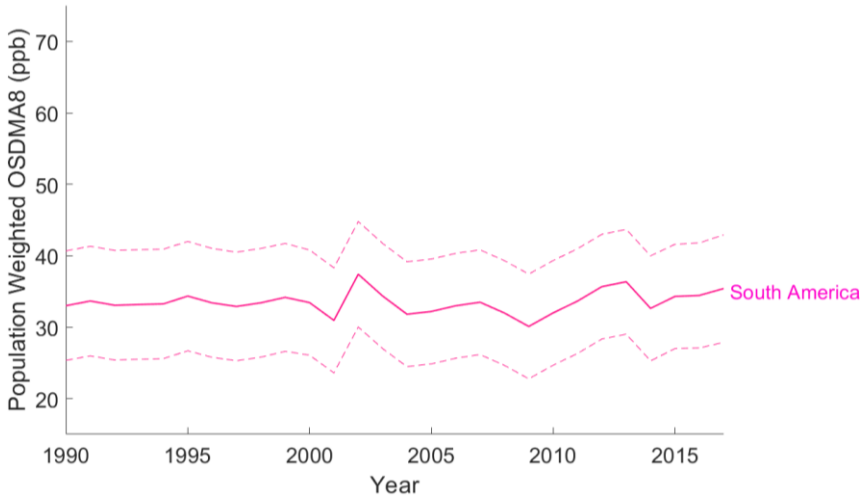

Figure S43: Oceania ozone trend with uncertainty interval.

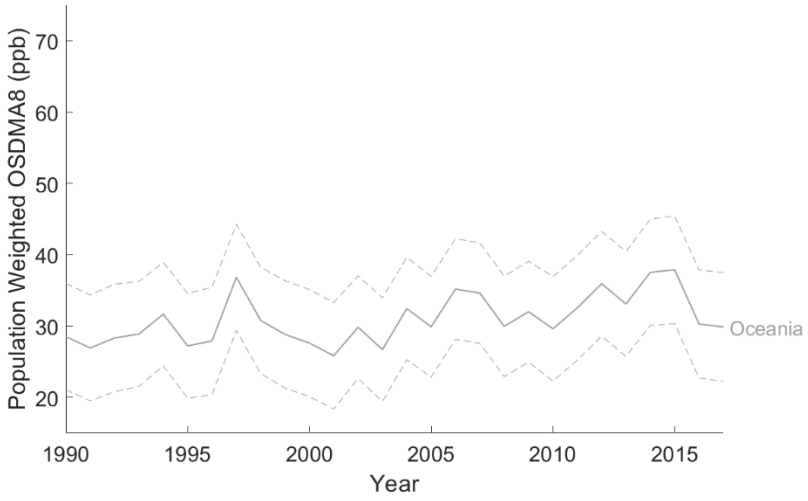

Figure S44: India (left) and Pakistan (right) ozone trend with uncertainty interval.

Figure S45: Bangladesh (left) and China (right) ozone trend with uncertainty interval.

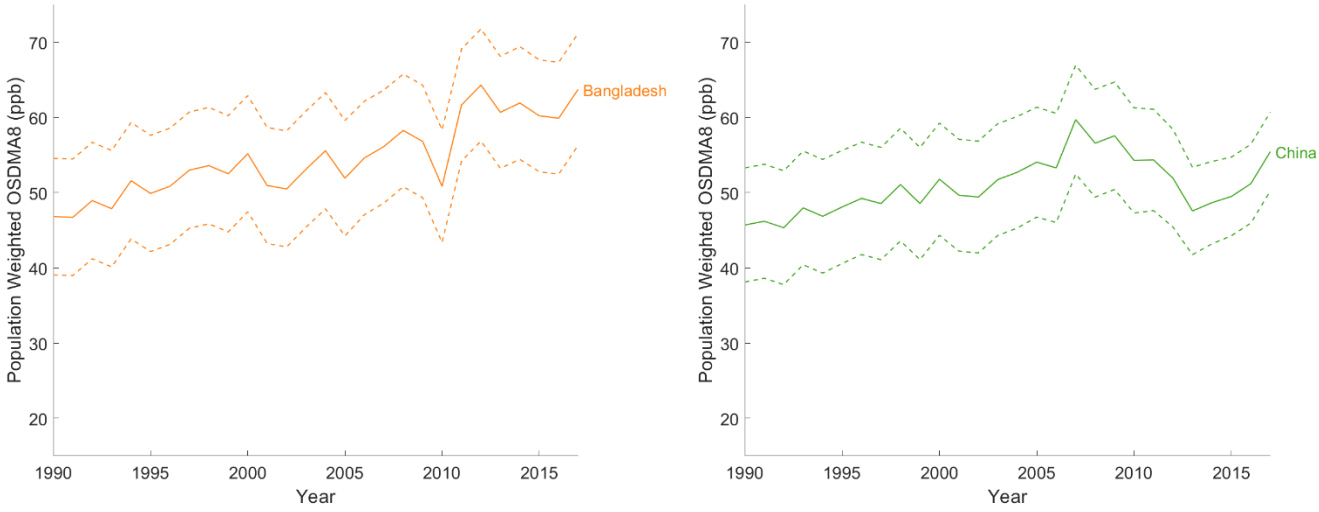

Figure S46: Nigeria (left) and United States (right) ozone trend with uncertainty interval.

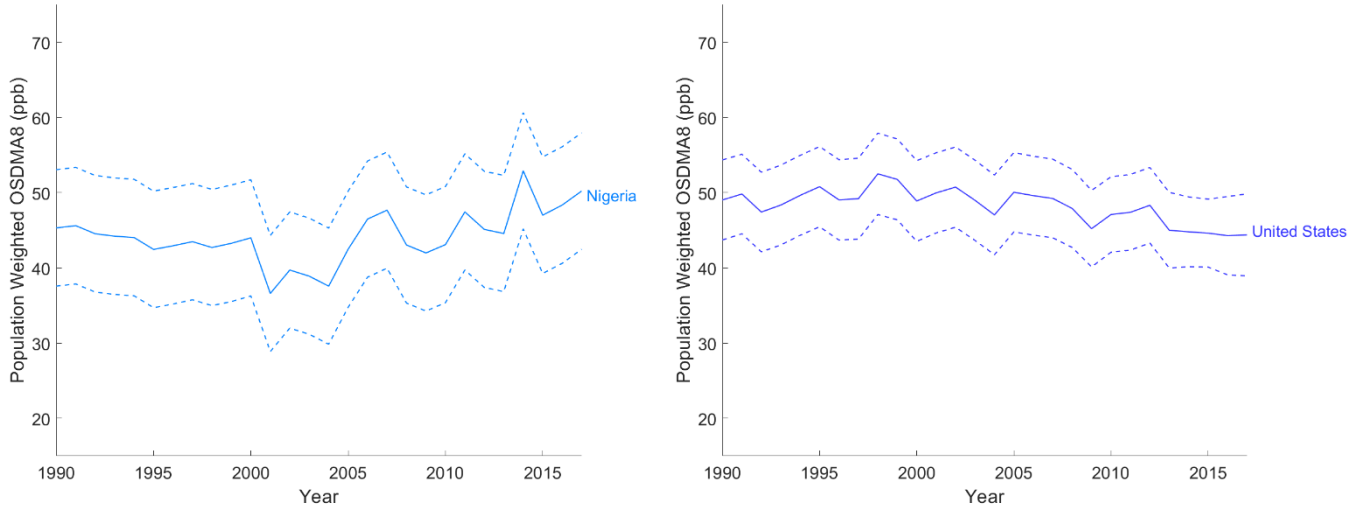

Figure S47: EU-28 (left) and Russia (right) ozone trend with uncertainty interval.

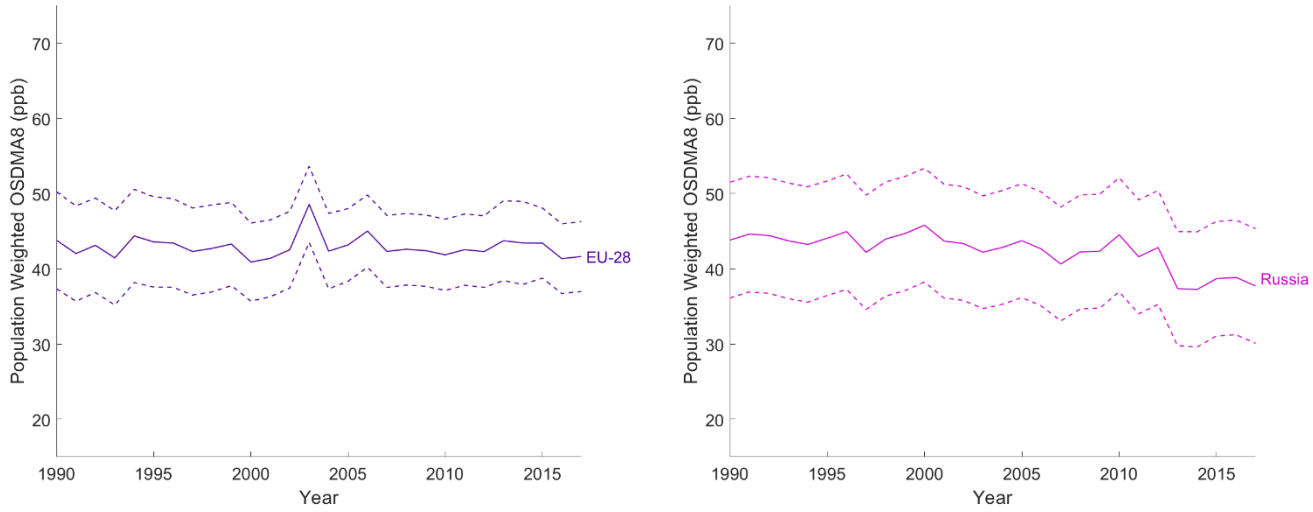

Figure S48: Brazil (left) and Indonesia (right) ozone trend with uncertainty interval.